A novel model of optogenetic kindling of neocortex

Elvis Cela

Integrated Program in Neuroscience (IPN)

Department of Neurology and Neurosurgery

Faculty of Medicine

McGill University

Montreal, QC

A thesis submitted to McGill University in partial fulfilment of the requirements

for the degree of Doctor of Philosophy

“Aut viam inveniam aut faciam”

I will either find a way or I will make one.

Hannibal Barca, circa 217 BC

Acknowledgements

Firstly, I would like to thank my PhD supervisor, Jesper Sjöström, for teaching me how and why we do science. I have had the privilege to work on a challenging project in a novel area in the lab and in the neuroscience field in general and thank Jesper for entrusting me with this project and allowing me the freedom to pursue additional experiments on my own volition. In addition, the scale of the project necessitated learning programming for the first time, for which I am fortunate as I uncovered a latent passion for it. My PhD occurred during a critical time in adulthood and it has undeniably shaped my thinking and character going forward; I am grateful to have spent it in a hard-working and stimulating environment and project.

Secondly, I would like to thank the members of my committee: Anne McKinney and David Stellwagen who have provided invaluable guidance, suggestions and support over the years. Both during committee meetings and outside they were always available to chat and lend helpful advice for which I am grateful.

Thirdly, I would like to thank all past and present Sjöström lab members for shared good times, outings and fun discussions that veered outside of science but were nonetheless amusing and often well-needed idleness. There are many past and present members to name but the recurring characters include: Hovy, Therese, Amanda and Christina. I have also had the great privilege to mentor several talented undergraduates and thank them for perpetually renewing my interest in science. In particular I am thankful to Amrit, Taiji, Debby, and Andrew.

Fourthly, I would like to thank all my colleagues and friends at the MGH and elsewhere who have made the PhD into a complete experience. The CRN has a very collegial

atmosphere and I've had the opportunity to meet many great colleagues. In particular I am thankful for all the discussions with Benny, Ibrahim, Andy, Marie, Horia, and Erin.

I would also like to thank my collaborators both within the MGH, the Murai lab, Adamantidis lab, as well the Deisseroth lab at Stanford who were instrumental in helping set up the ChR2 viral expression system and getting unpublished reagents from. In particular I would like to extend thanks to Charu for timely communication and Thomas for feedback on building the *in-vivo* stimulation setup. In addition, I am grateful for Jonathan's (MIT) help with the extracellular slicing solution for older animals. At the MGH, I have relied heavily on experimental support from Gael, Sabrina and Todd.

Finally, I would like to thank my family for their support and understanding during my PhD.

Preface

In this thesis, I describe the development of a novel neocortical optogenetic kindling model of seizures and subsequent characterization of this model. Further work that I contributed to such as a two-hit model which allows for accelerated seizure development and preliminary experiments using ChR2 assisted circuit mapping, to investigate corresponding circuit changes after seizure induction are also described.

The main novelty herein is the ability to target a defined cell population with light *in-vivo*, without grossly damaging nearby tissue and induce seizures gradually over time in initially healthy animals. Importantly, this is the only work to date to use optogenetics for kindling and long-term monitoring in healthy awake behaving animals. Other work has relied on induction of seizures using classical methods and/or genetic mutations or relying on acute seizure induction. This model opens up new avenues of research into the study of epileptogenesis such as the cell type specific contributions to plasticity that underlie the transition from a healthy to a diseased state.

Contributions of authors

Chapter 1: Parts of this introduction are published in *Frontiers in Neuroscience*.

Cela E and Sjöström PJ (2019) Novel Optogenetic Approaches in Epilepsy Research. *Front. Neurosci. 13:947*

EC and PJS wrote the manuscript.

Chapter 2: This chapter is published in *Scientific Reports:*

Cela, E., McFarlan, A.R., Chung, A.J., Wang, T., Chierzi, S., Murai, K.K., and Sjöström, P.J. (2019). An Optogenetic Kindling Model of Neocortical Epilepsy. *Scientific Reports 9*, 5236.

PJS and EC designed the project. EC carried out *in-vivo* experiments with help from SC, AJC, and TW. AM carried out immunolabelling with help from WTF, EC and KM. EC, PJS, and AJC analyzed electrophysiology results.

Chapter 3: Parts of this chapter are in preparation for submission*:*

Elvis Cela, P. Jesper Sjöström. *CB1R blockade accelerates seizures during neocortical optokindling.*

PJS and EC designed the project. EC carried out experiments. EC analyzed results.

Chapter 4: Data in this chapter may be used in future manuscripts.

Elvis Cela, Gaël Quesseveur, Keith K Murai, P. Jesper Sjöström. *CRACM analysis of circuit changes following optokindling.*

EC carried out *in-vivo* and *in-vitro* recordings, optogenetic stimulation and analysis. PJS wrote acquisition and analysis software and oversaw the project. GQ and KKM provided *in-utero* electroporated animals.GQ constructed plasmids for *in-utero* electroporation.

Table of contents

Abstract

Epilepsy is a major neurological disorder that is under intense scientific and medical investigation. The emergence of seizures is associated with other comorbidities and decreases the quality of life of patients. In addition, around 30% of patients do not respond to standard line of treatment using anti-epileptic drugs (AEDs). Furthermore, it is still unclear how seizures arise in the otherwise healthy brain. Therefore, it is critical to have well developed models where a causal understanding of epilepsy can emerge.

While the development of seizures has been studied in many animal models, such as those using electrical induction, deciphering the results of such studies has been difficult due to the uncertainty of the cell population being targeted as well as potential confounds like brain damage from the procedure itself. The kindling model of epilepsy, an enduring electrical induction model has been used over time to dissect the steps of seizure development in animals that underlie epilepsy. We used the classical kindling model as a base to develop novel models from and addressed the disadvantages associated with current induction models.

This thesis describes the development of a novel optogenetic kindling model of seizures along with a two-hit counterpart which can be used separately, as well circuit analysis methods these models can be combined with to study epileptogenesis. Using a combination of optogenetic stimulation and EEG recordings in awake freely moving animals, we tested the hypothesis that activity alone from repeated stimulation eventually causes seizures. The resulting seizures display several hallmarks features consistent with classical kindling such as a decrease in seizure threshold, worsening seizure symptoms and an elevated retention of seizure susceptibility in kindled animals. Using two-photon targeted paired

whole-cell recordings and ex-vivo optogenetic manipulation of cellular activity we found that intrinsic excitability of cells from kindled brains did not differ from controls. To circumvent the labour and time constraints imposed by our optogenetic kindling protocol, we developed a two-hit model using rimonabant injections to test if CB1R blockade could accelerate optokindled seizures. Finally, we ran proof of principle experiments using optogenetic stimulation in acute slices that could serve as an alternative to paired recording for rapid circuit mapping following seizures.

Taken together, our results demonstrate promoter-specific manipulation of excitatory cell populations can give rise to seizures, a variant model for accelerating seizure development and possible circuit mapping methodologies to dissect circuit changes following seizures. I anticipate my findings may serve as the inspiration for future studies using optogenetics and other modern techniques to probe potential mechanisms of seizure development and increase the probability of developing novel treatment options.

Résumé

L'épilepsie est une maladie neurologique majeure qui fait l'objet d'intenses activités de recherche scientifique et médicale. L'émergence des crises est associée à d'autres comorbidités et diminue la qualité de vie des patients. En outre, environ 30% des patients ne répondent pas à la ligne de traitement standard utilisant des DEA. Cependant, on ne sait toujours pas comment les crises surviennent dans un cerveau par ailleurs sain. Par conséquent, il est essentiel d'avoir des modèles bien développés d'où peut émerger une compréhension causale de l'épilepsie.

Alors que le développement de crises a été étudié dans de nombreux modèles animaux, tels que ceux utilisant l'induction électrique, l'interprétation des résultats de ces études a été difficile en raison de l'incertitude de la population cellulaire ciblée ainsi que d'autres variables confusionnelles telles que les lésions potentielles associées à la procédure elle-même. Le modèle de l'allumage de l'épilepsie, un modèle d'induction électrique durable, a été utilisé au fil du temps pour disséquer les étapes du développement des crises chez les animaux. Nous avons utilisé le modèle de l'allumage classique comme base pour développer de nouveaux modèles et aborder les désavantages associés aux modèles d'induction actuels.

Cette thèse décrit le développement d'un nouveau modèle de l'allumage optogénétique des crises d'épilepsie avec un homologue deux coups qui peut être utilisé séparément, ainsi que des méthodes d'analyse de circuit avec lesquelles ces modèles peuvent être combinés afin d'étudier l'épileptogenèse. En utilisant une combinaison de stimulation optogénétique et d'enregistrements EEG chez des animaux éveillés se déplaçant librement, nous avons testé l'hypothèse que l'activité seule montre que la stimulation répétée provoque des crises. Les crises présentent plusieurs caractéristiques classiques de l'allumage, comme

une diminution du seuil épileptique, une aggravation des symptômes de crises et une rétention élevée de la susceptibilité aux crises chez les animaux modèles. En utilisant des enregistrements de cellules-entières en paires simultanément à de l'imagerie à deux photons et une manipulation optogénétique ex-vivo de l'activité cellulaire, nous avons trouvé que l'excitabilité intrinsèque des cellules provenant des cerveaux du l'allumage ne différait pas des témoins. Pour contourner les contraintes de temps et de travail imposées par notre protocole de l'allumage optogénétique, nous avons utilisé des injections de rimonabant pour tester si la manipulation de CB1R pouvait accélérer les crises d'épilepsie optogénétique. Enfin, nous avons effectué des expériences de preuve de principe en utilisant la stimulation optogénétique de tranches fraîches de cerveau qui pourrait servir d'alternative à l'enregistrement en paires pour cartographier rapidement le circuit après des crises.

Dans l'ensemble, nos résultats démontrent que la manipulation spécifique du promoteur dans les populations de cellules excitatrices peut donner lieu à des crises, un modèle pour accélérer le développement des crises et des méthodes de cartographie des circuits pour disséquer les changements de circuit suite à des crises. Je prévois que mes résultats pourraient servir d'inspiration pour de futures études utilisant l'optogénétique et d'autres techniques modernes pour sonder les mécanismes potentiels du développement des crises et augmenter la probabilité de développer de nouvelles options de traitement.

List of figures

List of Abbreviations and Acronyms

AAV:	Adeno-associated virus
ASD:	Anti-seizure drug
AD:	Afterdischarge
ChR2:	Channelrhodopsin 2
NpHR:	Halorhodpsin
PV:	Parvalbumin
TLE:	Temporal lobe epilepsy
PDS:	Paroxysmal depolarizing shift
IS:	Interictal spikes
LTP:	Long-term potentiation
HFOs:	High frequency oscillations
mGluR:	Metabotropic glutamate receptors
LFP:	Local field potential
EEG:	Electroencephalography
SE:	Status epilepticus
PV:	Parvalbumin
AP:	Action potential
GFAP:	Glial fibrillary acidic protein

AMPARs: α-amino-3-hydroxy-5-methyl-4-isoxazolepropionic acid receptors

NMDARs: N-methyl-D-aspartate receptors

LTP: Long term potentiation

CamKIIα: Ca^{2+}/calmodulin-dependent protein kinase

CRACM: ChR2 assisted circuit mapping

IUE: In-utero electroporation

1 INTRODUCTION

1.1 Preamble to Chapter 1

In this chapter, a general introduction to the contents of this thesis is provided serving as a literature review of the field. It is composed of a brief introduction to epilepsy, animal models used to study it and the recent application of optogenetics to the study of seizures. Insights of how we can deepen our understanding of underlying circuit mechanisms and consequences of epileptogenesis using optogenetics are also discussed. Finally, I highlight what questions future models must take into account to effectively transform classical electrical induction models into optokindling models.

1.2 Epilepsy as a neurological disease

Epilepsy is widely recognized as a common neurological disorder affecting about 1% of the global population (Brodie et al., 2009; Engel and Pedley, 2008). It is defined as a chronic condition associated with at least one seizure and associated neurological, psychological as well as cognitive consequences (Fisher et al., 2014). A seizure is defined as a transient

occurrence of symptoms thought to result from aberrant neuronal activity in the brain (Kwan et al., 2011).

Seizures do not usually occur as single episodes. Instead, it is widely believed that once seizures arise, they are more likely to reoccur, giving rise to the idea of seizures begetting seizures (Ben-Ari et al., 2008). Once a seizure arises, it can and does terminate itself without any outside interference. However, if a seizure doesn't self-terminate, it leads into a state termed *status epilepticus (SE)* which is defined as any seizure lasting 5 minutes or longer (Brophy et al., 2012). SE is the 2nd most common neurological emergency carrying a major risk for morbidity and mortality (Rossetti and Lowenstein, 2011). SE that persists despite treatment with benzodiazepines and at least one anti-epileptic drug (AED) is termed refractory and occurs in ~30% of patients with SE. Refractory SE carries short-term fatality rates of 16 - 39% which is roughly three times higher than non-refractory SE (Rossetti and Lowenstein, 2011).

Seizures can originate in different brain areas and have varying symptoms associated with the area of initiation (Brodie et al., 2009; Kwan et al., 2011). Broadly, convulsive seizures are associated with body movements while non-convulsive seizures such as absence seizures are not. Epilepsy can also be crudely categorized into generalized or focal epilepsies, even though epilepsies that start as focal may eventually generalize (Engel, 2005). Furthermore, partial seizures which originate in a focal region of the cortex can be further divided into simple partial seizures, which do not impair consciousness, and complex partial seizures, which do. Both simple or complex partial seizures can spread to other cortical networks and may result in secondary generalized tonic-clonic seizures, which are characterized by widespread bilateral involvement of cortical regions and which are accompanied by convulsions and loss of consciousness (Chang and Lowenstein, 2003). Generalized seizures can be further classified as absence, tonic, or clonic depending on

impaired consciousness, stiffening of the extensor muscles, or rhythmic muscle contractions of the upper trunk, respectively (Brodie et al., 2009b). In contrast, simple partial seizures originating in motor cortex give rise to rhythmic movements of contralateral limbs whereas those arising from sensory cortices give rise to visual or auditory hallucinations.

Seizure types can also be divided into those that arise from genetic predispositions and those that are acquired. Genetic predispositions for developing seizures can arise as a result of channelopathies, which are each associated with specific seizure types and probabilities of having certain symptoms (Chang and Lowenstein, 2003; Glasscock et al., 2007). Other examples include mutations in transcriptional regulators such as JAK-STAT (Grabenstatter et al., 2014), proteins involved in cell growth such as mTOR (Way et al., 2012), or expansions in non-coding regions (Ishiura et al., 2018). On the other hand, acquired epilepsy can arise for many different reasons including: traumatic brain injury, infection, cancer, cerebrovascular disorder, autoimmune disorder, and developmental malformation (Berkovic et al., 2006).

Although traumatic brain injury gives rise to epilepsy in 5% of cases, typically a considerable period of time has to pass before the first seizures emerge (Herman, 2002). This latent period of epileptogenesis is thought to be due structural reorganization and network rewiring, although the details are poorly understood. For this reason, epileptogenesis is a central focus of animal studies in efforts to improve treatment outcomes (Chauvette et al., 2015).

Of the focal epilepsies, lateral temporal lobe epilepsy (TLE), in which seizures originate from the hippocampus and related structures, is the most common form and has been well studied (Chang and Lowenstein, 2003). Other forms of focal epilepsy that involve seizures which arise from different parts of the neocortex such as the frontal, sensorimotor, frontotemporal, parietal or posterior cortex have also been well studied given their high prevalence in humans (Manford et al., 1992). As an example, seizures arising from the motor

cortex are mainly simple focal motor seizures with symptoms depending on the side and spread of the area involved. Initially, they can involve clonic jerking of the affected muscle groups but as the seizure becomes generalized and seizure spreads from the initial focus, other parts of the body become involved in what is termed a Jacksonian march (Nathanson et al., 1978; Ohara et al., 2004).

Once epilepsy has been diagnosed, there are several options for treatment with two common avenues being surgical resection of diseased tissue and treatment with ASDs (Kwan et al., 2011). ASD treatment is typically prescribed but unfortunately 30% of patients do not respond to this type of treatment (Kwan et al., 2011). Furthermore, patients taking ASDs may suffer from a plethora of side effects, such as drowsiness, dizziness, blurred vision and tremor (Perucca and Gilliam, 2012). Factors that contribute to a poor prognosis include presence of multiple seizure types, presence of generalized tonic-clonic seizures, and high seizure frequency before treatment (Kwan and Brodie, 2000; Kwan et al., 2011). Limitations of ASDs in managing seizures may arise from problems that plague many drugs, such as failure of optimal dosage and reliance on drug serum concentrations in lieu of monitoring clinical symptoms (Kwan et al., 2011). The lack of treatment specificity, along with the high percentage of ASD non-responders who as a consequence suffer a lower quality of life, necessitates a more advanced understanding of the basic mechanisms of epileptogenesis. Importantly, treating seizures with ASDs does not generally undo the process of epileptogenesis, as evidenced by the seizure remittance and relapse rates (Shorvon and Goodridge, 2013). This is not surprising, since epileptogenesis presumably involves structural and morphological changes that are unlikely to be reversed by ASDs. ASDs work best in suppressing generation, propagation and severity of seizures themselves (Chen et al., 2018b). Essentially, we need to better elucidate how seizures initially arise in the healthy brain and establishing better animal models is the key to this.

1.3 Animal models of epilepsy

1.3.1 Acquired models of chronic epilepsy

As discussed, one of the central issues that belies effective treatment of intractable epilepsy is AEDs intended to prevent seizures may not be targeted to cure the underlying disease. Thus, a major thrust of epilepsy research has been to recapitulate seizures and their associated symptoms in animal models and study the progressions of disease over time. As a result, a variety of animal models have been developed to study the different aspects of seizures and epilepsy (**Figure 1.1**) (Löscher, 1999).

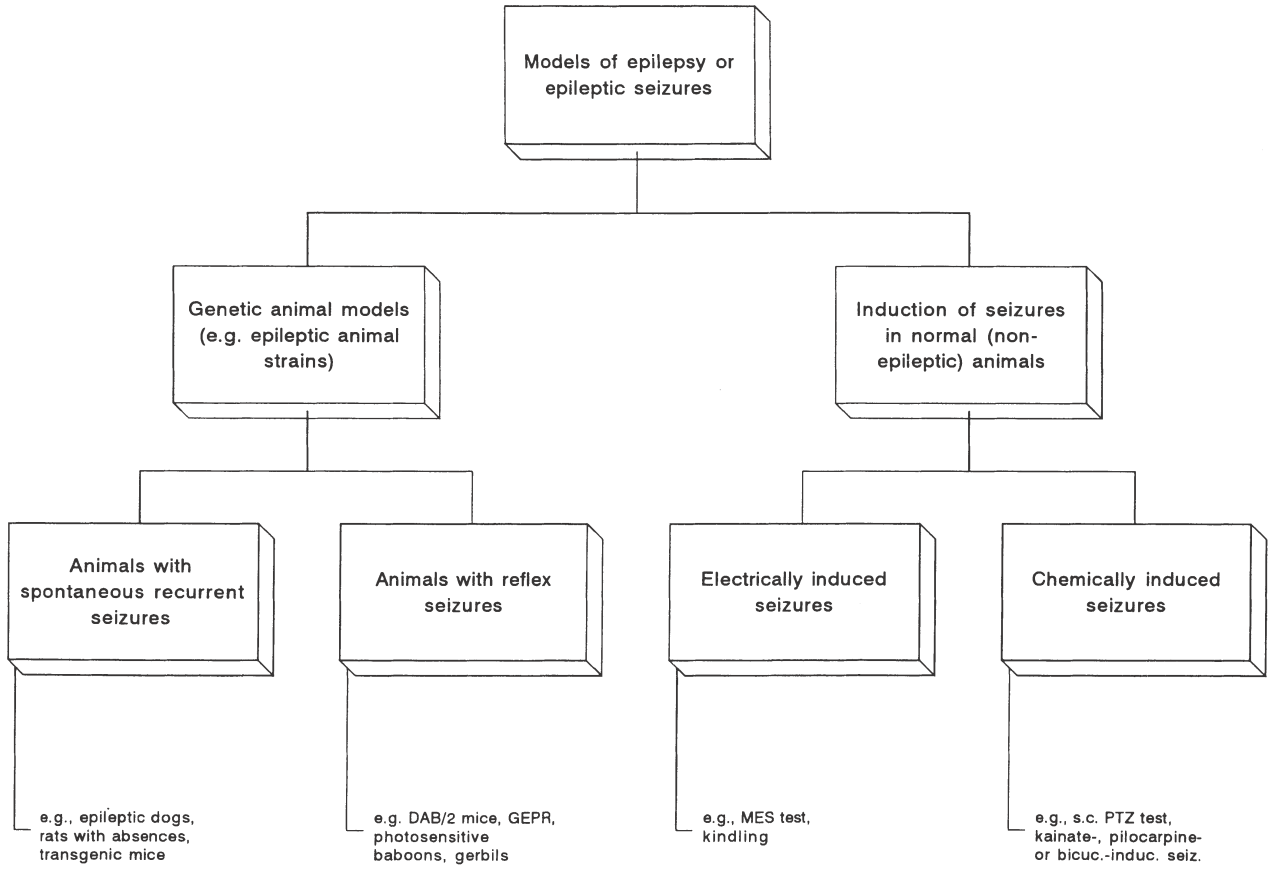

Figure 1.1 Overview of chronic animal models of epilepsy.

An outline of animal models of epilepsy divided into those with pre-existing conditions (genetic) or those in which seizure are elicited in initially healthy animals (induction) (Löscher, 1999).

Animal models of seizures can be split up into those with acquired epilepsy which include chemical and electrical induction as well as those of idiopathic/genetic origin (Löscher, 1999). Two enduring groups of models used to study chronic epilepsy are genetic and acquired, further subdivided into electrical or chemical induction (Löscher, 2002). Genetic animal models can involve animals with spontaneous or induced mutations resulting in recurrent seizures. For example, mutations in GluA4 AMPARs have been causally linked to absence seizures (Paz et al., 2011). On the other hand, acquired electrical models, such as kindling, rely on gradual development of seizures after repeated stimulation in initially healthy animals (Löscher, 2011a).

In chemical induction models, proconvulsants such as pentylenetrazol, kainic acid, or pilocarpine are injected into an animal to induce chronic seizures (Löscher, 2002). These chemicals act on receptors critically involved in synaptic transmission, thereby disturbing the excitatory-inhibitory balance and resulting in seizures (Fisher, 1989). On the other hand, 4-aminopyridine (4-AP) — another commonly used proconvulsant — acts mainly upon voltage-activated potassium channels, where it promotes elevated action potential firing due to faster recovery after inactivation (Storm, 1988), while kainic acid acts upon glutamate receptors (Olney et al., 1974). Several widely used convulsants carry out their action through antagonism of the GABA receptors (GABARs), thereby promoting excitability in the brain (Fisher, 1989). However, chemical kindling may also be elicited by agents such as cholinesterase agonists, opiates, local anaesthetics, neurotoxicants, as well as excitatory amino acids (Cain, 1983; Gilbert, 1992; Mori and Wada, 1989; Stripling and Ellinwood, 1977).

Administration of chemical convulsants can be intracerebral or systemic. Subthreshold doses of chemical convulsants can be combined with electrical stimulation as subconvulsive stimuli, or can be delivered alone repeatedly in a kindling paradigm (Cain, 1981). Finally, chemicals administered alone can cause *status epilepticus* if administered at high enough doses (Clark et al., 1992). For example, Clark (1992) found that higher doses of cocaine (65 mg/kg) were able to cause acute seizures whereas several subconvulsive doses (40 mg/kg) were required to eventually elicit seizures.

What advantages does chemical kindling present over other animal model of epilepsy? First, chemoconvulsants such as kainic acid preferentially target the hippocampus, even when administered systemically, mimicking temporal lobe epilepsy (TLE) in humans (Nadler et al., 1978). Secondly, chemical kindling results in structural changes that resemble those in partial seizures, as seen with pilocarpine injections (Cavalheiro et al., 1991). Thirdly, chemoconvulsants such as PTZ or strychnine can be used as acute seizure models to screen ASD action without necessarily resulting in chronic epilepsy (Löscher, 2011b).

There are also several drawbacks to using chemoconvulsants to study epilepsy. A main disadvantage is the lack of control over timing from chemoconvulsants injection to first seizure. Further, variability in drug metabolism and dissemination from injection site adds uncertainty to the timing of the response and this is hard to control for. Finally, systemic injection of drugs can have off-target effects with unintended consequences secondary to seizure initiation. For example, kainic acid, which acts upon kainate receptors, has been used to model TLE seizures but the receptor distribution is not limited to the limbic structures (Li et al., 2001).

1.3.2 The electrical kindling model of epilepsy

One model that has been particularly useful in furthering our understanding of chronic epilepsy has been the electrical kindling model of epilepsy (Goddard, 1967). In this model, healthy animals receive repeated electrical brain stimulation with what is initially a subconvulsive stimulus but becomes convulsive over time. The classic procedure involved delivering 50Hz rectangular pulse trains at low current intensity through bipolar microelectrodes at repeated intervals (Goddard et al., 1969). Inter-trial intervals of 24 hours or more were classically used to space kindling sessions, though later the minimum interval of 1-2 hours was used without increasing the number of stimulations required (Goddard et al., 1969; Racine et al., 1973). There is evidence that kindled seizures produce gradually dissipating inhibition which may restrict the inter-trial interval (Mucha and Pinel, 1977).

Repeated induction of focal seizures through kindling is highly reliable and initially expressed at the stimulated site. Stimulation efficacy was found to vary among stimulation sites with amygdala requiring the fewest stimulations and increasing in kindling difficulty: piriform cortex, entorhinal cortex, caudate putamen, hippocampus and neocortex (**Figure 1.2**) (Goddard et al., 1969). The brain region-specific differences in response to kindling are thought to arise in part from differential reactivity in stimulation sites themselves as well as the areas that they connect to (Sato et al., 1990). The amygdala, for example, has strong connections with motor areas and is able to generate interictal spikes early during kindling, indicating that epileptogenesis may be taking place (Hopkins and Holstege, 1978; Racine et al., 1988). Kindling efficacy can be further enhanced by bilateral instead of unilateral stimulation (Kogure et al., 2000).

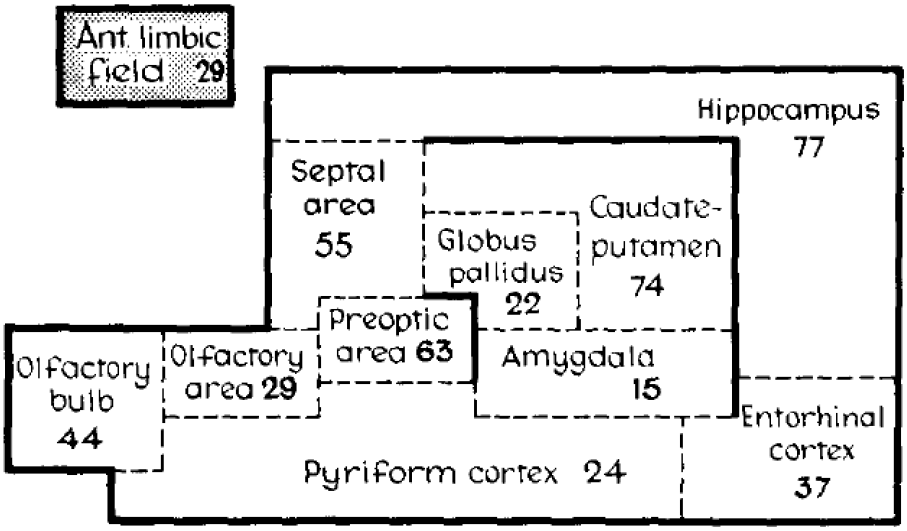

Figure 1.2 Different brain regions have variable responses to kindling.

Variability in brain area susceptibility to kindling. Numbers represent mean number of trials to first convulsion (Goddard et al., 1969).

The site of initial kindling also has an effect on subsequent secondary sites either contralateral to the initial site, or in related brain structures. For example, in amygdala kindling experiments it was found that the contralateral amygdala required fewer stimulations before stage 5 seizures occurred (Goddard et al., 1969). One explanation for this is that recurrent connections between the secondary and primary site become “sensitized” to repeated stimulation (Racine, 1978). Recruitment of secondary brain areas after unilateral kindling is not limited to contralateral areas. Often activity spreads from kindled primary areas to other brain structures. For example, audiogenic kindling involves brainstem sites during early stages but at later stages recruit secondary structures like amygdala and this latter activation is required for expression of the eventual clonic seizures (Feng et al., 2001; Sato et al., 1998). Interestingly, it is thought that regardless of kindled site, the piriform lobe is one of the first regions to show activation after the primary brain structure is kindled and

evidence suggests that this region may be even required for the eventual development of generalized seizures (Clark et al., 1991; Dragunow, 1988; Sato et al., 1998).

Further enhancement of kindling outcomes in terms of seizure development and efficacy can be achieved by performing bilateral instead of unilateral kindling of target brain structures. In limbic kindling experiments, bilateral hippocampal stimulation doubled the percentage of animals that successfully kindled (Kogure et al., 2000; Tsuchiya and Kogure, 2012). However, while bilateral stimulation can enhance kindling efficacy, kindling two different non-symmetrical brain sites can decrease efficacy of responders. This phenomenon of kindling antagonism was first demonstrated between the amygdala and the entorhinal cortex in rats and has progressively been shown in other brain regions (Duchowny and Burchfiel, 1981). It is thought that one site becomes dominant and suppresses the networks in the other site, a process that may be facilitated by noradrenergic systems (Applegate and Burchfiel, 1990).

Though initially defined in rodents, kindling has also been found to be effective in a variety of animal species (Goddard et al., 1969; Morimoto et al., 1993; Wada et al., 1975). The early behavioural responses of freezing in response to stimulation eventually progress to generalized seizures with bilateral clonic activity (Racine, 1972b). Correspondingly, the initial brief afterdischarge (AD) that follows stimulation becomes altered resulting in increased duration amplitude and frequency with a decreased seizure threshold (Racine, 1972b). Also, kindled animals retain a reduced threshold for seizures over months, which has been thought of as analogous to learning (Goddard et al., 1969) .

Initially, Goddard and colleagues stumbled upon the kindling model while they were studying learning and found that brain areas have different propensity for kindling with some areas being able to give rise to seizures much faster than others (Cain, 1982; Goddard, 1967).

This initial study has led to many others which have in unison found kindling to describe certain parts of seizure development well so that knowledge gleamed from this model can be more broadly applied to our understanding of seizure development. However, some parts of seizure emergence in human epilepsies cannot be adequately described by the kindling model such as lack of spontaneous seizures (Bertram, 2007).

The relevance of kindling to human epilepsy continues to be debated even though there are several similarities between kindling in animal models and the development of seizures in humans. First, the progressive changes in the brain brought about by repeated kindling mimic features observed in human epileptic brains and include increasing seizure susceptibility, gradually worsening memory, and alterations in inhibitory circuits (Sayin et al., 2003). In order to better understand the comorbidities of seizures in humans, researchers have studied the side effects of kindling in animals, in particular, those of hippocampal structures. They found that kindled rats develop long-lasting deficits in spatial memory impairments (Gilbert et al., 2000; Hannesson et al., 2001) associated with cumulative hippocampal sclerosis when probed through multiple assays (Kotloski et al., 2002). In parallel, long-term studies of patients with temporal-lobe seizures have noticed adverse consequences on cognitive functions such as IQ (Oyegbile et al., 2004). These memory and behavioural dysfunctions in kindled rats are probably caused by repeated hippocampal circuit reorganization leading to runaway pathological activity, a mechanism not unlike that in temporal lobe seizures in humans (Corcoran and Moshé, 2005). Another use of the kindling model closely tied with clinical outcomes is its utility as a tool for preclinical evaluation of AEDs. For example, AEDs developed for TLE such as phenytoin and carbamazepine which act on voltage-dependent Na^+ channels were found to elevate seizure thresholds in a limbic kindling model (Morimoto et al., 1997).

What advantages does electrical kindling present over other animal models of epilepsy? First, electrical kindling allows precise focal activation of specific brain sites through anatomical targeting with the stimulating electrode. Second, it allows for reliable development of chronic seizures, as well as readily manipulated ictal and postictal periods. Lastly, behavioural alterations during stimulations start focally and evolve into generalized seizures, mimicking partial to complex seizure evolution in humans (Sato et al., 1990).

However, there are also several limitations to electrical kindling models. For example, using electrical kindling to study chronic epilepsy can be labour and time-intensive. Kindling typically also fails to capture a critical feature of epilepsy — recurrent spontaneous seizures — unless the animal is "over-kindled" through a large number of sessions (Michael et al., 1998; Pinel and Rovner, 1978). Finally, kindling is associated with injury and inflammation, which has been linked to higher seizure rates, making the contribution of pathological activity hard to distinguish from that of injury (Cavazos et al., 1994; Pitkänen et al., 2009a).

To sum up, both electrical and chemical induction models reproduce many of the steps in seizure progression and related pathology underlying human epilepsies. However, because the cell population that is perturbed is unclear and because of the tissue trauma associated with the induction procedure, new approaches to study seizures are needed, e.g. using cell-specific targeting and activity manipulation. As we shall see below, optogenetics provides an indispensable tool here.

1.3.3 Cortical trauma-induced epilepsy models

It has long been recognized that traumatic brain injury (TBI) is a major risk factor for developing epilepsy (Annegers et al., 1998). Studies have revealed that TBI increases the rate of developing seizures in both early (within 24 hours of TBI) and as late as two years after

initial TBI (Haltiner et al., 1997; Temkin, 2003). Further, it is known that cortical trauma can lead to pathological activity in the majority of patients within 24 hours (Kollevold, 1976) and incidence of posttraumatic TBI is related to the initial severity of injury (Ferguson et al., 2010).

With this knowledge in mind, researchers have been able to produce trauma models which recapitulate some of the changes thought to occur during injuries that may lead to seizures. One common model that has been used for decades called the cortical undercut model is used to mimic the damage in the cortex and white matter that occurs in many brain-penetrating wounds (Prince and Tseng, 1993). In this model, it is thought that cortical damage produces deafferentiation that lead to increases in local excitability as the inhibitory constraints are reduced or removed which eventually produces seizures. The white matter underneath the cortex is intact so as to limit the cortical damage and study the consequences of partially isolating neocortex in epileptogenesis (Chauvette et al., 2016).

Other models used to study post-traumatic epilepsy depend on repeated injury to the brain in a controlled manner such as fluid percussion injury (Pitkänen et al., 2009b) and controlled cortical impact (Feeney et al., 1981). Both of these models can give rise to spontaneous seizures following injury though not as much is known about the underlying acute or chronic changes in excitability as those that occur in the undercut model (Pitkanen and McIntosh, 2006).

1.4 Novel genetic and optical approaches to epilepsy

1.4.1 Methods for light-driven perturbation of neuronal activity

The cellular basis of seizure formation continues to evade researchers, in part owing to the unknown populations that electrical kindling impinges upon. Therefore, a causal

understanding of epileptogenesis necessitates genetic identification and manipulation of activity in specific target neurons. Optogenetics can circumvent these drawbacks by allowing genetic tagging and manipulation of activity in specified neuronal populations (Zemelman et al., 2002). This technique allows light-driven activation or inactivation of neurons, by the expression of light-gated ion channels such as Channelrhodopsin-2 (ChR2) or pumps such as Halorhodopsin (NpHR), respectively (Boyden et al., 2005; Chow et al., 2010; Lima and Miesenböck, 2005; Nagel et al., 2002; Yizhar et al., 2011) (**Figure 1.4**). The rhodopsin later termed ChR2 was discovered in the algae *Chlamydomonas reinhardtii*, where it generates photocurrents contributing to phototaxis (Harz and Hegemann, 1991). Aside from NpHR, another widely used inhibitory opsin is Archaerhodopsin (Arch) which inhibits neuronal activity through influx of H^+ compared to NpHR's extrusion of Cl^- ions (Chow et al., 2010; Nagel et al., 2002; Zhang et al., 2007).

Along with the first developed opsins used to activate and inhibit neurons, other variants include but are not limited to: G-protein-coupled receptors (opto-XRs) (Airan et al., 2009), vSWO/vLWO (Masseck et al., 2014), chloride channels (iC1C2, SwiChR) (Berndt et al., 2014) and chloride channel variants (JAWS) (Chuong et al., 2014), as well as sodium pumps (Inoue et al., 2013). Another approach has been to create a light-gated version of the ionotropic glutamate receptor (iGluR), which shares the advantage of millisecond manipulation of neuronal activity with optogenetics (Volgraf et al., 2006). Finally, reactive oxygen species can be used to inhibit neurotransmission after coupling to a light absorption by light-oxygen voltage domain (Shu et al., 2011). In summary, light-activated proteins open up novel approaches to studying epilepsy by permitting control of genetically defined neuronal populations, typically with millisecond precision.

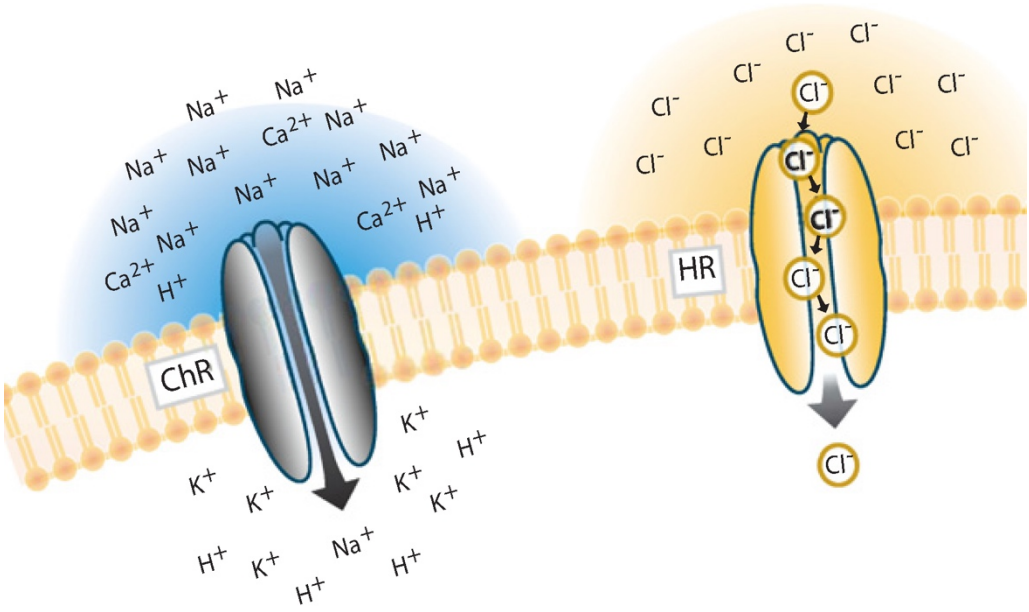

Figure 1.3 Optogenetic tools for activating (ChR) and silencing (HR) neurons

Channelrhodopsin (left) activates neurons through influx of non-specific cations (Na^+, Ca^{2+}, H^+) while Halorhodopsin (right) deactivates neurons through influx of Cl^- ions

Modified from Yizhar et al. (2011)

1.4.2 Genetic targeting of opsins

One key advantage of optogenetics is modulation of activity in specific neurons, but how can opsins be targeted to different neuronal populations? First, opsins can be delivered using adeno-associated virus (AAV) or lentivirus containing a promoter targeting the cells of interest (Dittgen et al., 2004; Ponnazhagan et al., 1997). Furthermore, the serotype of the AAV itself can confer a degree of selectivity though specific tropism (Burger et al., 2004). Secondly, opsins can be expressed in transgenic animals using a combination of the Cre/loxP (Sauer, 1987) and/or Flp/Frt systems (Buchholz et al., 1998), which can add even more specificity through selective promoters (Fitzsimons et al., 2002). Finally, specific cell

populations can be targeted using monosynaptic and/or transsynaptic tracing techniques. Retrograde tracing can be done using rabies virus (Chatterjee et al., 2018; Rancz et al., 2011) or wheat germ agglutinin (Libbrecht et al., 2017) in combination with Cre-dependent ChR2 expression (Gradinaru et al., 2010). Anterograde tracing can be done using Herpes simplex virus (Lo and Anderson, 2011) or certain AAV serotypes (Zingg et al., 2017). These techniques can also be combined to improve spatial and/or temporal selectivity, by employing intersectional targeting strategies. For example, Cre or Flp can be fused to an estrogen receptor (ER) ligand-binding domain (LBD) that is only sensitive to synthetic 4-hydroxytamoxifen (4-OHT). Upon 4-OHT administration, the ER-LBD translocated to the nucleus where it can mediate recombination (Dymecki and Kim, 2007; Sjulson et al., 2016). Thus, recombination can be temporally regulated by 4-OHT injection.

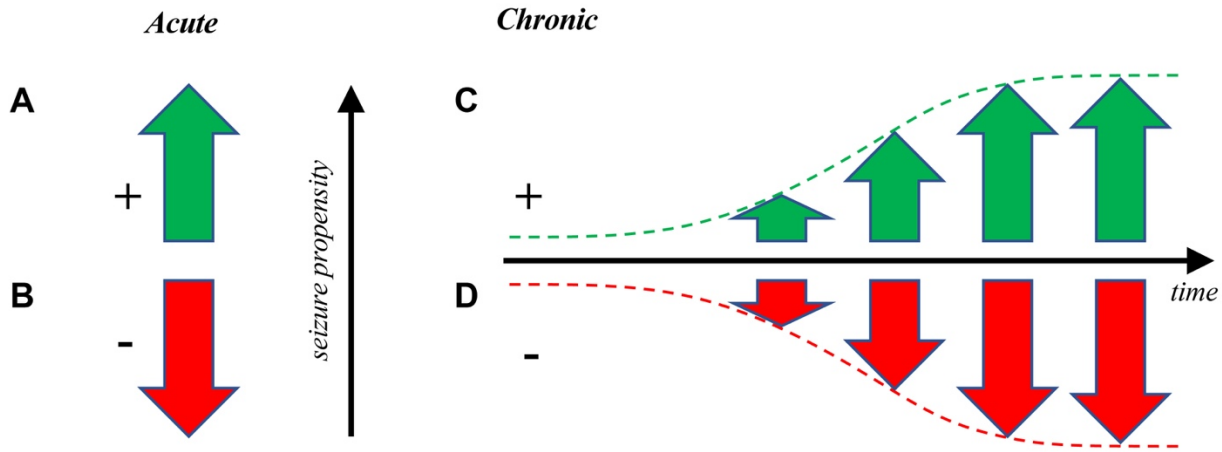

Figure 1.4 Optogenetic manipulation of seizure propensity

(**A**) Optogenetics can be used to drive seizures acutely (Khoshkhoo et al., 2017) or to (**B**) put a brake on already active seizures (Krook-Magnuson et al., 2013; Wykes et al., 2012a) as a form of pro- or anti-convulsant, respectively. This latter approach has potential clinical applications for interrupting ongoing seizures (Paz et al., 2013), whereas both are useful for studying epilepsy.

(**C**) Seizures can also be gradually elicited over time via optogenetic kindling, or optokindling (Cela et al., 2019). Optokindling is fundamentally distinct from directly driving seizures by optogenetic stimulation, since optokindling requires long-lasting changes of neuronal circuits (Cela et al., 2019), whereas direct optogenetic drive does not (Khoshkhoo et al., 2017).

(**D**) It may also be possible to gradually decrease seizure propensity via optogenetic dekindling. As far as we know, this remains to be experimentally demonstrated optogenetically, but such findings have been reported with electrical stimulation (Bains et al., 1999; Ozen and Teskey, 2009). The kindling and dekindling modes may both enable the study of epileptogenesis, e.g. to test therapies that slow down or reverse the development of seizures.

1.4.3 Putting a brake on seizures with optogenetics

Optogenetics has found multiple uses in neuroscience, including studying epilepsy where it has been used to both halt and initiate seizures (**Table 1.1**) (Cela et al., 2019; Paz et al., 2013). The majority of studies attempting to optogenetically abate seizures have used classical animal models to induce epilepsy (Wang et al., 2017; Wykes et al., 2012a).

Interneurons (INs) play a central role in many types of epilepsy and different populations of INs have been critically linked to both the initial seizure activity (Khoshkhoo et al., 2017) and eventual generalization of seizures (Wang et al., 2017). In a handful of pioneering studies, it was shown that spontaneous seizures in a TLE induction model can be controlled by either stimulation of GABAergic cells or direct optogenetic inhibition of PCs in the hippocampus (Krook-Magnuson et al., 2013; Ladas et al., 2015; Lu et al., 2016). Inhibiting excitatory PCs using NpHR to stop or alleviate seizures has also been shown in hippocampus

(Berglind et al., 2014; Krook-Magnuson et al., 2015; Sukhotinsky et al., 2013; Tonnesen et al., 2009). Finally, it was found that stroke-induced seizures can be stopped using optogenetic inhibition of thalamocortical neurons via NpHR (Paz et al., 2013).

However, inhibition is not always local. For example, it has been shown that TLE seizures can be inhibited by optogenetically stimulating the cerebellum (Krook-Magnuson et al., 2014). TLE seizure generalization is modulated differently by mossy and granule cells and these seizures are correlated with decreased spatial discrimination performance, mirroring similar deficits in human epilepsies (Bui et al., 2018). In another study, researchers used inhibitory opsins to suppress PC activity and abort seizures in a tetanus-toxin-induced model of neocortical epilepsy (Wykes et al., 2012a). High-frequency light stimulation was both shown to inhibit 4-AP-induced seizures *in-vivo* and *in-vitro* (Chiang et al., 2014). Finally, seizure suppression has also been achieved in dorsal raphe and superior colliculus, highlighting the utility of optogenetics across several brain areas (Soper et al., 2016; Zhang et al., 2018a).

Optogenetics has also been used to modulate seizures arising in genetic models where animals have a predilection to developing seizures. In absence epilepsy models, both activation of tonic spiking in thalamus and optogenetic stimulation of cerebellar neurons abated seizures *in vivo* (Kros et al., 2015; Sorokin et al., 2017). Taken together, these studies highlight different ways optogenetics can be used for seizure cessation, to potentially enable therapeutic treatments.

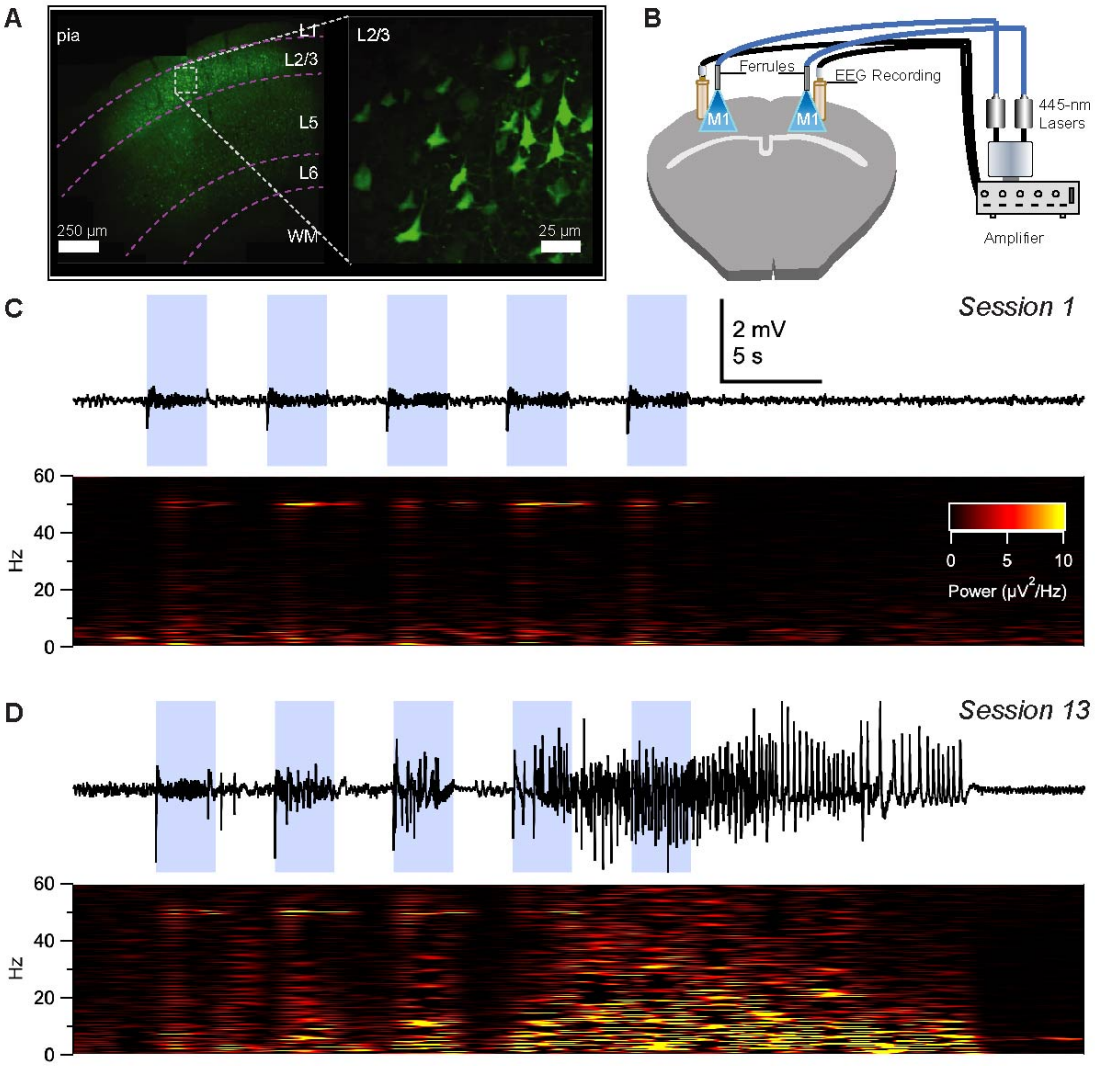

Figure 1.5 Optokindling leads to gradual seizure development over time

(A) Coronal M1 section immunostained for EYFP indicated ChR2 expression in layer 2/3 (L2/3), 5, and 6, though predominantly in L2/3. Inset shows close-up of L2/3 ChR2-expressing PCs.

(B) To simultaneously activate ChR2 and acquire EEG, ferrules and recording screws were implanted bilaterally above M1, without penetrating the cortex. Fiber optic cables were air-coupled to 445-nm lasers. EEG signals were processed by an extracellular amplifier, but not pre-amplified. A computer (not shown) TTL-gated the lasers and digitized amplified EEG signals.

(C) In each stimulation session, M1 was kindled with 15 bouts of 3-second-long 50-Hz bursts of 5-ms 445-nm laser pulses, divided into three sweeps delivered once a minute. Sessions were repeated at least 25 times every two days. The first session shows EEG responses to light stimulation but no seizure (Top). Spectrogram shows directly light-driven response in 50-Hz band but no seizures (Bottom).

(**D)** The EEG recording at session 13 shows a prominent seizure (Top). Spectrogram reveals both light-driven response in 50-Hz band as well as increased power in low-frequency bands (Bottom).

Reproduced with permission after Figure 1 from Cela et al. (2019)

1.4.4 Promoting seizures with optogenetics

Optogenetics has also been used to study the initiation of seizures and contributions of different cell types to seizure activity. Several studies have been able to induce seizures using only light stimulation. For example, stimulation of ChR2-expressing cells in the hippocampus led to seizure-like events (Osawa et al., 2013). Optogenetic stimulation of hippocampal PCs can also give rise to progressively intense seizures (Berglind et al., 2018). High-frequency optogenetic stimulation of PCs in dorsal or intermediate hippocampus give rise to different behaviours such as face twitching or clonus providing an explanation for the heterogeneity of seizure types seen in patients with hippocampal pathology (Weitz et al., 2015). Another study found kindling-like effects after optogenetic stimulation of dentate gyrus, in the form of increased in duration and severity of seizure responses (Krook-Magnuson et al., 2015).

PCs are not the only neurons participating in seizure activity, INs have been also implicated on different aspects of seizure formation. For example, activation of PV INs can induce seizures during the inter-ictal period but inhibit them during the ictal period (Assaf and

Schiller, 2016). Further, optogenetic induction of seizures in neocortex revealed different roles of distinct IN populations with VIP inhibition increasing seizure threshold and somatostatin (SOM) and parvalbumin (PV) prolonging seizures during ictal activity (Khoshkhoo et al., 2017). Indeed, INs may play a role in the transition to ictal events through rebound excitation (Chang et al., 2018). Thus, seizure onset is not determined solely by PCs; it is increasingly recognized that certain IN populations such as VIP play a key role (Khoshkhoo et al., 2017).

Promoting seizures with optogenetics does not have to rely on light stimulation alone. Indeed, several studies took advantage of the established electrical kindling protocol and used it in parallel with light stimulation to investigate epileptogenesis (Berglind et al., 2018; Wang et al., 2017). Using light stimulation alone eliminates the amount of damage caused by the stimulating electrode during electrical kindling and allows optogenetic targeting of diverse cell populations to study the breadth of epilepsies occurring.

While optogenetic stimulation alone has been proven sufficient in several cases (Cela et al., 2019; Khoshkhoo et al., 2017; Osawa et al., 2013) many studies use a genetic model or chemical proconvulsants in conjunction with optogenetics. For example, light stimulation of somatosensory cortex of mice with genetic mutations increasing susceptibility to absence epilepsy also initiates seizure events (Wagner et al., 2015). In addition, electrical kindling can be combined with optogenetic stimulation to give rise to progressively worsening generalized seizures (Wang et al., 2017). Another study exploring the graded development of seizures in hippocampus following repeated light stimulation found progressively worsening and eventual spread of seizure activity (Berglind et al., 2018). These studies showed that optogenetic stimulation is sufficient to induce seizures, but more work remains to be done using long-term stimulation as well as monitoring additional seizure properties in awake behaving animals.

Furthermore, several recent studies using optogenetics to investigate the contribution of different neuronal population to seizures have reported conflicting results. In CA3 for example, optogenetic activation of PV INs led to excitatory GABA transmission and a boost of seizure activity (Ellender et al., 2014). In apparent contradiction, activation of GABA INs in the subiculum delayed generalized seizures after TLE (Wang et al., 2017). In addition, optogenetic PV IN activation leads to ictal discharges *in-vitro* (Shiri et al., 2015) as well as during 4-AP application (Yekhlef et al., 2015). However, a previous study using ChR2 to activate PV cells near the seizure focus led to cessation of seizures (Sessolo et al., 2015). These conflicting results relied on optogenetics to highlight the complexity of IN contribution to seizure dynamics and underscore the need for further study. Future studies would benefit from looking at other IN types such as VIP and SOM to investigate the relative contribution of different IN populations to seizure formation.

1.4.5 Optogenetic kindling models of epilepsy

Table 1.1 Optogenetic epilepsy studies

Studies to date using optogenetics either to interrupt ("Brake"), promote seizures ("Drive") or kindle ("Kindle"). DG denotes the Dentate gyrus, CA1 *Cornu Ammonis* subfield 1, CA3 *Cornu Ammonis* subfield 3, LCN lateral cerebellar nuclei, and MCN medial cerebellar nuclei.

Reference	**Brake**	**Drive**	**Kindle**	**Area**	
Cela et al. (2019)			✔	Motor	Cortex
Khoshkhoo et al. (2017)		✔		Motor	

Wykes et al. (2012a)	✔			Motor	
Assaf and Schiller (2016)	✔	✔		Somatosensory	
Chang et al. (2018)		✔		Somatosensory	
Berglind et al. (2014)	✔			CA3	Hippocampus
Berglind et al. (2018)	✔			CA3	
Bui et al. (2018)	✔			Dentate gyrus	
Chen et al. (2018a)	✔			CA1+ DG	
Chiang et al. (2014)	✔			CA3	
Krook-Magnuson et al. (2013)	✔			CA1	
Krook-Magnuson et al. (2015)	✔	✔		Dentate gyrus	
Ladas et al. (2015)	✔			Dentate gyrus	
Lu et al. (2016)	✔			Dentate gyrus	
Osawa et al. (2013)		✔		CA3+DG	
Sessolo et al. (2015)		✔		Temporal cortex	

Shiri et al. (2015)		✔		Entorhinal cortex	
Tonnesen et al. (2009)	✔			Hippocampus	
Wang et al. (2017)	✔			Subiculum	
Weitz et al. (2015)		✔		Hippocampus	
Yekhlef et al. (2015)	✔			Entorhinal cortex	
Krook-Magnuson et al. (2014)	✔			Lateral	Cerebellum
Kros et al. (2015)	✔			LCN and MCN	
Soper et al. (2016)	✔			Superior colliculus	Midbrain
Paz et al. (2013)		✔		Ventrobasal	Thalamus
Sorokin et al. (2017)	✔	✔		Ventrobasal	

Multiple studies have shown that seizures can be acutely elicited with optogenetics (**Table 1.1**). In light of this, is there a place for using optokindling? We argue that there are several key advantages. Because optokindling allows graded development, increased severity of electrographic and behavioral seizures over time, as well as long-term susceptibility of seizure properties akin to long-term memory (**Table 1.2**) (Goddard, 1967; Teskey, 2001a), it is possible

to use optokindling to study aspects of epileptogenesis rather than simply studying directly driven seizures. These features make kindling a reliable animal model for the study of the transition to seizures from a healthy brain over the long term (Sato et al., 1990).

Additionally, kindling can be combined with a second factor in a two-hit model of seizures to examine synergistic effects (Berkovic et al., 2006). For example, the two-hit model can be used to study how early-life seizures impinge on seizure propensity later in life (Koh et al., 2001).

With these advantages in mind, we recently developed an optokindling model (**Figure 1.5**) in neocortex that replicated several hallmark features of electrical kindling such as gradual seizure development as well as long-term seizure retention (**Table 1.2**) (Cela et al., 2019). With optokindling, we were able to induce seizures whilst avoiding tissue damage, which might otherwise confound interpretation of results (Pitkänen et al., 2009a). We found that optokindling can mimic the gradual development of seizures in epileptogenesis (Morrell, 1985).

Going forward, in order to effectively develop optogenetic variants to classical kindling, classical changes accompanying kindling must be measured such as long-term retention of seizure susceptibility, worsening electrographic and behavioral seizures, as well as changes in seizure threshold and possible propagation of seizures (**Table 1.2**) (Goddard et al., 1969; Teskey, 2001a). These variables are critical to differentiate optokindling models from direct optogenetic drive of seizures (see also **Table 1.1**).

Furthermore, optogenetics also opens up new avenues of examining dekindling, or the gradual decrease in seizure propensity, i.e. the opposite of epileptogenesis (**Figure 1.4**) (Morrell, 1960; Salanova et al., 1996). With optogenetics, it may be possible to reverse the synaptic changes occurring during epileptogenesis. Future studies also need to examine other

brain areas aside from neocortex to ensure that the optokindling effect can be replicated elsewhere in the brain as was done with electrical kindling (Cela et al., 2019; Goddard et al., 1969).

Table 1.2 Criteria for kindling

Key properties of kindling, as outlined by Teskey (2001a).

	Metric	**Description**
1	Electrogenic seizure severity	Kindling causes an increase in duration, amplitude, frequency, and complexity of seizures.
2	Behavioral seizure severity	Behavioral seizures appear and increase in severity.
3	Seizure threshold	Seizure threshold is reduced, so that initially inert stimulation may eventually elicit seizures.
4	Seizure propagation	Seizure eventually propagates from stimulation site to distant brain regions.

1.4.6 Future directions in optogenetic applications to seizures

Over several decades, the field of epilepsy has benefited from multiple animal models of epilepsy, as described above. More recently, optogenetics has been used to study epilepsy with the goal of linking circuit properties to seizures in defined neuronal populations. Here, we have discussed how optogenetics was used to both activate and inactivate target cells leading to either prolonging or reducing seizure duration in several different brain regions (**Table 1.1**).

However, several issues remain before optogenetics will likely gain widespread use in epilepsy research. First the virus injection and ferrule implantation procedure that is required for optogenetic activation is time consuming and labour intensive. This has already begun to be addressed by near infrared (IR) versions of ChR2 which do not need ferrule implants for light delivery and can instead be activated transcranially (Lin et al., 2013). These IR variants also reduce the possibility of heat-induced light damage from prolonged stimulation (Christie et al., 2013; Hososhima et al., 2015). Secondly, the EEG recording, which also requires time-consuming implantation procedures, can be replaced by all-optical interrogation of neural circuits using genetically encoded sensors for readout and optogenetic actuators for control of cellular activity (Emiliani et al., 2015). Thirdly, the advantage of optogenetics in targeting different neuronal populations is restricted by the specificity of factors such as promoters and viral serotype.

As the genetic toolkit for exogenous protein expression continues to expand (Sjulson et al., 2016), it will allow for the activity of neural circuits contributing to seizure formation to be recorded and manipulated by light, which in turn will enable the development of novel epilepsy models with improved spatiotemporal precision (Zhang et al., 2018b). This will likely be particularly useful in closed-loop systems where real-time adjustment can be made based on behaviour or ongoing brain activity, e.g. at the start of seizures to shut them down.

Optokindling is a particular subset of this genetic toolkit — studies such as ours (Cela et al., 2019) will improve our understanding of circuit changes in epileptogenesis rather than of acute seizure induction. This is important since long-term seizure development may closely mimic certain aspects of human epilepsies that involve circuit alterations while acute seizures models may be more useful to study circuits and seizure properties as such (Lillis et al., 2015; Sutula, 2004).

Optogenetics is not the only genetic neuronal activation system useful for the study of epilepsy. Another system that has been used is pharmacogenetics using designer receptors exclusively activated by designer drugs (DREADDS). DREADDS are G-coupled receptors and can be used to inhibit (hMD4i receptor) or excite (hM3Dq receptor) cells (Pei et al., 2008) upon addition of the drug clozapine N-oxide (CNO). DREADDS have been used to both halt and initiate seizure development, e.g. seizure suppression in organotypic hippocampal slice cultures (Avaliani et al., 2016), seizure blockade in amygdala-kindled mice (Wicker and Forcelli, 2016), as well as silencing of pilocarpine-induced seizures *in-vivo* (Katzel et al., 2014).

A recent study has highlighted the possibility of using optogenetics along with pharmacogenetics to induce seizures with the former while abating their activity with the latter (Berglind et al., 2018). DREADDs can be used to chronically inhibit or promote activity in genetically defined neurons similar to optogenetics but while DREADDS can serve some of the main properties of optogenetics in studying seizures, they have significant disadvantages. First, DREADDS have reduced temporal specificity compared to optogenetics. Chronic manipulation of activity levels imposed by DREADDS lack the millisecond-scale precision mimicking synaptic transmission afforded by optogenetics. Second, the supposedly otherwise inert agonist (CNO) can in fact be metabolized back to clozapine and have off-target effects such as lowered seizure threshold, which could of course cloud the interpretation in epilepsy studies (Manvich et al., 2018; Sajatovic and Meltzer, 1996). Optogenetics may thus prove to be a better method of activity manipulation in epilepsy studies.

In conjunction with genetic methods for manipulating neuronal activity, the roles of injury and inflammation can be explored using the two-hit model (Berkovic et al., 2006). Optical induction models such as optokindling have a narrower focus on activity-dependent plasticity, since — compared to their electric or chemical counterparts — they result in

relatively little tissue damage or inflammation (Cela et al., 2019). It may in fact be possible to optokindled transgenic mice without the need for viral injection or surgery (Cela et al., 2019), thus bypassing injury and inflammation completely. This may make them especially useful for discovering novel therapies, to halt or slow down pathological plasticity in epileptogenesis.

The application of optogenetic intervention in human epilepsies has been delayed because several hurdles need to be overcome. For example, there are health concerns associated with using viral vectors for gene delivery. Furthermore, the human brain is much larger than that of rodents, which means much more powerful light sources are required to access deep brain structures (Couzin and Kaiser, 2005; Delbeke et al., 2017). Furthermore, optogenetic seizure interruption requires highly accurate real-time seizure detection, which is still a largely unsolved issue (Dheer et al., 2017).

Although it remains unknown what precisely the future holds in store, what should be clear from this review is that optogenetics is here to stay as a key tool to control activity in primary epilepsy research as well as in future treatments. Recent optogenetic studies have already revealed e.g. the differential IN population role in seizure initiation as well as different ways of halting seizures depending on the brain area (Ellender et al., 2014; Khoshkhoo et al., 2017; Paz et al., 2013). With optogenetics, more circuit components underlying seizures will be dissected and novel therapeutic interventions will be discovered.

1.5 Mechanisms and consequences of epileptogenesis

1.5.1 General mechanisms of seizure generation

Epileptogenesis, or the process by which the brain become epileptic, is a critical but not well understood part of the epilepsy literature. One difficulty arises from the fact that many single processes which are thought to be important may work in synergy and it is not entirely clear

how this can happen. It is known for example that the development of seizures is accompanied by changes at the cellular level such as neuronal loss, gliosis and mossy fibre sprouting (Houser, 1999; Sutula et al., 1992). Other changes that accompany seizures are electrographic in nature instead of anatomical and will be discussed further below.

Under normal non-pathological circumstances, the brain maintains a balance between the excitatory and inhibitory tone. Consequently, ictal events are believed to be the result of the shift in balance between excitation and inhibition and this imbalance can be reached in several ways (Chang and Lowenstein, 2003; Galarreta and Hestrin, 1998; Nelson and Turrigiano, 1998). For example, an overall reduction of excitation is a major factor accompanying lesion-dependent epilepsy (Timofeev et al., 2014). Since 80% of the neurons in neocortex are excitatory, damage done during a focal lesion are largely responsible for impinging on the excitatory network (Gabbott and Somogyi, 1986).

To better understand what roles excitation and inhibition play during seizure development, investigators have conducted experiments which are focused on different. properties of neurons and types of cell populations that may be impinged upon during seizures. One of these properties has been intrinsic excitability and factors which have been investigated in epileptic animals include resting membrane potential, input resistance, and membrane time constant (Mody and Staley, 1994). There has been considerable controversy with these findings with many studies comparing control and epileptic tissues to find no differences in intrinsic properties (Avoli and Olivier, 1989; Prince and Wong, 1981). On the other hand, some studies have shown these differences exist and confirmed the hypothesis that passive membrane properties change in chronically epileptic tissue (Franck et al., 1988; Mody et al., 1988; Prince and Tseng, 1993). This discrepancy may be explained at least in part by the fact that most recording studies examine only “epileptic” principal neurons. However, since the animal models used cannot distinguish between PCs that are affected, the

variability in cell choice affects the measurement outcome. Furthermore, other mechanisms that increase intrinsic excitability such as low Ca^{2+} conditions or those that impinge on overall synaptic transmission such as blocking K^{+} channels can also produce ictal events (Deisz, 2009). Further studies with more refined techniques comparing affected and non-affected neurons may be necessary to resolve this controversy.

1.5.2 Morphological changes associated with epilepsy

In addition to synaptic level changes and ionic composition, local circuit arrangement can contribute to the development and progression of seizures. In the hippocampus for example, the recurrent excitatory connectivity is conducive to synaptic synchronization and spread of seizures. CA3 PCs can fire bursts of action potentials and recruit the right number of neurons to lead to ictal events (Traub, 1982). According to the Hebbian postulate, if repeated seizures cause a brain to become more strongly interconnected through repeated co-activation of neurons, as is hypothesized to occur in many types of epilepsy, then an increase in the presence of efficacious synapses is one of the consequences of this prediction (Hebb, 1950). Indeed, with repeated synchronized activity, these pathways can strengthen their connections and sprout new ones as the brain advances from a healthy to a diseased state (Chen et al 2013).

Morphological changes accompanying epilepsy have been heavily studied in TLE models of epilepsy. The prediction of Goddard, in which he hypothesized that kindling might induce structural changes within neurons, were first supported by the findings of mossy fibre sprouting in the dentate gyrus following repeated seizures (Cavazos et al., 1991; Goddard, 1967; Represa et al., 1989). Mossy fibre sprouting is also seen in humans with temporal lobe

epilepsy and is thought to arise from repeated seizures as well (Sutula et al., 1988). Recurrent excitation has been implicated for this mechanism since experiments *in vitro* have shown that recurrent excitation emerges when inhibition is reduced or changes in the extracellular milieu occur (Lynch and Sutula, 2000; Wuarin and Dudek, 1996). Seizure-induced recurrent excitatory circuits may be necessary to allow propagation of seizures that would otherwise be inhibited, thereby contributing to the progression of epilepsy.

In addition, hippocampal kindling is thought to lead to an overall decrease in the number of synapses and it may lead to a shift toward the higher efficacy perforated over non-perforated synapse which may account for some of the increases in electrophysiological responses following kindling (Geinisman et al., 1988a,1992). Following neocortical kindling, aside from similar changes as those observed in hippocampal kindling, there is a transient increase in dendritic length and branches two days after which transitions into a decrease three weeks later (Teskey et al., 2006). In addition, there is an increase in synapse density of layer V local connections in kindled animals compared to controls (Teskey et al., 2006). Finally, neocortical kindling is accompanied by a decrease of neuronal density, up to 30% following several weeks of kindling (Teskey et al., 2006) .

The consequences on the brain from repeated seizures are not limited to morphological changes visible in different cell types. Gross neuronal changes like apoptosis and necrosis can also accompany seizures. Neuronal death in animal models of kindling can be observed from the first seizure onset and additional repeated seizures can cause widespread apoptosis as seen in hippocampal structures and neocortex, which mimics classical human sclerosis of the hippocampus (Cavazos et al., 1994; Kotloski et al., 2002). As mentioned previously, kindling-induced seizures can cause significant reductions in neuronal numbers and this result has been replicated in several studies using electrical induction of seizures (Cavazos and Sutula, 1990; Kotloski et al., 2002; Sloviter et al., 1996). The

molecular mechanisms underlying seizure-induced apoptosis are not fully elucidated but are thought to involve glutamate-mediated excitotoxicity resulting in intracellular calcium overload and eventual apoptosis (Meldrum, 1993,2000).

1.5.3 Inhibitory circuits and their role in seizure formation

While neuronal network activity and synchronization across brain areas are a part of normal brain operation, aberrant pathological firing may depend on similar mechanisms, at least initially, to get the brain in a synchronous state. For example, INs such as those belonging to the PV family are thought to play a critical role in synchronizing PC firing (Cobb et al., 1995). However, pharmacological manipulations that block GABAergic inhibition such as bicuculine or picrotoxin do not just block synchronization between PCs, they have the capability to produce ictal and interictal events (Avoli, 1996; Stanton et al., 1987). Furthermore, even though focal lesions may impinge heavily on the excitatory networks which eventually lead to seizures, some INs are thought to be more sensitive to pathological activity following local cortical lesions (Avramescu et al., 2009).

The kindling model of epilepsy also shows several changes associated with seizure onset and generalization linked to INs. A reduction in IN number has been observed during kindling-induced seizures, specifically cholecystokinin and GABA transporter 1-positive INs (Sayin et al., 2003). It is particularly interesting that these two classes are affected since they provide mainly axo-somatic and axo-axonic inhibition that directly affects AP propagation in the axon hillock (Freund and Buzsaki, 1996). Following these changes are decreases in the evoked inhibitory postsynaptic currents and overall reduction in inhibition (Sayin et al., 2003). PV neurons are also reduced in human epileptic hippocampi examined post-mortem

(During et al., 1995; Zhu et al., 1997) and their role as generators of the gamma rhythm has become increasingly evident in recent times (Sohal et al., 2009).

Many studies have furthered our understanding of the consequences of inhibitory circuit changes following seizures by studying the hippocampal circuitry in animals and humans. In the hippocampus, a disconnection of inhibitory INs may occur in the CA1 region after electrically-induced seizures (Mangan et al., 1995). In the same circuit, presynaptically, the mossy fibres of granule cells appear to express a GABA-synthesizing enzyme after seizures (Schwarzer and Sperk, 1995). Further experiments in human epileptic tissue have demonstrated impairments in GABA transporter function in the hippocampus suggesting that these transporters may dampen excitation under normal conditions but have a diminished role in epileptic tissue (During et al., 1995). Investigators have further posited that the normally inhibitory $GABA_A$ receptor may mediate excitatory transmission during seizures in response to increased activity levels (Staley et al., 1995).

1.5.4 Excitatory circuits and their role in seizure formation

Early studies suggested that epilepsy, similar to learning, might involve similar cellular and molecular mechanisms. For example, synaptic and circuit alterations in kindling also required protein synthesis and if this process was blocked with inhibitors, secondary epileptogenesis was also blocked (Morrell et al., 1975). Later studies showed that giving the protein synthesis inhibitor anisomycin 15 minutes before high frequency stimulation to amygdala could block potential kindling that would otherwise occur (Cain et al., 1980). In fact, evidence for what is considered the modern candidate for memory, long-term potentiation (LTP) began to be derived from studies on mirror foci and kindling, happening during the time LTP was discovered. The similarities between kindling and LTP do not end there. It is well established

that once a primary epileptogenic focus is active, it will provide high-frequency efferent outflow to its targets (Wilder et al., 1968). While high frequency electrical stimulation can induce LTP, increases in afferent activity after induced seizure foci can also induce LTP (McNamara, 1994; Teyler and DiScenna, 1987). Finally, recent evidence has emerged showing that kindling can occlude potential LTP in slices even after kindling has been terminated (Esmaeilpour et al., 2017).

The emergence of seizures is associated with many changes in receptors that are critical for excitatory neurotransmission in the brain. For example, repeated kindling induces an increase in the NMDAR-dependent synaptic transmission that is long-lasting but not permanent (Behr et al., 2001). Interestingly, kindling-induced seizures may tip the excitation/inhibition balance further since NMDARs have been found to have enhanced transmission (Kohr et al., 1993). Also, repeated seizures over time give rise to a novel NMDAR that is less sensitive to agonists (Nadler et al., 1994). Thus, NMDARs play a critical role in the initial seizure induction and but not persistence of seizure susceptibility at least with respect to the kindling model of seizures.

Glutamate-activated EPSPs depend heavily on activation of AMPA receptors (AMPARs). Studies from epileptic post-mortem tissue in humans have shown up-regulated AMPARs (Hosford et al., 1991). Changes in AMPARs can also occur after electrical kindling (Kamphuis et al., 1994). During seizures, it is thought that AMPARs may contribute not just to shifting the excitatory/inhibitory balance but through cell death as well. For example, in hippocampal CA4 neurons, AMPARs seem to switch to calcium permeable which increases the probability of subsequent calcium induced excitotoxicity (Friedman et al., 1994). In other parts of the hippocampus, different mechanisms may play a role in enhancing hyperactivity. In granule cells, the altered AMPAR subunits show an enhanced response to agonists and may result in increased excitatory tone (Kamphuis et al., 1994). Given several lines of

evidence implicating the roles of AMPARs during ictogenesis, modulating the effect of AMPAR activity may be a potential way of targeting AEDs. Indeed, blocking AMPARs and NMDARs receptors retarded epileptogenesis in an animal TLE model of seizures (Schidlitzki et al., 2017).

Metabotropic glutamate receptors (mGluRs), especially those belonging to group 1 have been recognized for decades as important contributors to epileptogenesis. Early studies discovered that mGluR agonists could recruit the hippocampus *in-vitro* and *in-vivo* to produce synchronized discharges (McDonald et al., 1993; Taylor et al., 1995). While addition of mGluR agonists produced ictal-like discharges, their removal did not restore baseline activity, suggesting that mGluRs are closely linked with network plasticity and initiation of an epileptogenic process (Anwyl, 2009; Merlin and Wong, 1997). Indeed, it is now apparent that mGluRs are critical for brain plasticity even in the absence of pathologic conditions and exert their effects through second messengers such as phospholipases and extracellular kinases (Niswender and Conn, 2010; Zhao et al., 2004).

As more studies have emerged from animal models of epilepsy, it has become more apparent that seizures cannot be fully explained by failure of inhibition. It is increasingly clear that there are several other changes that occur concurrently during and after seizure emergence that are important for the transition from a healthy to an epileptic state. As an example, second messengers have been increasingly looked at for their role in the development of seizures. Following kindling, it is believed that there is a loss of intracellular calcium-binding proteins such as calbindin and an increase in Ca^{2+} current which may be explained by increased Ca^{2+} channel density on the cell membrane (Kohr et al., 1991; Vreugdenhil and Wadman, 1992). However, these results do not completely rule out that changes in second messenger systems are a result of and not a consequence of kindling (Mody and Staley, 1994).

1.5.5 Genetic pathways associated with epileptogenesis

The long-lasting consequences of seizures are a major stumbling block to effective treatment. Thus, a major research effort is focused on identifying key genes that participate in the long-term consequences of seizures. The lasting effects may be in part underlied by activation of immediate early genes and neurotrophins such as BDNF and TrkB which contribute to long-term circuit alterations (Binder et al., 1999; Elmer et al., 1996). Other genes that are altered following excessive neuronal activity such as kindling-induced seizures are neuroactive peptides, potassium channels, extracellular proteases, as well as glutamic acid decarboxylase (GAD) (Iadarola et al., 1986; Qian et al., 1993; Rosen et al., 1992; Sonnenberg et al., 1991; Tsaur et al., 1992). Notably, the genetic changes in protein or mRNA expression that accompany kindling may be short lived but their gene products may nevertheless be able to impart lasting changes on brain circuits (Mody, 1993). Some genetic and molecular changes can be induced by minor hyperactive episodes, for example by ADs (Gall, 1992). Thus, even in the earlier stages of kindling, the cascade of events eventually leading to generalized seizures may have already begun.

Another heavily studied protein with regards to ictogenesis has been mTOR and its downstream targets, which have been associated with multiple diseases involving developmental brain malformations (Huang and Manning, 2008). Inactivating genes that inhibit mTOR signalling causes mice to develop seizures after one month (Uhlmann et al., 2002). On the other hand, excessive stimulation of the mTOR pathway causes disorganization of cell layers and astrogliosis, amongst other changes, and these pathological changes as well as the onset of seizures can be reversed by inhibiting the mTOR pathway (Uhlmann et al., 2002; Zeng et al., 2008). In humans, mutations of mTOR pathway molecules such as tuberous sclerosis complex 1 cause severe and intractable epilepsy as well as related focal

cortical malformations (Wong, 2008). Thus, there are multiple genetic and molecular changes that act in concert with structural changes and impinge upon the transition from a healthy and epileptic state.

1.5.6 Contributions of glia to epileptogenesis

Changes in morphology and synaptic function of neurons are not the only factors that may contribute to the development of seizures. Increasingly, glia have been found to play key roles in the initial steps of seizure development and progression of epilepsy. Post-mortem tissue analysis from patients with epilepsy have shown evidence of gliosis and activated astrocytes; their role in neurotransmitter management may suggest how glia can contribute to seizure-generation (Cohen-Gadol et al., 2004; Petroff et al., 2002). In animal models of epilepsy, it was found that repeated kindling-induced seizures upregulate GFAP mRNA and protein levels along with increasing glial proliferation and growth (Hansen et al., 1990; Khurgel and Ivy, 1996). Aside from astrocytes, microglia can also be activated in epileptic tissue in response to proconvulsant application or electrical stimulation (Borges et al., 2003). Once activated, microglia may modulate several functions which can contribute to epilepsy such as aberrant neurogenesis or a pronounced inflammatory response (De Simoni et al., 2000; Luo et al., 2016).

Possible mechanisms of glial contribution to seizure formation include how glia interact and can modify the extracellular space between neurons. It is known that seizure activity is associated with an increase in extracellular K^+ concentration and a decrease in extracellular Ca^{2+} concentration (Somjen, 2009). As the seizure occurs, the extracellular space surrounding cells actual closes (Amzica and Neckelmann, 1999). These changes alone dramatically affect intrinsic excitability of neurons due to ionic redistribution. The increase in

K^+ shifts the reversal potential to more depolarized values and enable I_h currents to generate action potentials (Timofeev et al., 2002). Yet another potential mechanism where glia could impinge on the development of seizures is through glutamate uptake. Alteration in the glial glutamate transporters EAAT1 and EAAT2 has been shown to be common in TLE (Seifert et al., 2006). Meanwhile, inhibition of glial glutamate transporters leads to prolonged synaptic currents and decreased threshold to seizures (Campbell and Hablitz, 2008).

Glia are also tightly involved with inflammation and may play a role in seizure promotion through inflammatory pathways (Dong and Benveniste, 2001). For example, febrile seizures, which are initiated by fever, are associated with increased levels of the cytokine IL-1β (Dube 2005). IL-1β may also act in concert with other cytokines such as TNFα to inhibit glutamate reuptake and promote hyperactivity (Bezzi et al., 2004; Ye and Sontheimer, 1996).

Finally, glia may modulate epileptogenesis through metabolic by-products such as ATP. ATP is broken down to adenosine which acts on presynaptic A1 adenosine receptors and can inhibit transmitter release (Pascual et al., 2005). Seizure induction results in decreased circulating adenosine concentrations (Li et al., 2008). Correspondingly, the enzyme that regulates adenosine phosphorylation, adenosine kinase, has generated increasing interest as a potential therapeutic agent to prevent epileptogenesis (Boison, 2008). Taken together, it is becoming increasingly clear that glia play important and non-overlapping roles in epileptogenesis through several different pathways.

1.5.7 Brain-wide changes associated with epilepsy

Since performing kindling experiments in humans directly is not permissible, there are only few reports of successful seizure generation after electrical stimulation (Monroe, 1982;

Sramka et al., 1976). Early experiments were instrumental in laying the foundation for human studies of epilepsy and uncovering the steps involved in seizure generation. One of the most intensely studied consequences of kindling has been on the somatotopic organization upon which movement representations are thought to be based on (Murphy et al., 1980; Penfield and Rasmussen, 1950). Further experiments showed that once seizure severity reached tonic clonic status, seizure activity could spread to adjacent muscle groups in the so-called "Jacksonian march" (Murphy et al., 1980). These findings were supplemented by those of Penfield who had discovered earlier the representation or somatotopic map within the human precentral gyrus (Penfield and Rasmussen, 1950). Later, researchers were able to show that movements in patients with epilepsy could be elicited from regions outside of the motor cortex (Uematsu et al., 1992).

In animal kindling studies, one of the first findings supporting this human work demonstrated that kindled animals showed an increase in the area of cortex from which forelimb movements could be elicited (Teskey et al., 2002). Increasing stimulation intensity during electrical kindling of cortex, also showed increasing number of forelimb muscle recruitment compared to controls (Teskey et al., 2002). In addition to changes in sensorimotor representation, neocortical kindling can also change tonotopic representation in auditory cortex. Kindled animals have less precise tuning curves potentially resulting from decreased thalamocortical input of stronger horizontal connections, giving rise to responses over a broader frequency range (Valentine et al., 2004). Also, during spontaneous activity, kindled animals show greater neuronal synchrony between neurons assayed with single-unit recordings in primary auditory cortex (Valentine et al., 2004).

1.6 Electrophysiological correlates of seizure development

1.6.1 HFOs

High-frequency oscillations (HFOs) are field potentials that are 80Hz or greater and last from several to hundreds of milliseconds (Buzsaki et al., 1992). They are thought to play several key roles in brain functions such as sleeping and waking cycles, cognitive processing, and memory consolidation (Engel and da Silva, 2012). Studies have suggested that HFOs may reflect inhibitory potentials from rhythmic IN firing (Cobb et al., 1995; D'Antuono et al., 2005). HFOs can be broadly divided into two frequency ranges, ripples (80-200 Hz) and fast ripples (250-500 Hz) (Bragin et al., 1999b; Buzsaki et al., 1992). Spontaneous ripple HFOs can be seen in the neocortex, hippocampus and during non-pathological conditions. Cortical HFOs are thought to be closely tied to sensory-evoked potentials (Jones and Barth, 1999; Kandel and Buzsaki, 1997). Ripples have also been implicated as critical participants of information transfer from hippocampus to neocortex during sleep (Buzsaki, 1996).

HFOs have also been found in animals and patients with epilepsy where the dominant frequencies detected are 250-600 Hz (Jacobs et al., 2009b; Zijlmans et al., 2009). Data thus far suggests that HFOs detected in pathological conditions may reflect bursts of population spikes from abnormally synchronized PCs (Jefferys et al., 2012). In animal models of chronic limbic epilepsy, fast ripples have been found only in rats that have spontaneous seizures, thereby providing a plausible association between fast ripples and the onset of spontaneous seizures (Bragin et al., 1999a; Bragin et al., 2000).

Several of the properties of HFOs in animals such as spectral frequency, duration and association with seizure-onset zones are recapitulated in humans (Bragin et al., 1999a; Staba et al., 2002). In patients with MTLE, it was found that higher rates of fast ripples

detected were positively correlated with severity of sclerosis that was observed as well as decreased densities of neurons in hippocampal circuitry (Ogren et al., 2009; Staba et al., 2007). In addition, the number of HFO-generating zones within pathological tissue correlate with seizure frequency and their power increases during the transition to hypersynchronous seizures (Bragin et al., 2005; Bragin et al., 2003).

In fact, HFOs have received increased attention as a potential biomarker for seizure activity (Schevon et al., 2009; Urrestarazu et al., 2007). For example, in TLE models, HFOs are found in areas of the hippocampus and related limbic structures where ripples do not occur under normal conditions (Bragin et al., 2004). Also, the rates of HFOs in pathologic conditions were strongly linked to the area of seizure onset but not anatomical lesion, suggesting that HFO generation may be a fundamental property of epileptogenesis (Jacobs et al., 2009a; Staley et al., 2011).

1.6.2 Interictal spikes

Other electrophysiological correlates of seizure development are interictal discharges/spikes - high-amplitude fast EEG transients typically followed by a slow wave that lasts several hundreds of milliseconds (de Curtis and Avanzini, 2001). The slow wave is termed a paroxysmal depolarizing shift (PDS) and is commonly observed when $GABA_A$-mediated inhibition is impaired (Schwartzkroin and Prince, 1980). Interictal spikes (ISs) include rapid potentials that are designated as spikes (even faster than 50ms) and slower potentials between 50-200 ms duration termed sharp waves (Gotman, 1980). In the cortex, ISs can recur and remain localized to one region or spread to another area that may involve secondary subcortical structures (de Curtis and Avanzini, 2001). Amongst other mechanisms in the neocortex that participate in PDS formation, calcium currents are thought to be critical and

blocking these results in reduction or abolishment of PDS and ISs (Brown and Griffith, 1983; de Curtis et al., 1999; Wong and Prince, 1978).

In neocortex, it is believed that deep layers such as 4 and 5 are responsible for promoting PDS and therefore IS generation (Chagnac-Amitai and Connors, 1989). Furthermore, it was found that PDS can be initiated by the gradual summation of excitatory inputs (Chamberlin et al., 1990). Since INs play a major role in synchronizing the firing of INs and PCs, it has been proposed that they are responsible for the synchronization needed to generate cortical ISs (Perreault and Avoli, 1992). Furthermore, it is thought that ISs may characterize the change from latent to chronic epilepsy (Bortel et al., 2010). Also, ISs' role may depend on developmental stage. Studies in juvenile animals have shown that they may play a role in axon guidance and the formation of initial axonal connections (Staley et al., 2011).

ISs have been increasingly recognized as a prognostic tool for seizure development and potential therapeutic target for clinical intervention. Studies have shown that the animals that eventually develop epilepsy have an increase in frequency of ISs (Huneau et al., 2010). ISs have also been detected in epileptic patients though there is still some controversy with regards to their true meaning since they have also been detected to a lesser degree in healthy subjects (Jabbari et al., 2000). In presurgical studies, using HFOs as markers for seizure generating sites had a better surgical outcome than using ISs (Jacobs et al., 2010). Other studies have suggested that the presence of HFOs with ISs was more sensitive in predicting seizure-onset area than ISs alone (Jacobs et al., 2008).

This suggests that ISs may not predict as well as HFOs the extent of the epileptogenic region targeted for surgical resection.

1.7 Rationale and aims of the thesis

Rationale

Current chronic animal models of epilepsy where seizures are induced are widely used and allow examination of the first stages in the transition from a healthy to an epileptic brain. Yet models of electrical induction like kindling suffer from a set of key problems. For example, it has been difficult to disentangle the contribution of tissue damage from plasticity mechanisms. Furthermore, the experimenter cannot readily control the subset of cells that are activated with classical kindling, making it difficult to establish causal links between cell type and pathological outcome. This lack of specificity may in turn contribute to less standardized outcomes across labs.

Here we describe novel approaches using combinations of optical and genetic methods for studying epileptogenesis. These approaches can circumvent some shortcomings associated with the classical animal models and may thus increase the likelihood of developing new treatment options. We aim to clarify the local circuit changes that are associated with the transformation of the brain into an epileptic state.

Aim 1

The 1st aim of my PhD research was to develop a novel neocortical optogenetic kindling model of epilepsy which addresses current shortcomings of electrical induction models of epilepsy. The optogenetic model shares key features with electrical kindling models such as: 1) repeated stimulation, while initially ineffective, eventually results in seizures; (2) the severity and duration of these seizures increases over time; and finally, (3) animals with seizures that are left unstimulated for a prolonged period display retention of seizure potential when stimulation recommences. I describe this model in **Chapter 2** and this manuscript is published (Cela et al., 2019).

Aim 2

The 2nd objective of my research was to optimize this kindling model by modifying the rate of seizure occurrence to widen the suitability of the model. To this end, I used a two-hit approach by injecting animal with the cannabinoid receptor type 1 (CB1R) blocker rimonabant on top of the stimulation paradigm established in Aim 1 to accelerate seizure development. These results are described in **Chapter 3**.

Aim 3

The 3rd objective of my research was to develop methods of testing the consequences of the novel optogenetic kindling model in neocortical circuits. To achieve this, I used a combination of two-photon imaging and acute slice recordings combined with optogenetic stimulation of presynaptic cells to characterize the intrinsic properties of cells in the kindled cortex compared to healthy brains and lay the foundation for future studies. These preliminary results are discussed in **Chapter 4**.

The findings presented in this Ph.D. thesis discuss a method to examine seizure development in the initially heathy brain with cellular resolution (optokindling), a feat that has only recently become possible. Furthermore, I modified optokindling to result in accelerated seizure development by combining it with a CB1R blocker in a two-hit model of epilepsy. Finally, in preliminary experiments, I used ChR2 mapping techniques in acute slices as a potential means of investigating circuit changes following seizures. Taken together, these findings may be important going forward to develop new therapeutic strategies for intervention at critical points during epilepsy.

2 AN OPTOGENETIC KINDLING MODEL OF NEOCORTICAL EPILEPSY

2.1 Preamble to Chapter 2

In **Chapter 1**, I outlined what features must constitute an optogenetic kindling model, and how this differs from current seizure induction models. In **Chapter 2** I describe the development of a neocortical optogenetic kindling (optokindling) model that fulfils the criteria outlined in **Chapter 1**. Using in-vivo EEG recording as well as behaviour monitoring in awake behaving mice, I studied the gradual progression of seizures upon optogenetic light stimulation. The optokindling model I developed allows for genetic targeting of neurons of interest whilst limiting gross brain damage. The optokindling I describe in this chapter is the first of its kind, to my understanding, to effectively encompass kindling properties in an optogenetic model. The results in this chapter will also inform subsequent chapters.

Abstract:

Epileptogenesis is the gradual process by which the healthy brain develops epilepsy. However, the neuronal circuit changes that underlie epileptogenesis are not well understood. Unfortunately, current chemically or electrically induced epilepsy models suffer from lack of cell specificity, so it is seldom known which cells were activated during epileptogenesis. We therefore sought to develop an optogenetic kindling method (optokindling) in which activatable cells are both genetically defined and fluorescently tagged. We briefly optogenetically activated pyramidal cells (PCs) in motor cortex (M1) of awake behaving

mice every two days and conducted a series of experiments to validate the effectiveness of the model. Although initially inert, brief optogenetic stimuli eventually elicited seizures that increased in number and severity with additional stimulation sessions. Seizures were associated with long-lasting plasticity, but not with tissue damage or astrocyte reactivity. Once optokindled, mice retained an elevated seizure susceptibility for several weeks in the absence of additional stimulation, indicating a form of long-term sensitization. We conclude that optokindling shares many features with classical kindling, with the added benefit that the role of specific neuronal populations in epileptogenesis can be studied. Links between long-term plasticity and epilepsy can thus be elucidated.

2.2 Introduction

In 1967, Graham Goddard published his influential paper (Goddard, 1967) on the kindling model of epilepsy, where he described how brief daily high-frequency electrical stimulation of specific sub-cortical brain areas eventually led to seizures in a subset of otherwise healthy and non-epileptic animals. Because kindled animals retained a reduced threshold for seizures in the long term, Goddard argued that the process was “analogous to learning,” (Goddard, 1967) as proposed by Donald Hebb (Hebb, 1949) and others (Markram et al., 2011), suggesting that epilepsy could arise from pathological activity patterns that recruit learning mechanisms in the healthy brain (Teskey, 2001b). Although it does not represent all forms of epilepsy equally well, the classical kindling model is today widely accepted as a functional epilepsy model in which pathological evoked activity gradually develops in otherwise healthy brains (Morimoto et al., 2004).

Yet, the original kindling model suffers from a set of key problems. For example, it has been difficult to disentangle the contribution of tissue damage from plasticity

mechanisms (Cavazos et al., 1994). Furthermore, the experimenter cannot readily control the subset of cells that are activated with classical kindling, making it difficult to establish causal links between cell type and pathological outcome. This lack of specificity may in turn lead to poorer standardization across labs.

To improve on these shortcomings, we developed an optogenetic kindling model (optokindling) of epilepsy in neocortex. Optokindling shared several key features with the classical kindling model of epilepsy (Goddard, 1967; Teskey, 2001b): (1) repeated stimulation, while initially ineffective, eventually resulted in seizures; (2) the severity and duration of these seizures increased over time; and finally, (3) animals with seizures that were left unstimulated for a prolonged period displayed retention of seizure potential when stimulation recommenced. Furthermore, it was robust and did not cause appreciable brain damage or glial reactivity. Since the optically driven set of cells is genetically defined as well as fluorescently tagged in our model, it enables the study of cell and circuit changes associated with epileptogenesis.

2.3 Materials and Methods

Ethics

All procedures conformed to the standards and guidelines set in place the *Canadian Council on Animal Care* (CACC) and the *Montreal General Hospital Facility Animal Care Committee* (FACC), with the appropriate license. For surgeries, animals were anesthetized with isoflurane (CDMV Inc., St-Hyacinthe, QC, Canada). For collection of acute slices, mice were anesthetized with Avertin (Sigma Aldrich, Oakville, ON, Canada) or isoflurane and sacrificed once the hind-limb withdrawal reflex was lost. Every attempt was made to ensure minimum discomfort of the animals

2.3.1 Stereotaxic viral injections and EEG screw implantation

We targeted ChR2 to primary motor cortex (M1) of male C57BL/6J mice aged postnatal day (P) 30-45 using bilateral stereotaxic injection of AAV-CaMKIIα-hChR2-E123T/T159C-p2A-EYFP (UNC Virus Core, North Carolina, USA), since two kindling sites are known to function better than one (Teskey et al., 1999). Males were chosen solely instead of females since the estrus cycle can affect seizure susceptibility (Curry, 1974). Virus from plasmid constructs contributed by Karl Deisseroth was packaged by UNC Vector Core into serotype 5 AAVs. Using a stereotactic apparatus (Just for Mouse 5731, Stoelting Inc, Wood Dale, IL, USA), we injected 1.2 μL of virus bilaterally, following previously described procedures (Cardin et al., 2010). Injection coordinates relative to bregma were 1.1 mm anteroposterior, 1.5 mm mediolateral and 0.8 mm dorsoventral. We subsequently placed and cemented 1.25 mm ceramic ferrules (CFC-230, Thorlabs, Newton, NJ, USA) over the injected region of each hemisphere at the same coordinates as injection. Ferrules contained 200-μm-diameter 0.37-NA multimode fiber to allow light delivery. Coincident with viral injection and ferrule placement, we also implanted recording and ground screws (1/8”, 000-120 thread, 90910A600, McMaster-Carr, Elmhurst, Illinois, USA), which were stabilized with dental cement (Lang Dental, Wheeling, IL, USA). Animals were evaluated for correct placement with EYFP staining (see below). The coordinates for recording screws typically centered around ±3 mm mediolateral, -0.6 mm anteroposterior while the reference screws were placed at ±3 mm ML and -4mm AP. The screws had conductive wire soldered on and were connected to gold-plated jacks (64-132, Warner Instruments, Hamden, CT, USA; or 33X1880, Newark Electronics, Pointe Claire, QC, Canada) for EEG recordings. We used a separate ground reference screw for the left and right hemisphere.

2.3.2 *In-vivo* recordings and optogenetic stimulation

Animals were given 21 days to recover from surgery after which, they were habituated for three days to the recording setup before commencing stimulation sessions. The recording cage consisted of a 30 cm diameter wide and 40 cm tall Plexiglas cylinder covered with copper mesh and with a copper bottom. To reduce noise by serving as a Faraday cage, the copper plate and mesh of the cage were connected to the amplifier chassis ground. Two 445-nm blue lasers (Monopower-455-150-MM-TEC, Alphalas GmbH, Germany) on kinematic V-clamp post mounts (C1513/M, Thorlabs, Newton, NJ, USA) for ease of alignment, were air coupled (aspheric FC/PC fiber port PAF-X-18-PC-A with HCP mounting bracket, Thorlabs, Newton, NJ, USA) to two two-meter-long fiber-optic patch cords (M83L01, Thorlabs, Newton, NJ, USA), coupled to 1.25-mm bilaterally head-mounted ceramic ferrules (CFLC230-10, Thorlabs, Newton, NJ, USA). The light power exiting the fiber was ~50 mW; it was measured before and after every stimulation session to ensure it remained stable. EEGs were collected at 2-10 kHz with an extracellular amplifier (Model 1700, AM Systems, Sequim, WA, USA) and were digitized on a PCI-6221 board (National Instruments, Austin, TX, USA) using in-house software running in Igor Pro 6.37 (Wavemetrics Inc., Lake Oswego, OR, USA) on a desktop computer (Micro Tower Desktop PC SL-DK-H61MX-ID, SuperLogics, Natick, MA) running Windows XP SP7. This computer also episodically TTL-gated the two 445-nm lasers. Animal behavior was recorded with two cameras, one above the recording setup, and one to the side (Logitech C525 webcam, Tiger Direct.ca Inc., Calgary, AB, Canada). Video was acquired using iSpy software (Version 6.7.9, https://www.ispyconnect.com) running on the EEG acquisition computer. To score severity of seizures from these videos, we used a modified Racine scale **(Table 2.1)**. If behavior seemed to straddle two Racine stages, the score was taken as the intermediate value, e.g. 4.5

if between 4 and 5. As a form of verification, the Racine score was determined independently of the automated seizure detection. We did not categorize paw movement due to direct optogenetic activation as clonus, since it is a trivial and direct consequence of activation of motor programs that is unrelated to epilepsy.

Mice were stimulated every two days with the same protocol lasting approximately 33 minutes. Stimulation sessions were numbered sequentially starting at one. Each session consisted of an initial 10-minute-long baseline period, a three-minute-long induction, and a second 20-minute-long baseline. Baseline stimulation consisted of two 10-ms 445-nm laser pulses delivered at 30 Hz every 10 seconds. The induction period consisted of five bouts of three seconds of 50-Hz stimulation at 50% duty cycle and three second inter-bout interval, repeated three times once a minute (**Figure 2.1**). We categorized frequency bands as follows (e.g. **Figure 2.9**): delta (0-4 Hz), theta (4-8 Hz), alpha (8-12 Hz), beta (12-30 Hz), gamma (30-80 Hz), ripples (80-250 Hz), and fast ripples (250-500 Hz).

We employed two types of control animals. In EYFP controls, EYFP alone was expressed using AAV5- CaMKIIα-EYFP (UNC Virus Core, North Carolina, USA), and the stimulation during baseline and induction was as described above. In ChR2 controls, the same ChR2 construct as stimulated animals was expressed, but the 50-Hz stimulation was omitted from the induction period; the baseline stimulation pattern was as above.

In rekindling experiments, mice were not stimulated for 36 days after the last of the initial 25 kindling sessions. Once stimulation was resumed, mice were stimulated every two days, as before. The first session after the 36-day-long pause was considered rekindling session one, with subsequent sessions were numbered sequentially.

2.3.3 Immunohistological analysis

Mice were anesthetized with a cocktail consisting of (in mg/mL) 50 Ketamine, 5 Xylazine, 1 Acepromazine (CDMV Inc., St-Hyacinthe, QC, Canada) and transcardially perfused with 0.1 M phosphate-buffered saline (PBS) followed by 4% paraformaldehyde (PFA, P6148, Sigma Aldrich, Oakville, ON, Canada). Brains were incubated in 4% PFA overnight, and then stored for two additional days in a 30% (w/v) sucrose solution. Next, brains were mounted in O.C.T. media (25608-930, VWR, Montreal, QC, Canada) using a bath of 100% EtOH and dry ice. Using a cryostat, embedded brains were sectioned at 50 μm thickness through the primary and secondary motor cortices and sections were placed in a 0.01 M phosphate-buffered saline solution. Sections underwent a twenty-minute wash in 0.01 M phosphate-buffered saline with 1% Triton-X (X100, Sigma Aldrich, Oakville, ON, Canada) followed by a ninety-minute wash in 0.01 M phosphate-buffered saline with 0.3% Triton-X and 10% normal donkey serum (NDS) (566640, Sigma Aldrich, Oakville, ON, Canada). All antibody incubations were performed in 0.01 M phosphate-buffered solution with 0.3% Triton-X and 1% NDS.

Sections were incubated overnight at 4ºC in the primary antibodies: rabbit anti-cleaved caspase-3 (1:500, Cell Signaling, Danvers, MA, USA), mouse anti-NeuN (1:500, Millipore, Billerica, MA, USA), rabbit anti-NeuN (1:500, Abcam, Cambridge, MA, USA), chicken anti-GFP (1:1000, Abcam, Cambridge, MA, USA), mouse anti-GFAP (1:500, Millipore, Billerica, MA, USA) and guinea pig anti-GFAP (1:500, Synaptic Systems, Göttingen, Germany). Twenty-four hours later, tissue underwent three 15-min washes in 0.01 M phosphate-buffered saline with 0.3% Triton-X and 1% NDS, followed by a 90-min incubation in the Alexa Fluor donkey secondary antibodies at 1:1000 (anti-rabbit 405, anti-mouse 568, anti-rabbit 568, anti-chicken 488, anti-mouse 647, and anti-guinea pig 647) (Life Technologies, Burlington, ON, Canada).

Next, the tissue underwent three twenty-minute washes in 0.01 M phosphate-buffered saline with 0.3% Triton-X and 1% NDS. Following this procedure, coronal slices

were mounted using coverslips with a 40 µl bolus of ProLong Gold Antifade mount (P10144, Life Technologies, Burlington, ON, Canada). Sections were imaged using a Fluoview FV1000 confocal laser scanning microscope and Fluoview software (Olympus Canada, Richmond Hill, ON, Canada). Analysis of antibody-labelled slices was performed manually using ImageJ(Schneider et al., 2012) and Igor Pro (Wavemetrics Inc., Lake Oswego, OR, USA). For GFAP, ~6 sections with two measurements each, covering all six cortical layers, were analysed per animal. M1 was compared to a non-labelled cortical region. For NeuN, four or five sections were analysed with 7-8 measurements per animal. M1 cell counts were carried out across the six cortical layers.

2.3.4 Automated electrographic seizure detection

To independently detect seizures offline, a simple automatic seizure detection software algorithm was developed. Although this approach had the disadvantage of missing the occasional seizure that was detected by inspection, it was preferred because it was unbiased and — as opposed to manual inspection —invariably gave the same results when rerun on the same EEG sweeps. We manually inspected all automatically detected electrographic seizures.

EEG Fourier power traces were first converted to z-score sweeps. For z-scoring purposes, the background power levels were determined from the median of at least 64 one-second-long EEG segments recorded in the absence of laser stimulation. The median was used to automatically exclude the occasional movement artifact, because such artifacts resulted in massive responses that typically saturated the amplifier for about a second at a time.

To detect electrographic seizures, a combined threshold and duration criterion was applied. If power exceeded z-score 4 for longer than 4 seconds, then this event was deemed a seizure. EYFP and ChR2 control animals were used to determine these threshold values, whereby

which no seizures were detected in the control mice. We estimated a false negative rate of ~9% by direct inspection of EEGs. Z-scores above 100 were always rejected as movement artifacts. The z-score threshold crossing was taken as the start of an electrographic seizure. Seizure duration was automatically determined from seizure start to the first z-score downstroke threshold crossing. No attempt was made to merge events separated by a brief time of relative inactivity, so automatically detected electrographic seizures were likely underestimated both in terms of number and duration.

2.3.5 *In-vitro* acute slice experiments

Mice were anesthetized by an intraperitoneal injection of an Avertin solution (10 g 2,2,2-tribromoethyl alcohol, Sigma Aldrich T4,840-2, mixed with 10 ml of tert-amyl alcohol, Sigma Aldrich 24,048-6) at 500 mg/kg body weight. The animals were then perfused transcardially with an ice-cold (4˚C) oxygenated N-methyl-d-glucamine (NMDG) solution containing (in mM: 93 NMDG, 93 HCl, 2.5 KCl, 1.2 NaH_2PO_4, 30 $NaHCO_3$, 20 HEPES, 25 glucose, 5 sodium ascorbate, 3 sodium pyruvate, 10 $MgSO_4$ and 0.5 $CaCl_2$ bubbled with 95% O_2/5% CO_2 (Ting et al., 2014). After decapitation, the brain was removed and placed into the same cold NMDG solution. Coronal 300-µm-thick acute brain slices were prepared on a Campden Instruments 5000 mz-2 vibratome (Loughborough, UK) using ceramic blades (Lafayette Instrument, Lafayette, IN, USA). The brain slices were then kept at 33˚C in oxygenated NMDG solution for 10 minutes, after which they were transferred to an incubation solution (containing in mM: 125 NaCl, 2.5 KCl, 1 $MgCl_2$, 1.25 NaH_2PO_4, 2 $CaCl_2$, 26 $NaHCO_3$ and 25 glucose, bubbled with 95% O_2/5% CO_2) and kept for 1 hour before recording. Neurons were patched with pipettes (4-6 MΩ) filled with a gluconate-based current-clamp solution containing (in mM): 5 KCl, 115 K-gluconate, 10 K-HEPES, 4 Mg-

ATP, 0.3 Na-GTP, 10 Na_2-phosphocreatine and 0.02-0.04 Alexa Fluor 594, adjusted to pH 7.2-7.4 with KOH and to 310 mOsm with sucrose. Patch pipettes were pulled from medium-wall capillaries using a P-1000 electrode puller (Sutter Instruments, Novato, CA, USA). Whole-cell recordings were obtained using BVC-700A (Dagan Corporation, Minneapolis, MN, USA). Voltage signals were digitized at 10 kHz using PCI-6229 boards (National Instruments, Austin, TX, USA) and custom software (Sjostrom et al., 2001) running in Igor Pro (Wavemetrics Inc., Lake Oswego, OR, USA). L2/3 PCs were targeted for recording using a 2PLSM rig custom-built from a SliceScope (Scientifica, Uckfield, UK) as previously described (Buchanan et al., 2012). A MaiTai BB laser (Spectraphysics, Santa Clara, CA, USA) tuned to 900-920 nm was used to generate GFP/Alexa 594 fluorescence.

To characterize ChR2 responses to light, we relied on the imaging and electrophysiology platform described above, with an additional 445-nm blue laser (eBay.ca, seller: newgazer) guided onto the same light path as the 2-photon beam and controlled with two galvanometric mirrors (Cambridge Technologies, Bedford, MA, USA). The laser was controlled by the same program running electrophysiological acquisition running home-made software in Igor Pro.

2.3.6 Measurement of light scattering in cortical tissue

To measure light scattering properties in cortical tissue, we dissected whole brains from P30-45 mice and placed them on top of plain microscope slides (12-550-A3, Fisher Scientific, Nepean, ON, Canada). Next, we mounted the same 1.25-mm ferrule and the same 445-nm laser used for stimulation on the stereotax we performed our surgeries on. After, we mounted the sensor from a Thorlabs power meter (PM100D meter, S121C sensor, Thorlabs, Newton, NJ, USA) directly below the slide. We descended the ferrule into the brain in 100 μm

increments while measuring the power that was able to reach the sensor. We took 3 measurements at each depth and repeated the experiment with two different brains.

2.3.7 Statistics

The results are reported as the mean ± SEM. Significance levels are denoted using asterisks (* $p < 0.05$, ** $p < 0.01$, *** $p < 0.001$). Unless otherwise stated, we used Student's *t* test for equal means for all pairwise comparisons. If an equality of variances *F* test gave $p < 0.05$, we employed the unequal variances *t* test. Individual data sets were tested using a one-sample *t* test. For multiple comparisons, pairwise comparisons were carried out if one-way ANOVA suggested this at the $p < 0.05$ significance level. Equal or unequal variances ANOVA was used depending on Bartlett's test for equal variances. Wilcoxon-Mann-Whitney's non-parametric test was always used in parallel to the *t* test, with similar outcome. Multiple pairwise comparisons were corrected *post hoc* using Bonferroni-Dunn's method. Statistical tests were performed in Igor Pro unless otherwise stated. For circular statistics (**Figure 2.10**), we used the *circstat* toolbox in MATLAB in conjunction with the Watson U^2 test (Mardia and Jupp, 2000).

2.4 Results

2.4.1 Establishing an optogenetic kindling approach

To create an optogenetic variant of Goddard's classical kindling model of epilepsy (Goddard, 1967), we expressed the high-efficiency E123T/T159C ChR2 variant (Berndt et al., 2011) in primary motor cortex (M1) PCs using the CaMKIIα promoter, by bilateral stereotaxic injection of adeno-associated virus (AAV) in male P30-45 C57BL/6 mice (see Methods). We

verified ChR2 expression by 2-photon laser-scanning microscopy (2PLSM) of the enhanced yellow fluorescent protein (EYFP) tag. This revealed dense expression in layer 2/3 (L2/3), sparse expression in L5 and L6, and no appreciable label in L1 or white matter (**Figure 2.1**), consistent with published expression patterns of the CaMKIIα promoter (Cardin et al., 2009).

We were concerned that the 445-nm laser light might not penetrate the entire cortical thickness, possibly leading to inefficient or unpredictable kindling. To investigate if light was delivered to subgranular layers in sufficient amounts to activate ChR2, we measured the transmission of light through neocortical tissue *ex vivo* (see Methods). We found that the penetration profile was consistent with previous reports (Aravanis et al., 2007) (**Figure 2.7**). As a rule of thumb, light intensity must reach >1 mW/mm^2 to ensure suprathreshold activation (Boyden et al., 2005). With dual 120-mW lasers and power loss through the fiber optic cable typically measured to <50% (data not shown), we used this profile (**Figure 2.7**) to estimate ~8 mW/mm^2 at the L6/white-matter boundary, well above the intensity limit for suprathreshold activation. Furthermore, we note that the bulk of ChR2-expressing PCs were considerably closer to the pial surface (**Figure 2.1**), thus affording us a substantial safety margin.

We next wanted to verify that we could drive neocortical neurons at frequencies sufficient for kindling (Cain, 1982). To do so, we used whole-cell recordings in acute slices (see Methods) to explore the frequency dynamics of the high-efficiency E123T/T159C ChR2 variant (Berndt et al., 2011) that we used. We found that recorded L5 PCs followed 50-Hz light pulse trains with 90% fidelity (**Figure 2.8**), which should be more than adequate for binding neocortical PCs together by long-term potentiation (LTP) (Sjostrom et al., 2001) as well as for kindling (Cain, 1982). Taken together, our findings established that it should be possible to substitute optogenetic for electrical stimulation in the kindling model of epilepsy.

2.4.2 Optogenetic and classical kindling share several hallmark features

We next kindled animals every two days with a brief laser stimulation paradigm (**Figure 2.1**). To quantify epileptogenesis, we recorded EEG with bilaterally implanted screws (**Figure 2.1**) and behavior with dual cameras, one placed above the animal, and one to the side. Inspired by classical *in-vitro* LTP experiments (Abrahamsson et al., 2016; Sjostrom et al., 2001), we also recorded EEG baseline responses before and after the kindling (**Figure 2.1**). This enabled us to look for long-term changes in amplitude and temporal dynamics of EEG responses (**Figure 2.1**; also see below and **Figure 2.5**).

Evoked seizures were quite apparent, both in terms of behavior and EEG (**Figure 2.1**). We were worried, however, about experimenter bias associated with manual scoring of seizures. To avoid this, seizures were always automatically detected from EEG sweeps using a simple in-house software algorithm (**Figure 2.9**). Briefly, EEG spectral power was converted to z-score, and events exceeding a baseline-noise-determined z-score threshold for at least four seconds were automatically categorized as seizures (see Methods). Properties such as seizure numbers and seizure duration were assessed using this automated analysis. Our custom software also enabled visual inspection by decomposing EEG signals into different frequency bands (**Figure 2.9**). Using our automated seizure detection in combination with our optogenetic kindling approach, we obtained evoked seizures in 9 out of 12 animals (**Figure 2.2**). As with classical electrical kindling(Teskey, 2001b), we never found spontaneous seizures.

To verify that the evoked seizures were specific for both laser stimulation and for ChR2 expression, we carried out two control experiments. First, we injected mice with ChR2-carrying AAV as before, but 50 Hz induction was omitted (**Figure 2.2**). Second, we injected mice with AAV carrying only EYFP (but no ChR2) and carried out induction as before

(**Figure 2.2**). As expected, no seizures were detected in either control group (**Figure 2.2**). These control experiments furthermore verified the specificity of our automatic seizure detection algorithm (**Figure 2.9**).

We next explored if optogenetic kindling shared properties with classical kindling (Goddard, 1967). Using a modified version of the Racine scale (Racine, 1972c) to score behavior during the 3-minute-long induction period (see Methods and **Figure 2.1**), we found that severity increased over sessions (**Figure 2.2)**. In initial sessions, seizures were not detected, but they gradually emerged after several sessions (**Figure 2.2)**. With each session that passed, detected seizures increased in duration and were elicited after shorter periods of light stimulation (**Figure 2.2**). It was not clear that seizure severity saturated in our experiments. Our optogenetic kindling approach thus shared several hallmark features with its classical counterpart (Teskey, 2001b), including a gradual emergence in combination with increased seizure severity and duration, as well as lowered seizure threshold.

It has been reported that seizure susceptibility has a circadian dependency (Quigg et al., 2000), preferentially striking during inactivity. We found no correlation between the incidence of evoked seizures and circadian time, or between seizure duration and circadian time. However, we did find a weak correlation between the time to seizure and circadian time (**Figure 2.10**), consistent with a lowered seizure threshold at night (Quigg et al., 2000).

2.4.3 Optogenetically kindled mice retain a long-term susceptibility to seizures

A key feature of Goddard's original model was that kindled animals retained a reduced threshold for seizures in the long term, which was interpreted as a form of memory (Goddard, 1967). We tested if this was true in our optogenetic model as well. After successful kindling

in a subset of animals, we halted stimulation for 36 days. We then reinitiated stimulation for a second rekindling period. We pairwise compared rekindled animals with their naïve and kindled selves.

We found that seizures elicited in rekindled sessions were more severe than in kindled sessions and also occurred sooner (**Figure 2.3**). However, seizure duration and threshold did not change after rekindling compared to kindled mice (**Figure 2.3**). Taken together, optogenetically kindled animals retained a reduced threshold for seizures in the long term, as in classical kindling (Goddard, 1967; Morimoto et al., 2004; Teskey, 2001b).

2.4.4 Seizures developed in the absence of gross brain damage and glial reactivity

Models of induced seizures are typically associated with injury, which has been linked to higher seizure rates (Pitkänen et al., 2009a). The contribution of pathological activity and plasticity to epileptogenesis is therefore difficult to disentangle from that of injury. To assess the amount of tissue injury in our optogenetic kindling produced, we looked for cell loss and reactive astrocytes using NeuN and GFAP staining, respectively (see Methods and **Figure 2.4**). To visualize the region of ChR2-expressing cells, we stained for EYFP. We compared three categories of animals: optogenetically kindled animals with seizures, ChR2-expressing animals that were not kindled, and laser-stimulated animals that did not express ChR2 (the same three cohorts as in **Figure 2.2**). In comparing these three groups, we could not detect any differences in astrocytic reactivity or in cell counts (**Figure 2.4**). In conclusion, pathological activity, but not injury, was the key causative agent in our optogenetic epilepsy model. We cannot, however, exclude minor or subtle contributions from injury.

2.4.5 Epileptogenesis is associated with long-term changes in EEG dynamics

Since Hebbian plasticity is intrinsically unstable (Turrigiano, 2017), we hypothesized that epileptogenesis might be driven by synaptic plasticity. If so, laser-light-evoked EEG responses should undergo long-lasting strengthening. To investigate if there were changes associated with the high-frequency induction stimulation, we compared EEG responses during the baseline periods after and before the induction (see **Figure 2.1**). To see if there were long-lasting changes that were maintained longer than the two-day spacing of sessions, we explored EEG responses during the pre-induction baseline period across all sessions.

We found that the first EEG response due to a paired-pulse laser stimulus was not potentiated (**Figure 2.5**), in disagreement with our hypothesis that classical Hebbian plasticity might underlie epileptogenesis in our optogenetic kindling model. The second EEG response, however, was strikingly potentiated within each session (**Figure 2.5**), as previously reported for hippocampal kindling (Wierenga and Wadman, 1999). This potentiation of the second response gradually waned across sessions as amplitude seemed to saturate (**Figure 2.5**).

Our results indicated that, although there is long-term plasticity of laser-evoked EEG responses, these probably did not correspond to Hebbian plasticity, since the second but not the first response due to a paired-pulse stimulus was potentiated. Perhaps long-term alterations of EEG dynamics were due to changes in synaptic short-term dynamics. Another not mutually exclusive possibility is a reduced inhibitory drive (Wierenga and Wadman, 1999).

2.4.6 High-frequency power peaks before lower frequency power in seizures

It has previously been reported that high-frequency oscillations often precede neocortical seizure onset (Worrell et al., 2004). Visual inspection of seizure bands indicated that this could be the case in our model (**Figure 2.9**). If so, then the delta frequency peak in seizures should generally be preceded by a peak in the high-frequency ripple range. Indeed, we found that high-frequency power peaked more than six seconds before low-frequency power by several seconds (**Figure 2.6**).

2.4.7 Postictal depression of EEG power follows optogenetically induced seizures

It has been reported that EEG power is typically temporarily reduced following seizures, a notion known as postictal depression (Khoshkhoo et al., 2017). In keeping with previous models of epilepsy[18], we found a period of reduced EEG power following seizures. During this postictal period, EEG power was reduced by ~34% compared with preictal periods (see **Figure 2.11**).

2.4.8 Evoked seizures do not affect EEG power in the long term

We next investigated how different frequency bands were individually altered by the kindling protocol over tens of minutes to days (**Figure 2.12**). We found that, after the induction (**Figure 2.1**), delta and theta band powers increased in power for many tens of minutes, while high- ripple and fast ripple band power decreased (**Figure 2.12**). This effect was not long lasting, however, as it did not persist across stimulation sessions — no changes in the power

of any frequency band was observed when comparing the baseline period before induction across sessions (**Figure 2.12**). This result was in contrast to that found with evoked EEG responses (**Figure 2.6**), which were modified in the long term, across stimulation sessions.

Taken together, our findings reveal a complex set of changes in intrinsic and evoked EEG dynamics, acting on different time scales. Although postictal depression of intrinsic EEG power followed immediately after optogenetically induced seizures (**Figure 2.11**), as previously shown (Khoshkhoo et al., 2017), this outcome depended on which frequency bands were analysed and for how long (**Figure 2.12**). Only the second of paired laser-evoked EEG responses were potentiated in the long term, across different sessions (**Figure 2.5**).

2.5 Discussion

2.5.1 Optogenetic and classical electrical kindling share key properties

Based on the classical kindling model (Goddard, 1967), we developed a robust neocortical optogenetic kindling model of epilepsy. Our optogenetic model recapitulated several hallmark features of its classical counterpart (Teskey, 2001b). First, a majority of animals developed seizures, in line with electrical kindling studies showing robust seizure development (Goddard et al., 1969; Wada et al., 1989). Second, seizures emerged gradually over several stimulation sessions. Similar to electrical kindling, optogenetic kindling required more than ten sessions before first seizure and more than twenty sessions for the development of generalized seizures (Lothman and Williamson, 1994; Wada et al., 1989). Some reports do show maximal behavioral responses resulting from kindling much earlier, but there is still variability in this response (Racine, 1975). This is intriguing, given that electrical kindling stimulates a more diverse population of cells than our optogenetic kindling protocol. Third, once seizure began occurring, they happened regularly and increased in severity across

sessions. In addition, the light threshold necessary for evoking seizures decreased (Teskey, 2001b). Finally, there was a long-term retention of seizure susceptibility in kindled animals. After a 36-day-long pause in stimulation, seizures were similar to those in kindled animals, suggesting that animals did not immediately 'reset' to the unkindled state once repeated stimulation sessions were halted. These findings are consistent with previous reports on the hallmark features of electrical kindling (Dennison et al., 1995; Goddard et al., 1969; Wada et al., 1974).

As a proof of principle, we used our optogenetic model to demonstrate several findings previously found in epileptic models. First, we found evidence that high-frequency oscillations precede low-frequency activity in seizures (Worrell et al., 2004). Second, we observed that postictal depression of intrinsic EEG power was associated with seizures, as previously shown in neocortex (Khoshkhoo et al., 2017). Finally, we found that epileptogenesis was associated with a graded change in evoked EEG dynamics, as previously found in local field potentials of kindled hippocampus (Wierenga and Wadman, 1999).

2.5.2 Advantages of optogenetic kindling

Our optogenetic kindling model has several advantages compared to its classical electric counterpart. First, seizures developed in the absence of gross brain damage, providing an experimental epileptogenesis paradigm with improved specificity for plasticity and for pathological activity. Although the initial viral injection presumably resulted in some degree of injury, we were not able to detect any many weeks afterwards. Importantly, viral injections with a control EYFP-AAV also did not result in any animals with seizures. If injury was still a concern, it could be addressed by working with ChR2-expressing transgenic mouse lines. Craniotomy can also be avoided by activating ChR2 through the skull (Cardin et al., 2010;

Lin et al., 2013). We do concede however that several reports of classical kindling also failed to find gross tissue damage (Pitkänen et al., 2009a).

Second, optogenetic kindling enables cell-type-specific recruitment. This is an important feature since neuronal plasticity depends on synapse type (Larsen and Sjöström, 2015), so kindling is expected to be cell-type dependent. Indeed, directly optogenetically driven seizures have been shown to depend critically on cell type (Khoshkhoo et al., 2017). Furthermore, indiscriminate activation of several types of local neurons and fibers is one of the setbacks of electrical kindling. Although we did not notice any obvious difference with specific activation of PCs, is highly unlikely that e.g. repeatedly activating INs would have resulted in kindling, since their output is negative. In the future, elucidating this cell-type dependence will help clarify the circuit mechanisms that underpin epileptogenesis.

2.5.3 Current limitations of optokindling

Our optogenetic kindling model also comes with some disadvantages, such as the absence of spontaneous seizures, which could reasonably be seen as a lack of realism. However, these have not been observed with classical electrical kindling either — unless the animal is over-kindled through hundreds of sessions (Michael et al., 1998) — so this result is in keeping with the prior literature. We do not know why there are no spontaneous seizures in our optogenetic model, but this means our model system provides an ideal starting point for investigating the fundamental question of what is required to achieve spontaneous seizures.

Another disadvantage is that our optogenetic paradigm is quite time consuming. To enable us to monitor the gradual emergence of seizures, we spaced stimulation sessions by two days. We were also motivated by a concern that too closely spaced stimulation sessions might lower the efficacy of epileptogenesis (Goddard et al., 1969; Racine, 1972a). Although

this approach provided gradual emergence of evoked seizures, which was desirable for studying epileptogenesis, the long delay between sessions required more than 50 days of repeated spaced stimulation, which may not be ideal for all applications. This disadvantage is shared with the classical electrical kindling model. In preliminary experiments, however, we found that optogenetic kindling can be achieved within five days with a stronger induction protocol (McFarlan, Sampalli, Cela, Sjöström CAN 2018 poster 1-G-144).

2.5.4 The role of plasticity in epileptogenesis

We demonstrated that due to repeated pathological activation of a relatively small cluster of pyramidal neurons in motor cortex, local circuits undergo plastic changes that lead to the appearance of generalized seizures. This circuit plasticity appeared to happen in the absence of gross brain damage and inflammation, further implicating plasticity mechanisms as key causative agents. Although all investigated EEG frequency bands were unaffected across sessions, we found long-term alterations of evoked EEG dynamics, additionally supporting the interpretation that plasticity at least partially underpinned the seizure-promoting circuit changes. However, since the amplitudes of evoked EEG responses were unaffected, this did not appear to be a form of Hebbian plasticity (Hebb, 1949). Although we were inspired by classical LTP protocols in designing our optogenetic paradigm, our study did not directly address how Hebbian LTP related to epileptogenesis (Morimoto et al., 2004; Teskey, 2001b), which would have required testing if kindling occluded subsequent LTP induction (Abrahamsson et al., 2016; Sjostrom et al., 2001). There were, however, marked changes in short-term dynamics of evoked EEG responses, which could have been due to alterations in synaptic short-term plasticity, or to reduced inhibitory feedback (Wierenga and Wadman, 1999). Plasticity was thus linked to epileptogenesis in our model, although the specific nature

of this plasticity remains to be uncovered. This link is consistent with Goddard's interpretation of the long-lasting increased susceptibility to seizures as a form of memory (Goddard, 1967), since plasticity has been postulated to underlie learning (Hebb, 1949; Markram et al., 2011).

2.5.5 Future directions

To our knowledge, our model is the first to systematically use optogenetics for neocortical kindling of awake behaving and otherwise healthy animals. One recent hippocampal study demonstrated the graded development of seizures using optogenetics (Berglind et al., 2018), but it did not explore if the elevated seizure susceptibility was retained in the long term like in the original kindling model (Goddard, 1967), nor was it possible to evaluate the behavioral component since the mice were sedated. There have also been several studies using optogenetics to halt (Krook-Magnuson et al., 2013; Paz et al., 2012; Sukhotinsky et al., 2013; Wykes et al., 2012a) and initiate seizures in hippocampus (Krook-Magnuson et al., 2015; Osawa et al., 2013) as well as cortex (Khoshkhoo et al., 2017; Wagner et al., 2015). Although these studies demonstrated optogenetically elicited seizures, they did not show kindling, e.g. no gradual change in seizure threshold or severity were demonstrated, which is essential for providing a link to plasticity. Also, these studies relied on optogenetic stimulation either in combination with classical induction models (Wang et al., 2017; Wykes et al., 2012a) or with pre-existing disease phenotypes (Wagner et al., 2015), thus making it difficult to disentangle the role of plasticity from that of injury and inflammation in seizure development. However, with optokindling, it is possible to isolate the distinct role of plasticity in epileptogenesis.

More generally, it is with optogenetics possible to circumvent several shortcomings associated with other seizure induction models, e.g. unknown cell identity and cell cluster

size. Future studies with optokindling may explore cell type specific contributions to epileptogenesis, or microcircuit plasticity associated with epileptogenesis, in addition to the roles of injury and inflammation in the two-hit model. Because of its more specific focus on plasticity, we believe optokindling will be useful for finding therapeutic treatments, to halt or slow down pathological plasticity in epileptogenesis.

2.6 Figures

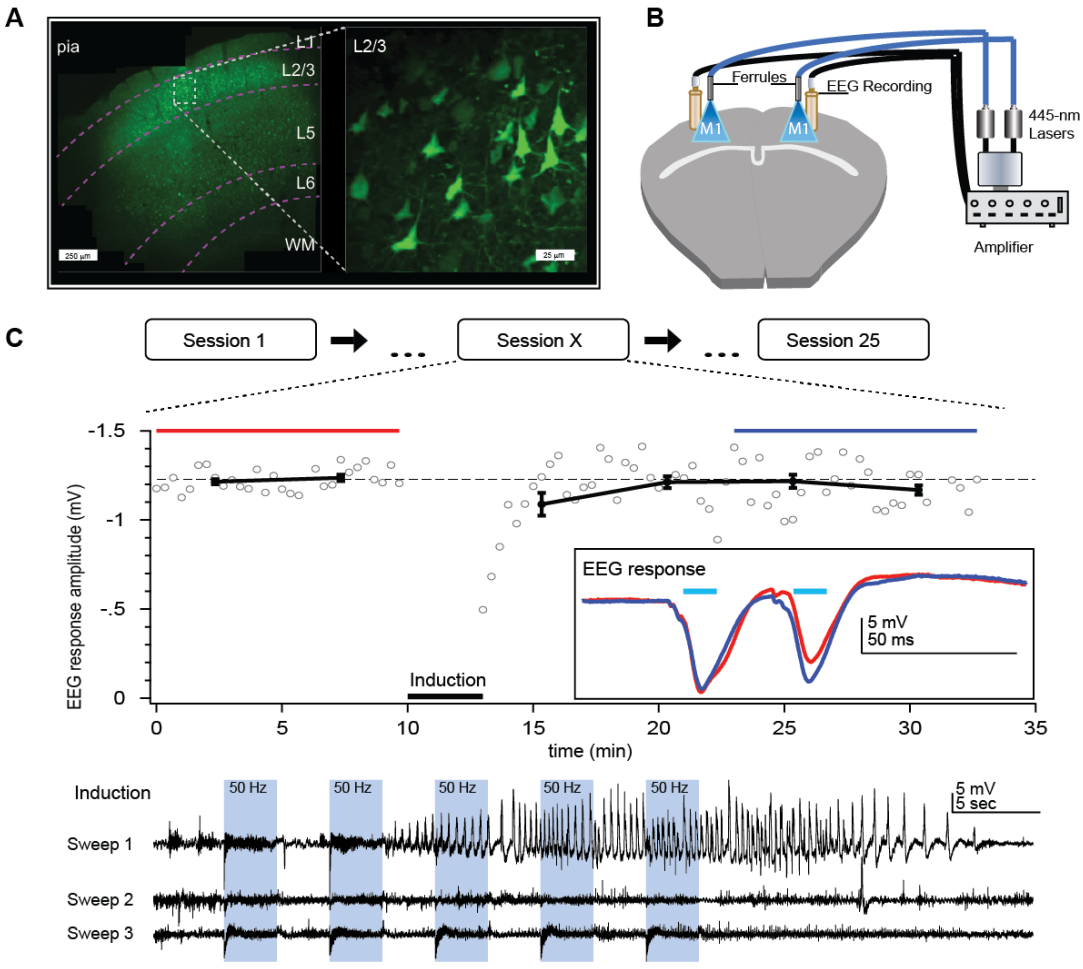

Figure 2.1 Optokindling via simultaneous EEG recording and ChR2 stimulation in awake freely-behaving animals.

(A) Coronal M1 section immunostained for EYFP indicated ChR2 expression in L2/3, 5, and 6, though predominantly in L2/3. Inset shows close-up of L2/3 ChR2-expressing PCs.

(B) To simultaneously activate ChR2 and acquire EEG, ferrules and recording screws were implanted bilaterally above M1, without penetrating the cortex. Fiber optic cables were air-coupled to 445-nm lasers. EEG signals were processed by an extracellular amplifier, but not pre-amplified. A computer (not shown) TTL-gated the lasers and digitized amplified EEG signals.

(C) In each stimulation session, M1 was kindled (during "Induction") with 15 bouts of 3-second-long 50-Hz bursts of 5-ms 445-nm laser pulses, divided into three sweeps delivered once a minute. Sessions were repeated at least 25 times every 48 hours. In this sample session from a non-naïve animal, a prominent electrographic seizure was evoked in the first induction sweep. EEG responses to 30-Hz paired-pulse laser stimuli were recorded for 10 minutes before and 20 minutes after the kindling induction. **Inset:** Paired-pulse EEG responses before (red) and after (blue) indicated a change in EEG dynamics but not amplitude.

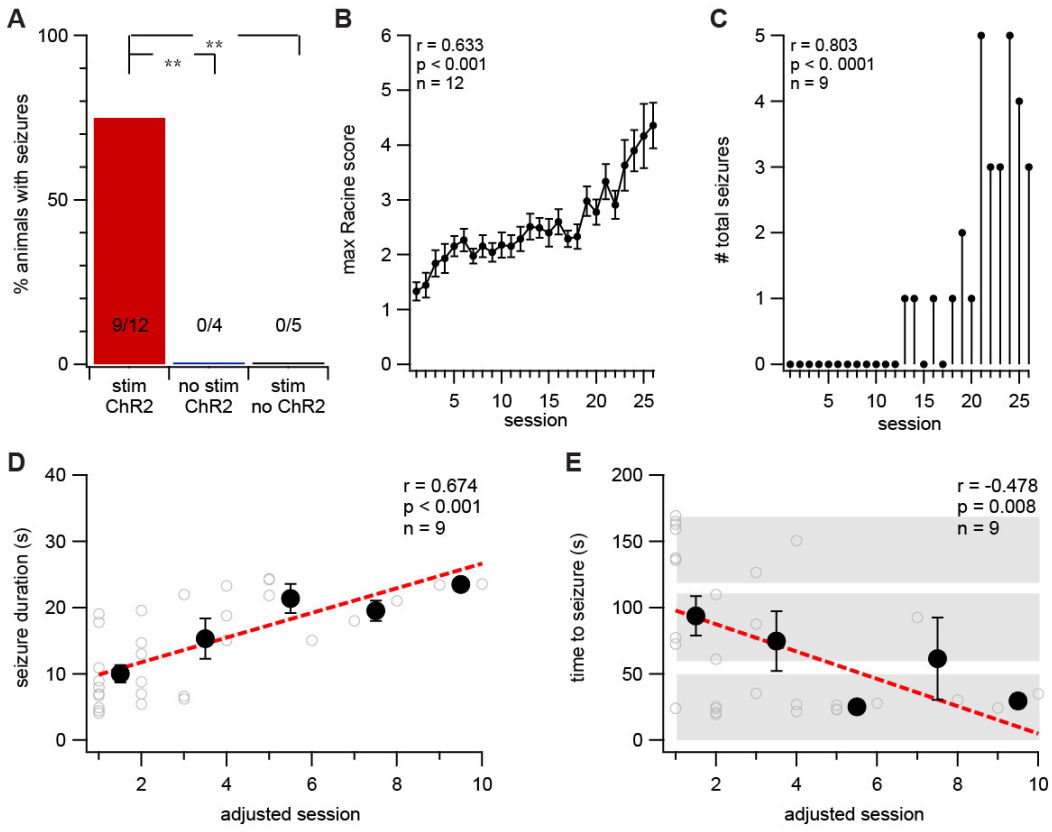

Figure 2.2 Optokindling and classical kindling share hallmark seizure features

(A) Optokindling required both laser stimulation and ChR2 expression. The number of stimulated ChR2-expressing animals that developed electrographic seizures (9 of 12 animals) was higher than unstimulated ChR2 controls (0 of 4) and stimulated no-ChR2 controls (0 of 5) (Fisher's exact test, $p = 0.001$).

(B) The behavioral seizure severity, as measured by a modified Racine score(Racine, 1972c), increased over sessions (Spearman's rank correlation test, rho = 0.957, $p < 0.001$, n = 12 animals).

(C) An increasing number of electrographic seizures developed in stimulated ChR2-expressing animals (Spearman's rank correlation test, rho = 0.862, $p < 0.001$, n = 30 seizures from 9 animals).

(D) Once seizures arose, seizure duration gradually increased over sessions ($r = 0.674$, $p < 0.001$, $n = 30$ seizures from 9 animals). Open circles represent individual seizures, whereas closed circles are averages over the one session before and after. Linear fits are made to the entire data set.

(E) Seizure threshold, measured as time to electrographic seizure onset from start of induction, decreased across sessions ($r = -0.478$, $p = 0.008$, $n = 30$ seizures from 9 animals; symbols as in D). Gray boxes denote the three 50-Hz induction epochs. Linear fits were made to the individual data points, not binned data.

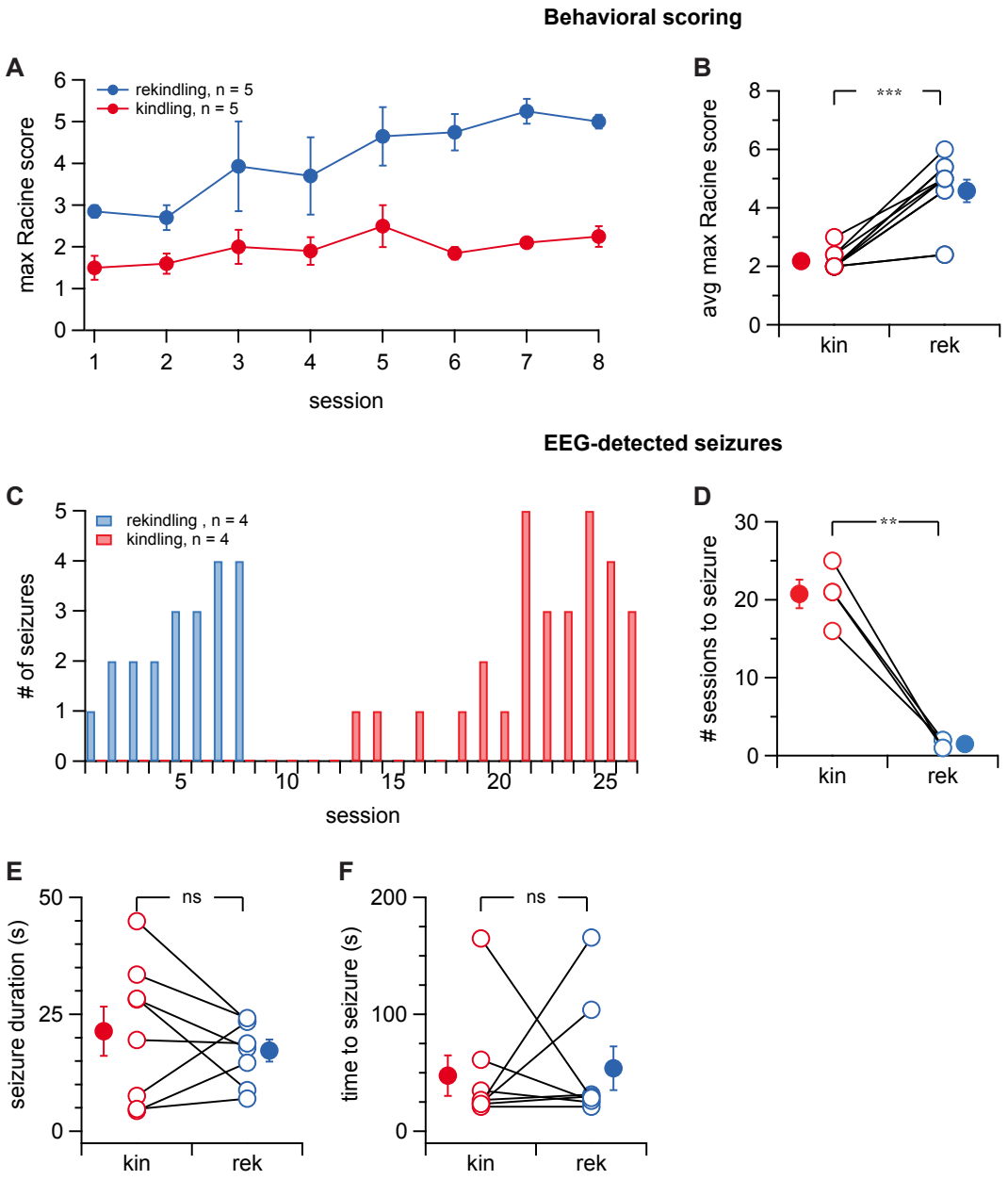

Figure 2.3 Kindled animals retained a long-term increase in seizure susceptibility

(A) Rekindled mice had more severe behavioral seizures compared to naïve animals (Kruskal-Wallis test, $p < 0.001$, n = 5 rekindled animals, n = 5 naïve animals). Racine scores from the eight rekindling sessions (blue) were compared with the first eight sessions in naïve animals (red).

(B) Rekindled animals (“rek”) had more severe behavioral seizures than naïve animals (“kin”; Student’s paired *t* test, $p = 0.009$, $n = 5$ animals).

(C) Electrographic seizures in rekindled animals occurred in earlier sessions than in naïve mice (Mann-Whitney’s $U = 183.5$, $p < 0.001$, $n = 4$ animals).

(D) Electrographic seizures in rekindled mice occurred after fewer sessions than in naïve animals (Student’s paired *t* test, $p = 0.003$, $n = 4$ animals).

(E) Electrographic seizure duration was indistinguishable between kindled and rekindled animals (Student’s paired *t* test, $p = 0.43$, $n = 4$ animals).

(F) The seizure threshold, as measured by time to electrographic seizure onset after start of light stimulation (see **Figure 2.1**), was not different in kindled and rekindled mice (Student’s paired *t* test, $p = 0.86$, $n = 4$ animals).

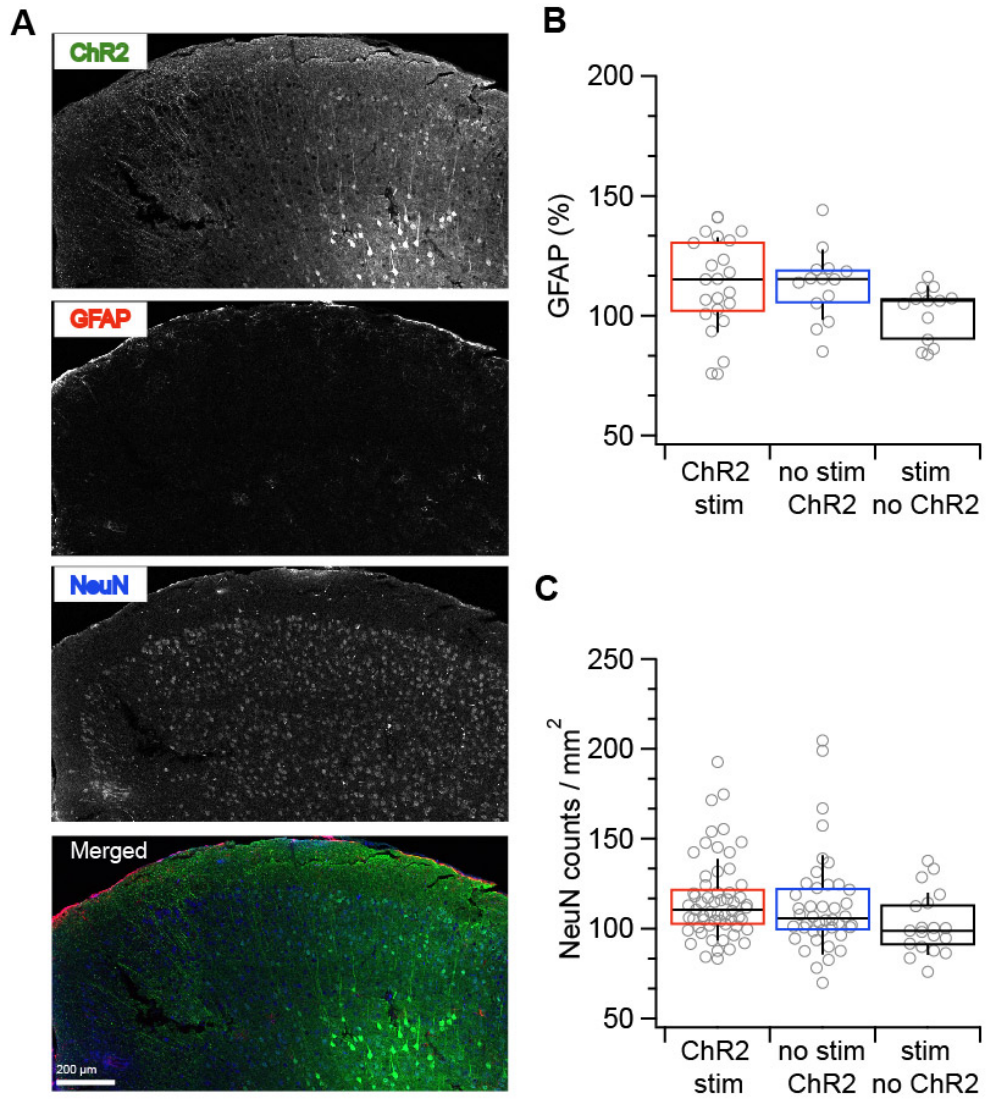

Figure 2.4 Immunohistology revealed no astrocytic reactivity or neuronal loss

(A) Sample coronal slices from an optogenetically kindled animal stained for EYFP to tag ChR2-expressing cells ("ChR2"), GFAP to label for astrocytic reactivity ("GFAP"), and NeuN to assess neuronal cell body counts ("NeuN").

(B) Astrocytic reactivity, as indicated by upregulated GFAP expression, was indistinguishable between animals with evoked seizures ("ChR2 stim", n = 59 sections) and the two control groups ("no stim ChR2", n = 42; "stim no ChR2", n = 19; one-way ANOVA, p = 0.11).

(C) Neuronal cell density did not differ between the three animal cohorts ("ChR2 stim", n = 23, "no stim ChR2", n = 14 and "stim no ChR2", n = 13, one-way ANOVA, p = 0.10; compare **Figure 2.4A**).

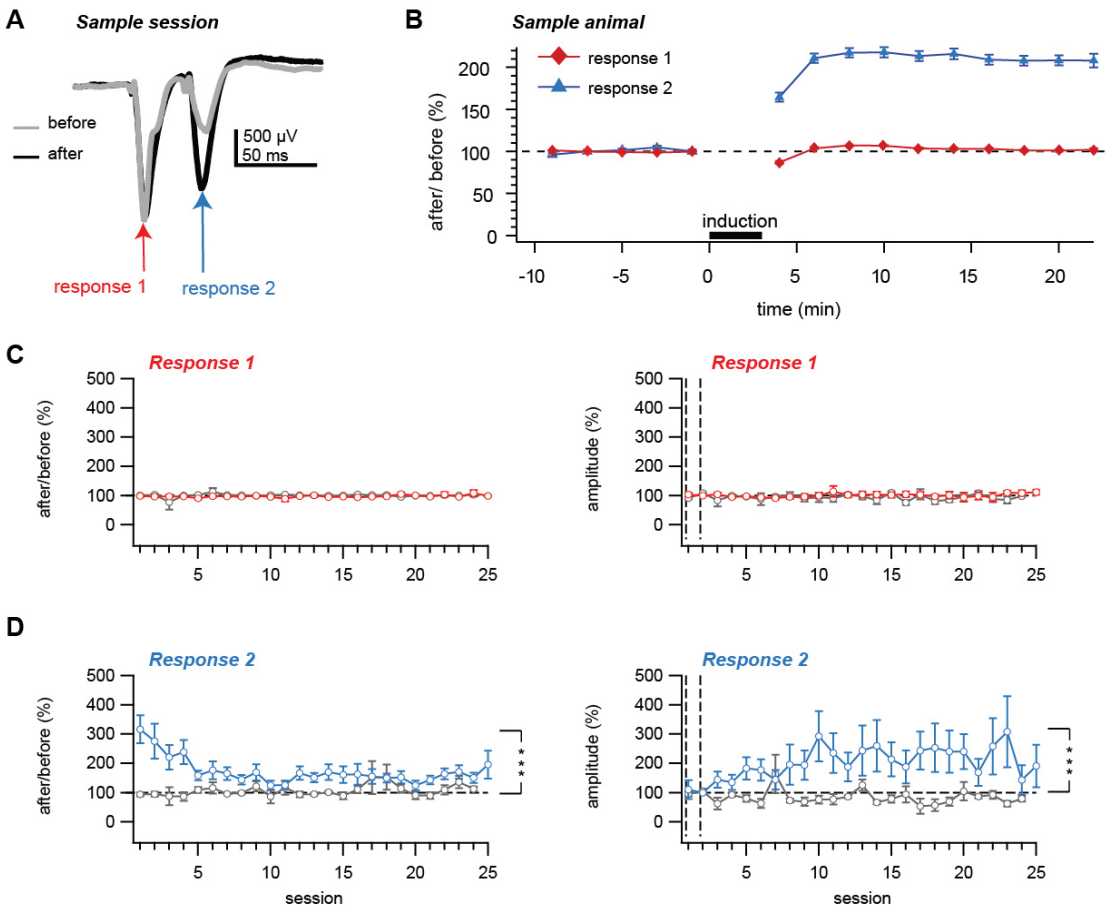

Figure 2.5 Evoked EEG responses exhibited long-term plasticity

(A) Example first and second EEG responses due to paired-pulse laser stimulation averaged during baseline periods before and after induction in one session.

(B) Ensemble EEG response amplitude averaged across all sessions in one animal showed a within-session potentiation of the second but not the first response.

(C) The magnitude of plasticity of the first EEG response remained unaffected across sessions and animals (left, $p = 0.32$, $n = 9$ stim ChR2 animals vs. $n = 4$ no stim ChR2 animals, Friedman test). The pre-induction baseline first response remained at the same amplitude across sessions and animals (right, responses normalized to the first two sessions indicated by vertical dashed lines, $p = 0.99$, stim ChR2 vs. no stim ChR2, Friedman test). Red: stim ChR2, gray: no stim ChR2.

(D) The magnitude of plasticity of the second EEG response remained elevated across sessions and animals (left, $p < 0.001$, stim ChR2 vs. no stim ChR2, Friedman test), although waned in the first five sessions. The pre-induction baseline second response remained potentiated across sessions and animals (right, normalized as in C, $p < 0.001$, stim ChR2 vs. no stim ChR2, Friedman test), although seemed to saturate, perhaps as plasticity waned (left). Blue: stim ChR2, gray: no stim ChR2.

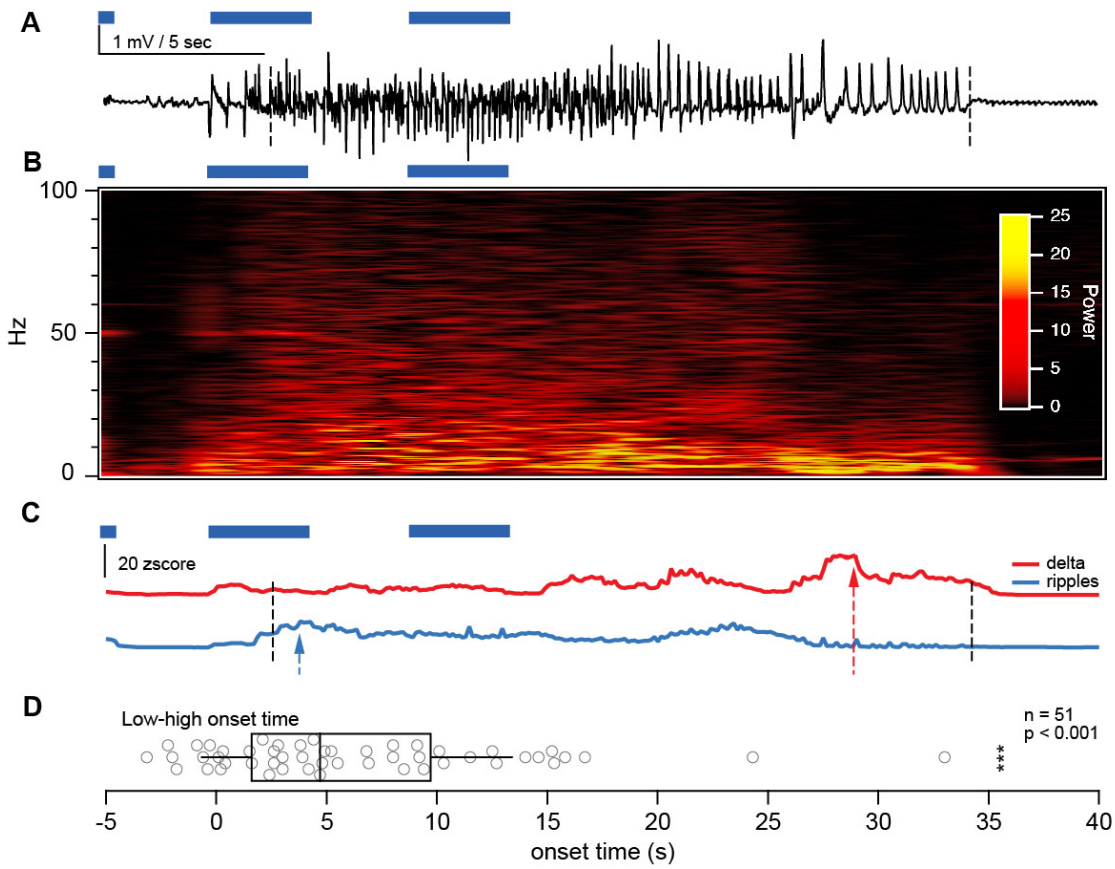

Figure 2.6 High-frequency oscillations peak before low-frequency oscillations

(A) Sample EEG trace illustrating an optogenetically evoked electrographic seizure, with automatically detected seizure start and end indicated by vertical dashed lines (see Methods). Note that seizure begins with rapid oscillations and ends with slow oscillations. Laser-light stimulation bouts are indicated in blue.

(B) Wigner transform of electrographic seizure in (A) showing graded decay in high-frequency components as well as a gradual increase in low-frequency power.

(C) FFT power z-score traces for delta (red, 4-8 Hz) and ripple bands (blue, 80-250 Hz) derived from the EEG trace in (A) shows how high-frequency oscillations peak (blue arrow) before their low-frequency counterparts (red arrow).

(D) Peak power of high frequencies occurred earlier compared with that of low frequencies (6.4 ± 1 sec, n = 51 seizures from 9 animals, $p < 0.001$, *t* test for difference of mean compared to time zero). Data points indicate the difference between the low and high frequency peak times for individual seizures. Box plot shows first quartile, median, and third quartile with whiskers denoting one standard deviation from the mean

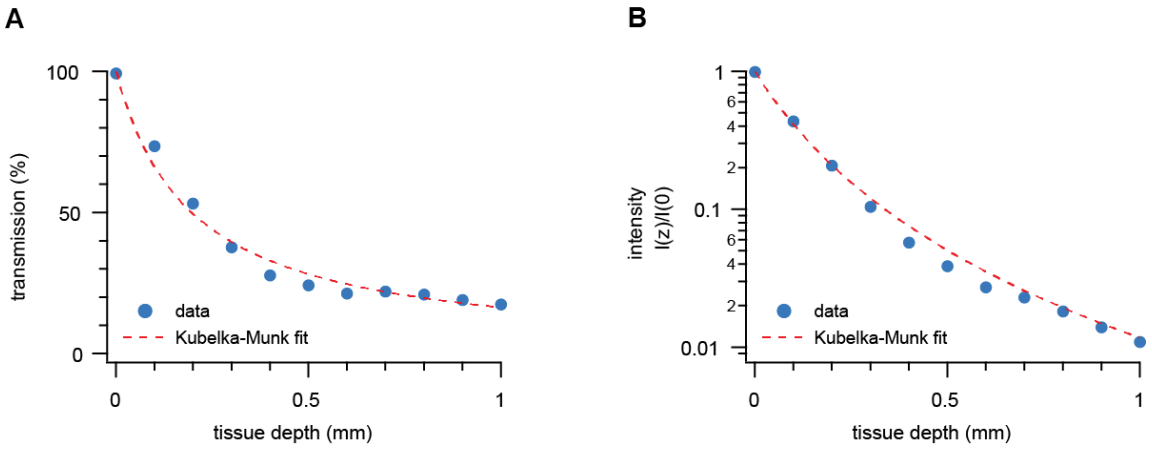

Figure 2.7 Laser light at 445 nm penetrated the neocortical thickness

(A) The Kubelka-Munk model of light transmission through diffuse scattering media (Kubelka, 1948; Mobley and Vo-Dinh, 2003) fit our acquired transmission data well (scatter coefficient $S = 5.09$/mm, $Chi^2 = 0.0013$; n = 2 measurements per data point).

(B) Normalized light intensity as a function of the tissue depth, *z*, was also well fit by Kubelka-Munk's equation (scatter coefficient $S = 4.35$/mm, Chi-squared = 0.013). This treatment accounts for geometric loss and scattering of light for a 200-µm-diameter 0.37-NA multimode fiber (Aravanis et al., 2007).

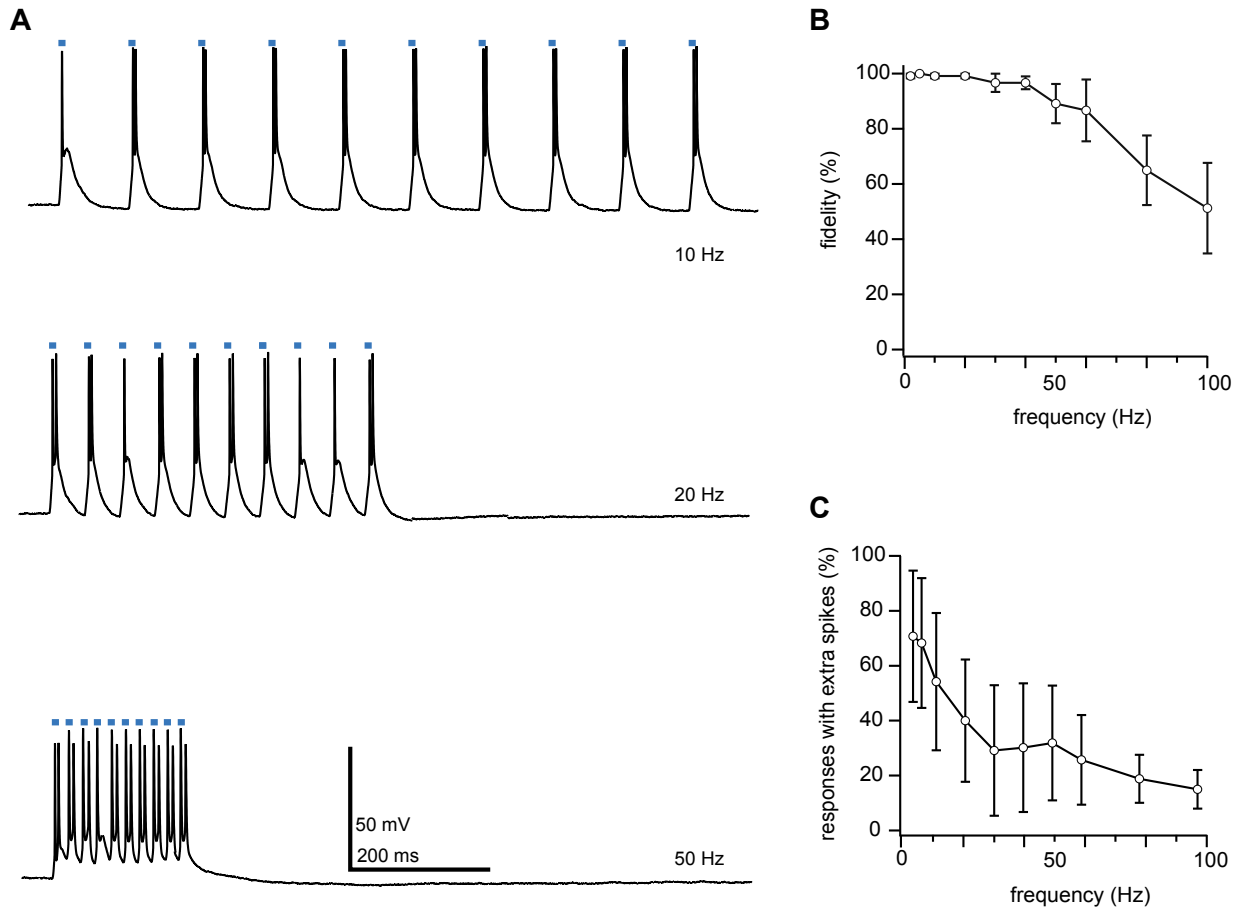

Figure 2.8 ChR2-expressing PCs can be reliably driven at 50 Hz

(A) Representative spike trains in response to 50, 20 and 10 Hz light stimulation (blue lines) recorded from PCs in current clamp.

(B) Spiking was reliably evoked at stimulation frequencies up to 50 Hz (n = 4 cells, 89% ± 7% fidelity).

(C) Percent responses from (B) with extra spikes. Responses with one or more extra spikes per stimulus were counted once per response. Percentage was calculated as number of responses out of the total that had extra spikes in response to light stimulation per given frequency (n = 4 cells).

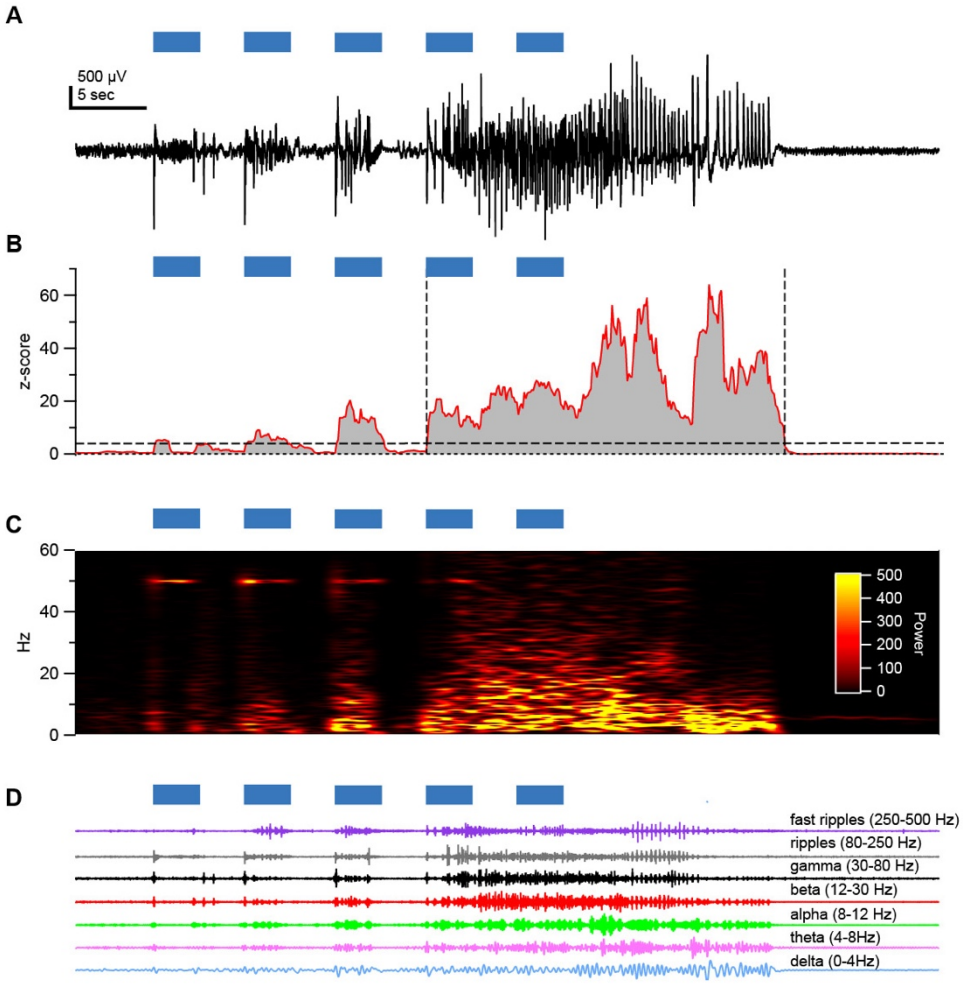

Figure 2.9 Automatic electrographic seizure detection.

(A) EEG of representative optogenetically-evoked seizure with light stimulation depicted in blue. Seizure is evoked after several bouts of light stimulation.

(B) Corresponding z-score values from seizure in (A) showing duration of seizure between dashed lines (horizontal and vertical) used in detection algorithm for identifying seizures. Criteria for detection of the seizure in (A) was met both in duration and amplitude.

(C) Wigner transform of trace in (A) showing prominent power signature at 50Hz as well as increases in lower power amplitudes as seizure emerges.

(D) Filtering of trace in (A) shows frequency bands from delta to fast ripples.

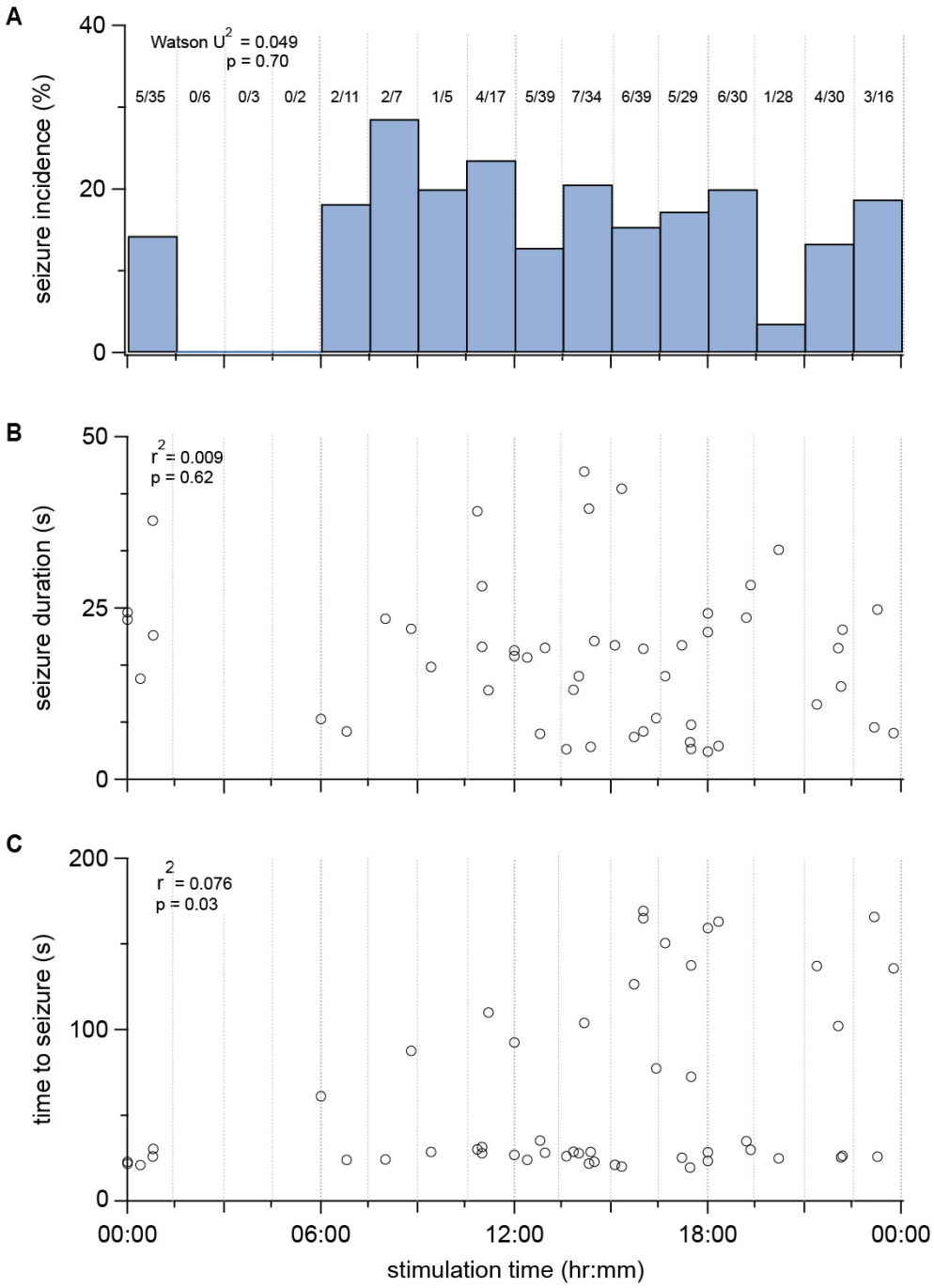

Figure 2.10 Seizure threshold depended weakly on circadian time

(A) Incidence of evoked seizures was not correlated with circadian time (Watson's Two Sample U^2 test, p = 0.70, n = 51 seizures from 9 animals). Kindling and rekindling seizures were pooled.

(B) Seizure duration was not correlated with stimulation time (Circular-linear correlation, $r^2 = 0.009$, $p = 0.62$, $n = 51$ seizures from 9 animals).

(C) Time to seizure from light onset — a measure of seizure threshold (**Figure 2.2)** — was weakly correlated with stimulation time (Circular-linear correlation, $r^2 = 0.076$, $p = 0.03$, $n = 9$ animals).

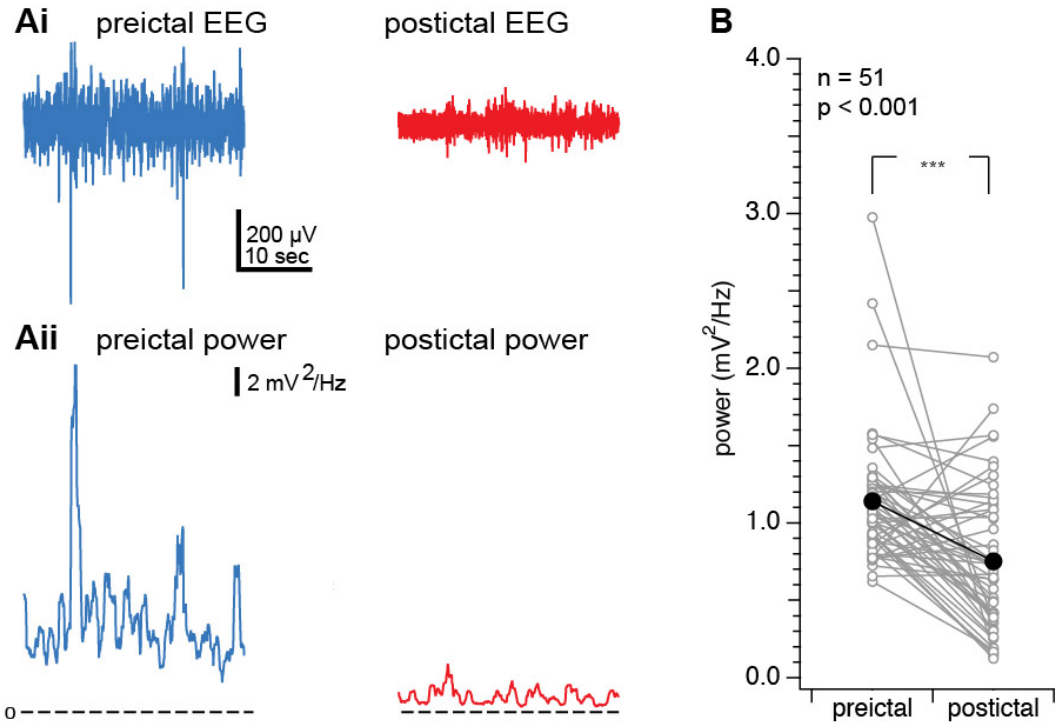

Figure 2.11 Post-ictal depression followed optogenetically elicited seizures

(A) Sample preictal EEG trace (Ai) from a laser-stimulated ChR2-expressing animal was of considerably larger power (Aii) than the corresponding postictal EEG (Ai right, Aii right). Dashed lines in Aii indicate zero power level.

(B) Average EEG power was lower after (0.75 ± 0.06, $n = 51$ seizures from 9 animals) compared with before seizures (1.14 ± 0.06, Wilcoxon signed rank test, $p < 0.001$). EEG postictal and preictal power was measured 200 seconds after and before evoked seizures.

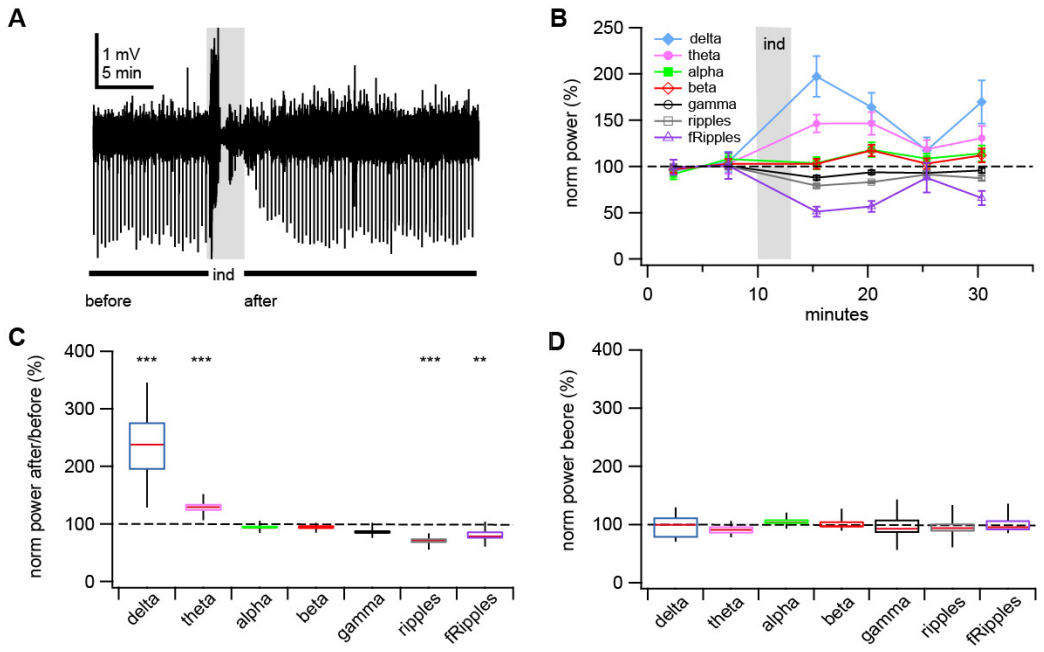

Figure 2.12 Frequency dynamics change within but not across sessions

(**A**) Representative EEG traces showing periods before, during and after induction in an optogenetically-kindled, ChR2-expressing animal.

(**B**) Normalized power of different frequency bands over one stimulation session in one animal corresponding to the EEG shown in (A). Induction period where 50Hz stimulation was applied is shaded in grey.

(**C**) To look for plasticity in the frequency dynamics, we measured the power of each band over the stimulation period (excluding the induction) and compared the normalized power after induction with that before (as in **Figure 2.12**), but across all sessions (analogous to **Figure 2.5**). On average, normalized power of delta, theta and fast ripples was elevated after induction while ripple power was reduced n = 9 animals, 25 sessions/animal, One-way ANOVA, delta $p < 0.001$; theta $p < 0.001$; ripples $p < 0.001$, fast ripples $p = 0.007$), indicating a form of frequency band plasticity within sessions.

(**D**) To see if the plasticity in frequency dynamics persisted across sessions, we measured the power of each frequency band in the baseline period before induction, averaged across sessions, and normalized to the power of each session to enable cross-animal comparison (analogous to **Figure 2.5**). Normalized power did not change across sessions for any frequency band (n = 9 animals, One-way ANOVA, delta, beta, ripples, gamma, fast ripples p = 0.99; alpha p = 0.78; theta p = 0.16), arguing against this possibility.

Table 2.1 The modified Racine scale used to score seizures

We used a modified variant of Racine's scale (Haas et al., 1990; Racine, 1972b) to score evoked seizure behavior in parallel movies recorded with two cameras (see Methods).

Racine score	Description of behavior
1	Mouth and facial movements
2	Head nodding
3	Unilateral forelimb clonus
4	Bilateral forelimb clonus with rearing
5	Rearing and falling
6	Wild running, jumping, vocalizations

3 CB1R BLOCKADE ACCELERATES SEIZURES DURING NEOCORTICAL OPTOKINDLING

3.1 Preamble to Chapter 3

In **Chapter 2** I built and characterized an optokindling model allowing seizure induction in initially healthy mice using repeated light stimulation over long time periods. The optokindling model recapitulated several key features of kindling such as long-term seizure retention and threshold reduction over time. However, while the model was highly effective (75% of mice eventually developed seizures), it took an average of ~13 session of stimulation before seizures emerged. Thus, I sought to reduce the labour and time constraints associated with optokindling. In this chapter, I explore how to accelerate seizure induction by combining optokindling with CB1R blockade in a two-hit model of seizures. Taken together, these experiments supplement and expand the utility of the optokindling model.

3.2 Abstract

Current chemically and electrically induced epilepsy models suffer from tissue damage and lack of cell specificity. Our recently developed optokindling model (Cela et al., 2019) circumvents these challenges but takes requires long-term continuous stimulation. We therefore sought to modify the current kindling protocol.

We wanted to test the possibility of using a two-hit approach in conjunction with our optokindling model. Thus, we employed co-administration of the cannabinoid-1 receptor (CB1R) antagonist rimonabant to animals before optogenetic stimulations to accelerate seizure development.

To induce seizures, Channelrhodopsin-2 (ChR2) expressing neocortical PCs of awake behaving C57BL/6 mice were briefly activated for at least 8 sessions every 48 hours. Behavioral severity was manually Racine-scored from video recordings, while seizures were automatically quantified offline from EEG.

Rimonabant injections accelerated seizure development and increased behavioral severity of seizures. However, neither seizure threshold nor seizure duration changed over sessions as with our original optokindling protocol.

To sum up, CB1R blockade can accelerate seizures in a two-hit model combined with optokindling.

3.3 Introduction

The electrical kindling model has been influential in scope and significance of discoveries of the epileptic brain (Goddard, 1967). However, it is associated with gross tissue damage and

the identity of stimulated cells is unknown (Pitkänen et al., 2009a). These factors have prevented the model from being utilized to investigate circuit properties during seizure formation at a neuronal level. We recently developed an optogenetic alternative that circumvents these problems and is able to effectively mirror several key properties of kindling. Nonetheless, this optokindling model has similar disadvantages as electrical kindling in labour and time costs required to prepare fully kindled animals. To circumvent the original time and labour constraints of electrical kindling, investigators have taken different approaches (Löscher, 2011b).

One approach to accelerate seizure development through kindling has been to take advantage of the multiple factors contributing to seizure generation which can act together in synchrony (Löscher, 2011b). As an example, in two-hit models of seizures, an initial seizure generating insult is paired with a second acquired or experimental factor that results in accelerated seizure generation (Berkovic et al., 2006). One potential factor that can accelerate seizures is modifying the activity of the CB1R. Indeed, CB1R has been well studied in context of epilepsy and it's known that knocking it out or reducing its activity both results in lowered seizure threshold and hyperexcitability (Marsicano et al., 2003; Vinogradova et al., 2011). We took advantage of this fact to inject the CB1R antagonist rimonabant before optokindling sessions.

In our experiments, rimonabant administration prior to optokindling accelerated seizure development and may prove as a useful alternative to the original optokindling protocol. Since the optically kindled neuronal identities are known, this two-hit approach enables circuit and neuronal changes associated with seizures to be studied on a shorter time scale than optokindling alone.

3.4 Materials and methods

Ethics

All procedures conformed to the standards and guidelines set in place the *Canadian Council on Animal Care* (CACC) and the *Montreal General Hospital Facility Animal Care Committee* (FACC), with the appropriate license. For surgeries, animals were anesthetized with isoflurane (CDMV Inc., St-Hyacinthe, QC, Canada). For collection of acute slices, mice were anesthetized with Avertin (Sigma Aldrich, Oakville, ON, Canada) or isoflurane and sacrificed once the hind-limb withdrawal reflex was lost. Every attempt was made to ensure minimum discomfort of the animals

3.4.1 Stereotaxic viral injections and EEG screw implantation

We targeted ChR2 to primary motor cortex (M1) of male C57BL/6J mice aged postnatal day (P) 30-45 using bilateral stereotaxic injection of AAV-CaMKIIα-hChR2-E123T/T159C-p2A-EYFP (UNC Virus Core, North Carolina, USA), since two kindling sites are known to function better than one (Teskey et al., 1999). Virus from plasmid constructs contributed by Karl Deisseroth was packaged by UNC Vector Core into serotype 5 AAVs. Using a stereotactic apparatus (Just for Mouse 5731, Stoelting Inc, Wood Dale, IL, USA), we injected 1.2 μL of virus bilaterally, following previously described procedures(Cardin et al., 2010). Injection coordinates relative to bregma were 1.1 mm anteroposterior, 1.5 mm mediolateral and 0.8 mm dorsoventral. We subsequently placed and cemented 1.25 mm ceramic ferrules (CFC-230, Thorlabs, Newton, NJ, USA) over the injected region of each hemisphere at the same coordinates as injection. Coincident with viral injection and ferrule placement, we also implanted recording and ground screws (1/8”, 000-120 thread, 90910A600, McMaster-Carr, Elmhurst, Illinois, USA), which were stabilized with dental

cement (Lang Dental, Wheeling, IL, USA). The coordinates for recording screws typically centered around ±3 mm mediolateral, -0.6 mm anteroposterior while the reference screws were placed at ± 3 mm ML and -4mm AP. The screws had conductive wire soldered on and were connected to gold-plated jacks (64-132, Warner Instruments, Hamden, CT, USA; or 33X1880, Newark Electronics, Pointe Claire, QC, Canada) for EEG recordings. We used a separate ground reference screw for the left and right hemisphere.

3.4.2 *In-vivo* recordings and optogenetic stimulation

Animals were given 21 days to recover from surgery after which, they were habituated for three days to the recording setup before commencing stimulation sessions. The recording cage consisted of a 30-cm diameter wide and 40-cm tall Plexiglas cylinder covered with copper mesh and with a copper bottom. To reduce noise by serving as a Faraday cage, the copper plate and mesh of the cage were connected to the amplifier chassis ground. Two 445-nm blue lasers (Monopower-455-150-MM-TEC, Alphalas Gmbh, Germany) on kinematic V-clamp post mounts (C1513/M, Thorlabs, Newton, NJ, USA) for ease of alignment, were air coupled (aspheric FC/PC fiber port PAF-X-18-PC-A with HCP mounting bracket, Thorlabs, Newton, NJ, USA) to two two-meter-long fiber-optic patch cords (M83L01, Thorlabs, Newton, NJ, USA), coupled to 1.25-mm bilaterally head-mounted ceramic ferrules (CFLC230-10, Thorlabs, Newton, NJ, USA). The light power exiting the fiber was ~50 mW; it was measured before and after every stimulation session to ensure it remained stable. EEGs were collected at 2-10 kHz with an extracellular amplifier (Model 1700, AM Systems, Sequim, WA, USA) and were digitized on a PCI-6221 board (National Instruments, Austin, TX, USA) using in-house software running in Igor Pro 6.37 (Wavemetrics Inc., Lake Oswego, OR, USA) on a desktop computer (Micro Tower Desktop PC SL-DK-H61MX-ID,

SuperLogics, Natick, MA) running Windows XP SP7. This computer also episodically TTL-gated the two 445-nm lasers. Animal behavior was recorded with two cameras, one above the recording setup, and one to the side (Logitech C525 webcam, Tiger Direct.ca Inc., Calgary, AB, Canada). Video was acquired using ISPYConnect software (https://www.ispyconnect.com) running on the EEG acquisition computer. To score severity of seizures from these videos, we used a modified Racine scale **(Table 2.1)**. If behavior seemed to straddle two Racine stages, the score was taken as the intermediate value, e.g. 4.5 if between 4 and 5.

Mice were stimulated every 48 hours with the same protocol lasting approximately 33 minutes. Stimulation sessions were numbered sequentially starting at one. Each session consisted of an initial 10-minute-long baseline period, a three-minute-long induction, and a second 20-minute-long baseline. Baseline stimulation consisted of two 10-ms 445-nm laser pulses delivered at 30 Hz every 10 seconds. The induction period consisted of five bouts of three seconds of 50-Hz stimulation at 50% duty cycle and three second inter-bout interval, repeated three times once a minute (**Figure 2.1**).

3.4.3 Automated seizure detection

To independently detect seizures offline, a simple automatic seizure detection software algorithm was developed. Although this approach had the disadvantage of missing the occasional seizure that was detected by inspection, it was preferred because it was unbiased and — as opposed to manual inspection —invariably gave the same results when rerun on the same EEG sweeps.

EEG Fourier power traces were first converted to z-score sweeps. For z-scoring purposes, the background power levels were determined from the median of at least 64 one-second-long EEG segments recorded in the absence of laser stimulation. The median was used to automatically exclude the occasional and relatively rare movement artifact, because such artifacts resulted in massive responses that typically saturated the amplifier for about a second at a time.

To detect seizures, a combined threshold and duration criterion was applied. If power exceeded z-score 4 for longer than 4 seconds, then this event was deemed a seizure. EYFP and ChR2 control animals were used to determine these threshold values, whereby which no seizures were detected in the control mice. Z-scores above 100 were always rejected as movement artifacts. The start of a seizure was taken as the z-score threshold crossing. Seizure duration was automatically determined from seizure start to the first z-score downstroke threshold crossing. No attempt was made to merge nearby events separated by a brief time of relative inactivity, so automatically detected seizures were likely underestimated both in terms of number and duration.

3.4.4 Rimonabant injection

Rimonabant (Sigma-Aldrich, SML0800) was mixed with DMSO 0.03% (v/v) solution and injected intraperitoneally 30 minutes before the onset of stimulation sessions. In control animals, we injected DMSO 0.03% (v/v) alone without rimonabant. The final concentration of the drug was 10mg/kg of body weight.

3.4.5 Statistics

The results are reported as the mean ± SEM. Significance levels are denoted using asterisks (*$p < 0.05$, **$p < 0.01$, ***$p < 0.001$). Unless otherwise stated, we used Student's *t* test for equal means for all pairwise comparisons. If an equality of variances *F* test gave $p < 0.05$, we employed the unequal variances *t* test. Individual data sets were tested using a one-sample *t* test. For multiple comparisons, pairwise comparisons were carried out if one-way ANOVA suggested this at the $p < 0.05$ significance level. Equal or unequal variances ANOVA was used depending on Bartlett's test for equal variances. Wilcoxon-Mann-Whitney's non-parametric test was always used in parallel to the *t* test, with similar outcome. Multiple pairwise comparisons were corrected *post hoc* using Bonferroni-Dunn's method. Statistical tests were performed in Igor Pro unless otherwise stated.

3.5 Results

To test the effects of rimonabant on seizure development, we injected rimonabant intraperitoneally 30 minutes before optogenetic kindling (**Figure 3.1**). We measured the number of sessions of stimulation required to elicit the first seizure and found that rimonabant-injected animals had earlier seizure emergence compared to control animals with seizures seen on the first session of stimulation (**Figure 3.2)**.

Next, we quantified the effects of rimonabant on seizure severity over session by Racine scores (n = 5 animals scored over 8 sessions). Rimonabant-injected animals had higher Racine scores, indicating more behaviourally severe seizures, compared to optokindled animals (**Figure 3.2**). Additionally, we measured seizure duration and seizure

threshold in rimonabant-injected animals over sessions and found that neither changed. (**Figure 3.2**)

Finally, to quantify changes in EEG dynamics we measured the differences in low-frequency power in rimonabant treated (n=18 EEGs) compared to DMSO treated controls (n = 5 EEGs) and found that rimonabant promotes higher powers of delta, theta and alpha frequencies (**Figure 3.3**).

3.6 Discussion

Epileptogenesis is a complicated process that involves multiple possible concurrent changes in synaptic and cellular functions (Semyanov et al., 2000; Sutula et al., 1988; Vezzani et al., 1995). As a result, animal models of epilepsy often yield a set of variables that are characteristic of the model but the saliency of these findings to seizure activity is not often clear. It is widely accepted there are multiple paths to seizure generation which is part of the reason delaying effective treatment options. Factors such as trauma, genetic predisposition and cortical malformations can predispose patients to seizures at rates higher than the general population (Annegers et al., 1996; Ferguson et al., 2010). Given the complexity of seizure development, the animal models used to study seizures should allow for the potential of exploring interactions amongst several contributing variables. This understanding has manifested itself through the “two-hit hypothesis” which posits that models may be manipulated to explore intersectional contributions to the epileptic brain (Hoffmann et al., 2004; Serbanescu et al., 2004).

One of the key players both in normal LTD and factors of excitability has been the CB1 receptor. This receptor plays critical roles in brain plasticity under normal conditions but has been increasingly found to promote hyperexcitability in the pathological brain as well

(Sjöström et al., 2003; Soltesz et al., 2015). Thus, we decided to test the two-hit hypothesis using our previously published optokindling protocol whilst modifying the activity of the CB1R receptor (Cela et al., 2019). We used IP injections of rimonabant, an inverse agonist of CB1Rs to test if injection into our optogenetically kindled animals would accelerate seizures. Rimonabant's proconvulsive properties are thought to arise by blocking depolarization-induced suppression of inhibition (Armstrong et al., 2009).

Rimonabant was able to accelerate seizure emergence so that seizures emerged earlier than with optogenetic kindling alone (**Figure 3.2).** This finding is corroborated by the literature findings that CB1R antagonism and rimonabant specifically can promote seizures either in conjunction with a second factor such as trauma or alone (Braakman et al., 2009; Dudek et al., 2010; Marsicano et al., 2003; Nissinen et al., 2017). Rimonabant-induced seizures also had worse severity, as measured through Racine score, than their optogenetically-kindled counterparts (**Figure 3.2)**. This in agreement with previous reports of an audiogenic seizure model where clonus incidence increased following rimonabant application (Vinogradova et al., 2011).

Since the severity of seizures was worse in rimonabant-injected animals than optogenetically-kindled, we wondered whether there would be a reflection of this in the power spectra as well. Furthermore, it was previously reported that other CB1R antagonists can increase convulsive seizures as well as change the power spectra at low frequencies (Perescis et al., 2017). These changes in lower frequency power may have behavioural correlates such as theta power being associated with locomotion and active wakefulness while alpha power dysfunction has been implicated in children with epilepsy (Coenen, 1975; Hsu et al., 1994; Hsu et al., 2016; van Lier et al., 2003).

While seizure onset was accelerated upon rimonabant administration, we found that seizure duration did not change over session while seizure latency decreased. In an audiogenic seizure model using rimonabant application in late sessions the reverse was found, a change of seizure latency but not duration was reported (Vinogradova et al., 2011). The discrepancy in the results may be due to the effect CB1R can mediate based on location of seizure initiation In the brain as well as the differences in using a genetic model compared to an acquired model (Ludanyi et al., 2008; van Rijn et al., 2010). The lack of change in seizure duration may be due in part by the fact that rimonabant gives rise to seizures that are all-or-none responses by promoting general hyperexcitability instead of relying on long-term circuit changes and gradual emergence of seizures, as kindling is thought to rely on (Lynch and Sutula, 2000). To sum up, we show that optokindling can be combined with other factors such as rimonabant to act complementarily on seizure occurrence in a two-factor model

3.7 Figures

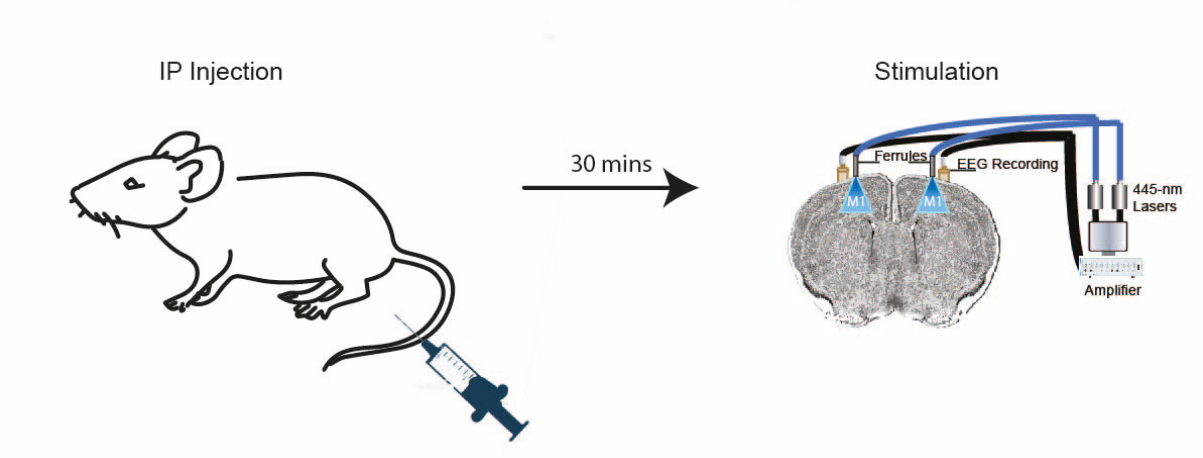

Figure 3.1 Rimonabant injection experimental paradigm.

Animals were injected with 10mg/kg rimonabant intraperitoneally and stimulated 30 minutes after injection. Thereafter they were stimulated with the same optogenetic kindling protocol outlined in **Figure 2.1.**

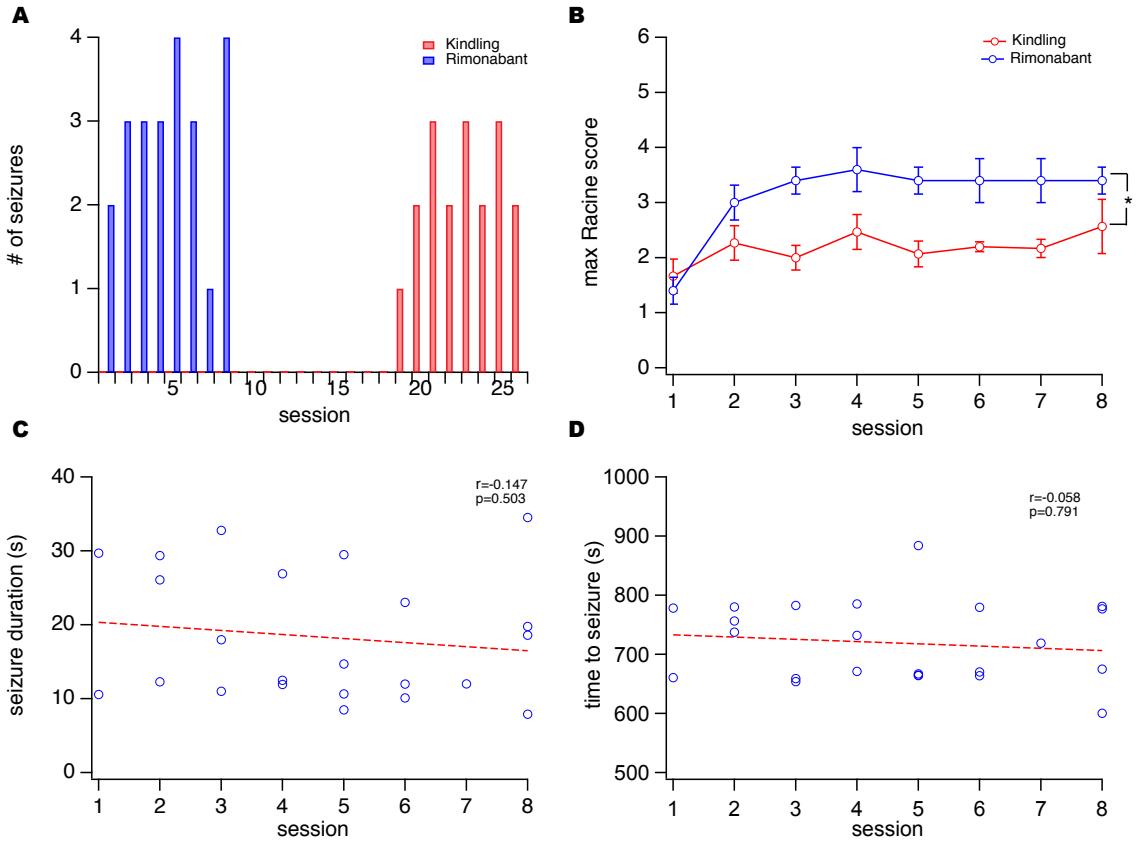

Figure 3.2 Rimonabant accelerates seizure development and severity during optogenetic kindling.

(A) Rimonabant-injected animals have their first seizure sooner than control animals (Mann-Whitney's U = 7.5, p = .001, n = 5 animals rimonabant, n =9 animals kindled).

(B) Rimonabant-injected animals have worse seizure severity than kindled animals (Wilcoxon signed-rank test, n = 5 animals rimonabant, n = 9 animals kindling, p = 0.015).

(C) Seizure duration in rimonabant-injected animals does not change over sessions (Spearman correlation, n = 5 animals, r = -0.147, p = 0.503).

(D) Seizure threshold in rimonabant-injected animals does not change over sessions (Spearman correlation, n = 5 animals, r = -0.058, p = 0.791).

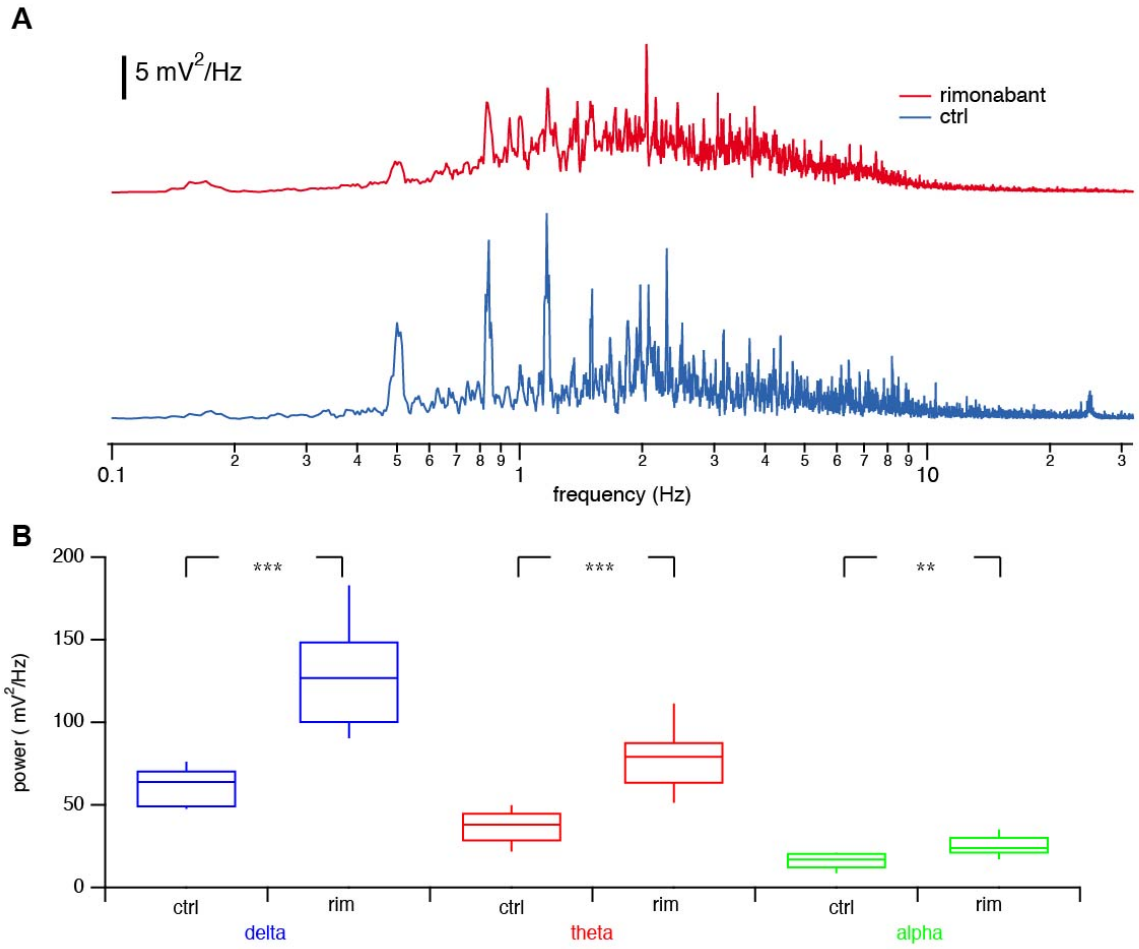

Figure 3.3 Rimonabant promotes lower frequency power during induction period.

(A) Average power band spectra from EEGs of rimonabant injected animals (n = 18 EEGs) and DMSO treated controls (n = 5 EEGs) after outlier removal.

(B) Comparisons of delta (0 - 4Hz,), theta (4 - 8 Hz) and alpha (8 - 12 Hz) average power spectra in EEGs of rimonabant injected animals and DMSO treated controls. Delta power (n = 18 rimonabant EEGs, n = 5 DMSO ctrl, Wilcoxon rank test, $p < 0.001$) theta power (n = 18 rimonabant EEGs, n = 5 DMSO ctrl, Wilcoxon rank test, $p < 0.001$) and alpha power (n= 18 rimonabant EEGs, n = 5 DMSO ctrl, Wilcoxon rank test, $p = 0.007$) are significantly higher in rimonabant EEGs.

4 METHODS FOR MEASURING CIRCUIT CHANGES ASSOCIATED WITH OPTOKINDLING

4.1 Preamble to Chapter 4

In **Chapters 2 and 3** I described the development of a novel optokindling protocol in neocortex and ways it can be modified to accelerate seizure development. Next, I wanted to explore potential methods that can be used to study the circuit changes following seizures *ex-vivo*. The main technique lending itself to this analysis is paired whole-cell patch clam recordings. However, even when using 4 electrodes where up to 12 connections can be tested simultaneously, the low connectivity rate in cortex makes finding connections a labour-intensive endeavour. Thus, I sought out alternatives. This chapter describes several preliminary experiments extending the potential toolset of studying optokindling in rodent animal models *ex-vivo*. The primary objective was to establish a foundation for future studies to use circuit mapping methods in lieu of paired recording to investigate circuit consequences following optokindling seizures. I present data from paired recordings in optokindled and control animals and also from experiments performed with CRACM.

4.2 Abstract

Epilepsy is a common neurological disorder whose cellular basis of pathology is not completely understood. Our recent discovery of optokindling presents a model to address circuit changes during seizures by allowing millisecond-precise activation of genetically defined neurons. We used optokindling in naïve mice to gradually drive seizures over the long-term (up to 25 sessions). Next, we sought to decipher at the neuronal level the effects of optokindling in M1 PCs, the primary target for optogenetic stimulation during optokindling. We first used paired recordings to compare intrinsic properties between optokindled and control animals. Next, we extended a proof-of-principle method for rapidly mapping circuit rewiring following seizures based on previous studies.

Acute brain slices from Channelrhodopsin-2 (ChR2) expressing M1 PCs of kindled and control mice were used for whole-cell patch clamp recording and optogenetic stimulation. In secondary experiments, we used the same ChR2-expressing acute slices with optogenetic illumination through the 4X objective using a 445-nm laser. Channelrhodopsin-assisted circuit mapping (CRACM) to rapidly map out circuit rewiring following seizures was carried out by moving the laser light in an 8 X 8 grid over the slice.

When performing paired recordings, we found no significant differences in several measures of intrinsic properties in optokindled compared to control slices. During our CRACM experiments we saw different efficiency of postsynaptic responses when comparing different delivery methods for ChR2. Further analysis of neocortical PC cell types will have to be performed to understand the complete circuit changes underpinning seizure development.

4.3 Introduction

Epilepsy is a common neurological disorder that involves gradual development of pathological activity in the initially healthy brain. Repeated seizures are the central hallmark of epilepsy and studies of how they arise have primarily focused on seizure generation in animal models though these mechanisms have not been fully elucidated (Fisher et al., 2014). This is in part due to the lack of understanding of the cellular underpinning of seizures due to inability of current models to target specific neuronal populations. Current animal models, while able to effectively induce seizures, are unable to decipher which neurons are impinged in the seizure process.

However, in the last decade, new methods such as optogenetics, along with developments in lasers and transgenic techniques have opened up the potential for new studies capable of resolving mechanisms of seizure generation at the cellular level (Khoshkhoo et al., 2017; Paz et al., 2013). Recently, we developed an optokindling model of epilepsy able to gradually induce seizures in initially healthy animals following stimulation of M1 PCs. Our optokindling protocol combines optical laser stimulation and ChR2 expression in identifiable PCs tagged by the EYFP report (Cela et al., 2019). This model has opened up avenues for exploring the dynamics of neuronal circuits during seizures.

The gold standard for examination of circuit dynamics, and more specifically, synaptic properties, is paired patch clamp recordings. However, this procedure is technically challenging since it requires the use of multiple recording electrodes and is laborious due to the low connectivity (20%) of some neuronal types such as PC-PC connections (Ko et al., 2011; Lefort et al., 2009). Given these disadvantages, methods have been developed which allow faster mapping of synaptic inputs. For example, laser-scanning phototstimulation (LSPS) where UV light is used to uncage glutamate on specific cells can be used (Callaway

and Katz, 1993). Uncaging can be combined with two-photon excitation, which further restricts stimulation to the XFP-tagged cells and is limited to the plane of excitation (Fino and Yuste, 2011). More recently, LSPS has been combined with optogenetic stimulation which allows millisecond activation of targeted ChR2-expressing cells using techniques such as Channelrhodopsin-2-assisted circuit mapping (CRACM) (Brill et al., 2016; Petreanu et al., 2007a; Petreanu et al., 2009). In CRACM, the laser travels in a grid like pattern to evoke presynaptic activation in an acute slice while the postsynaptic cell is recorded in whole-cell configuration. In summary, CRACM presents a viable mapping method for circuits between presynaptic neurons defined by ChR2 expression and postsynaptic neurons that are patched. Therefore, CRACM and LSPS/optogenetic methods be used in lieu of paired recording to interrogate circuit changes following seizures.

Here, we used complementary approached to combine LSPS and optogenetic stimulation in a modified CRACM technique. We combined postsynaptic voltage whole-cell recordings in postsynaptic targeted cells with laser stimulation of presynaptic ChR2 GFP-tagged cells to evaluate the potential of these methods to gauge circuit perturbations following seizures. Second, we used paired recordings to characterize intrinsic properties and connectivity of L2/3 cells in M1. We carried out experiments in optokindled and control animals to evaluate potential circuit changes correlated with seizures. Our LSPS/optogenetics experiments validated the potential of the method to rapidly map multiple presynaptic inputs in affected slices. Using paired recordings, we showed no differences in intrinsic excitability of optokindled compared to control slices. To sum up, we present a complementary approach to circuit mapping using simultaneous laser stimulation of presynaptic ChR2-tagged cells coupled to postsynaptic whole-cell patch recordings in acute slices.

4.4 Materials and Methods

Ethics

All procedures conformed to the standards and guidelines set in place the *Canadian Council on Animal Care* (CACC) and the *Montreal General Hospital Facility Animal Care Committee* (FACC), with the appropriate license. For surgeries, animals were anesthetized with isoflurane (CDMV Inc., St-Hyacinthe, QC, Canada). For collection of acute slices, mice were anesthetized with Avertin (Sigma Aldrich, Oakville, ON, Canada) or isoflurane and sacrificed once the hind-limb withdrawal reflex was lost. Every attempt was made to ensure minimum discomfort of the animals

4.4.1 Stereotaxic viral injections of ChR2

We targeted ChR2 to primary motor cortex (M1) of male C57BL/6J mice aged postnatal day (P) 30-45 using bilateral stereotaxic injection of AAV-CaMKIIα-hChR2-E123T/T159C-p2A-EYFP (UNC Virus Core, North Carolina, USA), since two kindling sites are known to function better than one (Teskey et al., 1999). Virus from plasmid constructs contributed by Karl Deisseroth was packaged by UNC Vector Core into serotype 5 AAVs. Using a stereotactic apparatus (Just for Mouse 5731, Stoelting Inc, Wood Dale, IL, USA), we injected 1.2 μL of virus bilaterally, following previously described procedures (Cardin et al., 2010). Injection coordinates relative to bregma were 1.1 mm anteroposterior, 1.5 mm mediolateral and 0.8 mm dorsoventral.

4.4.2 *In-vitro* acute slice recordings

Mice were anesthetized by an intraperitoneal injection of an Avertin solution (10 g 2,2,2-tribromoethyl alcohol, Sigma Aldrich T4,840-2, mixed with 10 ml of tert-amyl alcohol, Sigma Aldrich 24,048-6) at 500 mg/kg body weight. The animals were then perfused transcardially with an ice-cold (4˚C) oxygenated N-methyl-d-glucamine (NMDG) solution containing (in mM: 93 NMDG, 93 HCl, 2.5 KCl, 1.2 NaH_2PO_4, 30 $NaHCO_3$, 20 HEPES, 25 glucose, 5 sodium ascorbate, 3 sodium pyruvate, 10 $MgSO_4$ and 0.5 $CaCl_2$ bubbled with 95% O_2/5% CO_2 (Ting et al., 2014). After decapitation, the brain was removed and placed into the same cold NMDG solution. Coronal 300-µm-thick acute brain slices were prepared on a Campden Instruments 5000 mz-2 vibratome (Loughborough, UK) using ceramic blades (Lafayette Instrument, Lafayette, IN, USA). The brain slices were then kept at 33˚C in oxygenated NMDG solution for 10 minutes, after which they were transferred to an incubation solution (containing in mM: 125 NaCl, 2.5 KCl, 1 $MgCl_2$, 1.25 NaH_2PO_4, 2 $CaCl_2$, 26 $NaHCO_3$ and 25 glucose, bubbled with 95% O_2/5% CO_2) and kept for 1 hour before recording. Neurons were patched with pipettes (4-6 MΩ) filled with a gluconate-based current-clamp solution containing (in mM): 5 KCl, 115 K-gluconate, 10 K-HEPES, 4 Mg-ATP, 0.3 Na-GTP, 10 Na_2-phosphocreatine and 0.02-0.04 Alexa Fluor 594, adjusted to pH 7.2-7.4 with KOH and to 310 mOsm with sucrose. Patch pipettes were pulled from medium-wall capillaries using a P-1000 electrode puller (Sutter Instruments, Novato, CA, USA). Whole-cell recordings were obtained using BVC-700A (Dagan Corporation, Minneapolis, MN, USA). Voltage signals were digitized at 10 kHz using PCI-6229 boards (National Instruments, Austin, TX, USA) and custom software (Sjostrom et al., 2001) running in Igor Pro (Wavemetrics Inc., Lake Oswego, OR, USA). L2/3 PCs were targeted for recording using a 2PLSM rig custom-built from a SliceScope (Scientifica, Uckfield, UK) as previously

described (Buchanan et al., 2012). A MaiTai BB laser (Spectraphysics, Santa Clara, CA, USA) tuned to 900-920 nm was used to generate GFP/Alexa 594 fluorescence.

4.4.3 *In utero* electroporation

Animals were housed under standard conditions with free access to food and water on a 12h/12h light/dark cycle. *In utero* electroporation was based on already published techniques (dal Maschio et al., 2012). Briefly, timed-pregnant female CD1 mice from Charles River Laboratories (Senneville, Quebec) had surgeries performed on them corresponding to embryonic day 15.5. Females were anesthetized with isoflurane and the uterine horns and embryos were exposed after abdominal incision. A 3ul DNA plasmid containing Fast Green dye (MilliporeSigma, Oakville, Ontario) (0.1% w/v) and the DNA construct pCAG-ChR2-YFP was injected into the ventricles of the embryo using a polished glass capillary. Next, 5x50ms 45 V pulses at 950ms intervals were applied using an ECM 830 square pulse generator (BTX, Holliston MA). During the procedure, the embryos were periodically flushed with 37°C sterile PBS. After placing the embryos back into the mother, the abdomen was sutured, and the mothers were returned to their home cage until full recovery.

4.4.4 Optogenetic stimulation

To characterize ChR2 responses to light, we relied on the imaging and electrophysiology platform described above, with an additional 445-nm blue laser (eBay.ca, seller: newgazer) guided onto the same light path as the 2-photon beam and controlled with two galvanometric mirrors (Cambridge Technologies, Bedford, MA, USA). The laser was controlled by the same program running electrophysiological acquisition running home-made software in Igor Pro.

4.4.5 Statistics

The results are reported as the mean ± SEM. Significance levels are denoted using asterisks (*p < 0.05, **p < 0.01, ***p < 0.001). Unless otherwise stated, we used Student's *t* test for equal means for all pairwise comparisons. If an equality of variances *F* test gave p < 0.05, we employed the unequal variances *t* test. Individual data sets were tested using a one-sample *t* test. For multiple comparisons, pairwise comparisons were carried out if one-way ANOVA suggested this at the p < 0.05 significance level. Equal or unequal variances ANOVA was used depending on Bartlett's test for equal variances. Wilcoxon-Mann-Whitney's non-parametric test was always used in parallel to the *t* test, with similar outcome. Multiple pairwise comparisons were corrected *post hoc* using Bonferroni-Dunn's method. Statistical tests were performed in Igor Pro unless otherwise stated.

4.5 Results

4.5.1 Laser-scanning ChR2-assisted optogenetic circuit mapping

We obtained acute slices from optokindled and control animals expressing the high-efficiency E123T/T159C ChR2 variant in M1 PCs under control of the CaMKIIα promoter (Cela et al., 2019). Using focal blue light (455-nm) illumination we excited ChR2-expressing cells in a semi-random order over an 8-by-8 grid under the 4X objective corresponding to roughly 1mm^2 of tissue (**Figure 4.1B**). The postsynaptic cell was whole-cell patch clamped and no synaptic blockers were used. 8-by-8 colour coded grids were made corresponding to the average of 20 responses (**Figure 4.1C**). Next we measured the relationship between power intensity and mean response amplitude starting at 100% power (13mW) and found a strong positive correlation (r = 0.994, p < 0.001) (**Figure 4.2A**). We also observed that

stronger optogenetic stimulation was correlated with increased variance of the response in the postsynaptic cell ($r = 0.966$, $p = 0.002$) (**Figure 4.2B**). The optogenetically-evoked responses on the postsynaptic cell had low temporal jitter and latency in milliseconds between presynaptic stimulation and response **(Figure 4.3)**. Though all the data thus far was collected from optokindled animals which had ChR2 virally expressed, we wondered if we can express ChR2 using alternative methods. To achieve this, pCAG-ChR2-EYFP was injected in the lateral ventricles using in-utero electroporation (IUE) at embryonic day 15.5 (E15.5). We noticed that IUE-infected slices had lower overall GFP expression (data not shown) and when measuring average optogenetically evoked-response, those from viral injected sliced had ~30% greater response amplitude **(Figure 4.4)**.

4.5.2 Intrinsic cellular properties were not affected by optokindling

Repeated high-frequency firing can alter the excitability of cortical PCs (Cudmore and Turrigiano, 2004). We therefore wondered if optokindling gave rise to changes in intrinsic neuronal properties such as spike threshold, input resistance, or resting membrane potential. To explore this possibility, we recorded in acute slices the spiking responses of L2/3 PCs to gradually increasing current injections (**Figure 4.5**). We found, however, that none of the intrinsic cellular properties that we investigated were affected by the repeated high-frequency stimulation of optokindling. Kindling may also involve structural changes such as connectivity differences in the long term. To explore if optokindling was associated with connectivity changes, we compared number of connections in optokindled and control slices recorded from L2/3 PC pairs (**Figure 4.6**). We found however no differences in connectivity rates.

4.6 Discussion

Epileptogenesis is thought to involve several changes in both morphology and structure that are associated with seizure initiation, yet the exact circuit underpinnings have not been resolved (Geinisman et al., 1988b; Teskey et al., 2006). Since animal models of seizures have been unable to target specific neurons until recently, we took advantage of our published optokindling model to evoke seizures through repeated PC stimulation (Cela et al., 2019). To study circuit changes following seizures, we took two approaches: using optogenetic/LSPS in optokindled and control slices as well as paired patch clamp recordings. We found no differences in intrinsic properties between PCs in L2/3 of optokindled animals and controls. Analysis of connectivity rates of PCs recorded from optokindled and control animals also revealed no differences. Finally, we performed proof-of-principle experiments based on CRACM as to demonstrate a means of mapping multiple presynaptic inputs following seizures.

4.6.1 Circuit changes accompanying following optokindling

Disfunction in intrinsic properties are well understood to underlie several neurological disorders including epilepsy (Beck and Yaari, 2008). The exact mechanisms in seizures are not yet clear but it is believed to involve changes in the excitatory/inhibitory balance and circuit dynamics (Shah et al., 2004). In our optokindling model, plasticity was linked to epileptogenesis in, although the specific nature of this plasticity remains to be uncovered. Our measurements of several intrinsic properties at the end of optokindling showed no difference compared to non-stimulated animals, suggesting other changes in the circuits are necessary to allow development of seizures, but it isn't clear what they are. Our results were consistent

with previous reports finding no differences in intrinsic properties in epileptic animals (Avoli and Olivier, 1989; Prince and Wong, 1981). Subsequent studies impacting different cell populations besides PCs may prove useful to uncover potential population-specific intrinsic changes. Further analysis of connectivity rates from optokindled and control slices also revealed no differences. Increased synaptic connectivity has been previously associated with epilepsy but not connectivity rate per se (Chu et al., 2010). It could be that recording in adult slices fails to capture the connectivity changes reported during developmental studies. Another possibility is that the excitatory-inhibitory balance could be perturbed in cell types that were not investigated such as interneurons. For example, enhanced intrinsic excitability in basket cells can maintain excitatory-inhibitory balance (Campanac et al., 2013). Finally, our optokindling protocol may be too mild to cause significant increases in functional connectivity compared to traumatic brain injury protocols (Jin et al., 2006).

4.6.2 Proof of principle experiments using optogenetic circuit mapping

For decades there has been a considerable interest in mapping circuit reorganization following seizures but due to the low hit rate for recording synaptically coupled PCs, investigators have used alternatives such as focal glutamate microsimulation (Christian and Dudek, 1988; Lynch and Sutula, 2000; Markram et al., 1997). We performed proof-of-principle initial studies using laser-guided optogenetic stimulation of acute slices expressing ChR2 in L2/3 and 5 inspired by the initial reports of CRACM and LSPS/optogenetics studies (Brill et al., 2016; Petreanu et al., 2007b).

When comparing viral delivery and IUE to express ChR2 we noticed that virally transfected slices had greater response across the slice (**Figure 4.4**). This is consistent with previous reports using non-viral vectors introduced by IUE showing episomal expression

may deteriorate during development (Waddington et al., 2005). Compared to IUE, AAVs can integrate stably into the genome for longer lasting expression (Kaplitt et al., 1994). However, a main strength of IUE is the ability to target specific populations of cells at the progenitor stage (Matsuda and Cepko, 2007). Viral expression may also suffer from adverse immune responses which are not a concern during IUE since the immune system is not yet mature during injection (Taniguchi et al., 2012). Thus, these concerns must be balanced when choosing a viable expression system.

The advantages of LSPS/optogenetic circuit mapping are that power can be modulated on the fly to dilute responses (**Figure 4.2**), stimulation is temporally precise (**Figure 4.3**), and a wide area of the cell can be covered simultaneously (**Figure 4.1**). However, a main caveat is that ChR2 expression levels were not controlled for when performing optogenetic stimulation. Taking averages of several cells partially solves this problem but a better alternative is to quantify GFP expression and use the pixel intensity to normalize the corresponding postsynaptic response to whilst keeping the laser power constant. Therefore, future experiments will have to better control for variability in ChR2 expression.

4.6.3 Conclusions and future directions

To our knowledge, we have carried out the first LSPS/optogenetic experiments in optokindled slices. Our experiments serve as proof of principle in extending LSPS/optogenetics towards identifying circuit changes that are correlated with epileptogenesis. In this study, we focused on experiments where ChR2 was expressed in PCs though there are multiple possibilities for investigation of other neuronal cell types such as INs. Indeed, INs may have different roles in the initiation and maintenance of seizures so

investigating their roles during and after full optokindling may reveal different connectivity states (Khoshkhoo et al., 2017; Wang et al., 2017).

Also, we looked at changes in postsynaptic responses at the end of optokindling where generalized seizures had already been established (Cela et al., 2019). Given the gradual evolution of seizure intensity through kindling sessions, it would be instructive to map the epileptic circuit at different stages of kindling (Sutula, 2004). Research suggests that early and late epileptogenesis may have different synaptic and morphological changes associated with each stage and optogenetic circuit mapping can shed some light on these differences (Morrell, 1985). To sum up, optokindling combined with optogenetic circuit mapping together allow for rapid cell-specific dissection of microcircuit plasticity changes following seizures and may open up new avenues for therapeutic treatment of epilepsy.

4.7 Figures

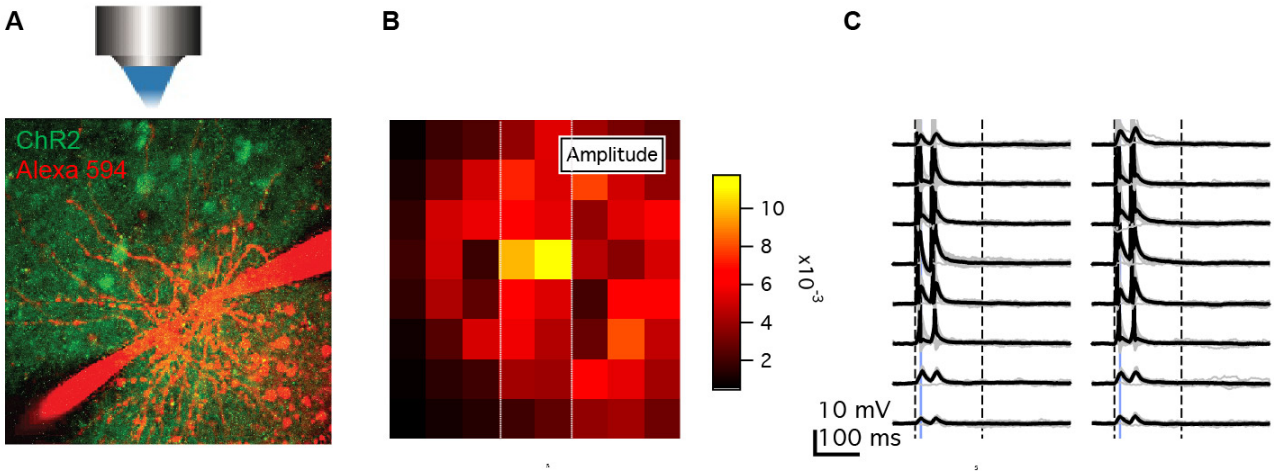

Figure 4.1 Rapid mapping of multiple presynaptic inputs using ChR2-assisted optogenetic stimulation.

(A) Optogenetic laser stimulation of PCs in a ChR2-expressing slice. 2PLSM flattened stack depicting whole-cell recording from PCs in L2/3 filled with Alexa-594 for visualization (red). EYFP expression depicts ChR2-expressing cells (green).

(B) 8-by-8 grid matrix of the amplitude of responses recorded in the postsynaptic cell after presynaptic stimulation of ChR2-expressing PCs in a grid like fashion across the slice. Actual responses inside white dashed lines are represented in (C).

(C) Evoked responses used to construct the diagram in (B) showing a close-up of the two central columns outlined by white dashed lines in the grid in (B).

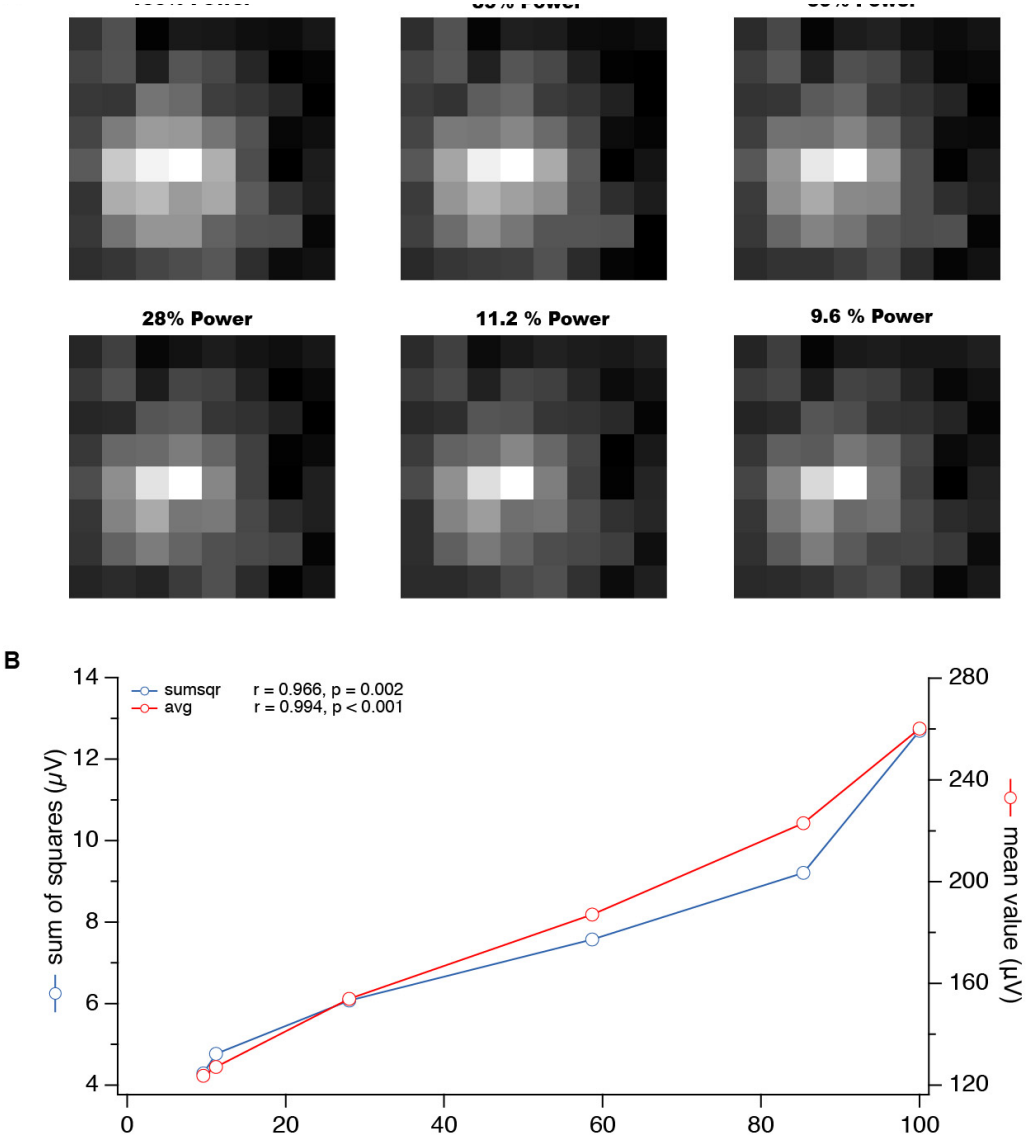

Figure 4.2 Characterization of CRACM responses through power level attenuation

(A) Power level was attenuated at the table using a half lambda plate and measurements were taken at the objective. ChR2-expressing slices were stimulated at different power levels and used to generate 8 by 8 grids. The matrices at each corresponding power level are shown.

(B) The average intensity and sum of square of each grid consisting of 64 different measurements was computed to arrive at a single value per matrix at each power level. Both average values ($r = 0.994$, $p < 0.001$) and sum of squares ($r = 0.966$, $p = 0.002$) increased significantly with power.

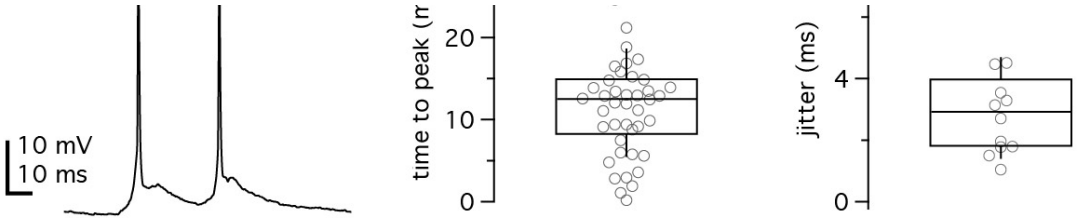

Figure 4.3 AP firing is temporally precise during CRACM *in-vitro*

(A) Action potentials (APs) elicited using light stimulation during whole-cell current clamp from L2/3 neurons in acute slices of M1. Instance of light stimulation with a 445nm laser indicated by dashed blue lines.

(B) Latency to peak of AP (n = 12 cells, 12.07 ± 0.99 ms). Jitter was measured as standard deviation of latency (n = 12 cells, 3.05 ± 0.47 ms). Box plot shows inter-quartile range, median and whiskers representing ± 1 st.dev.

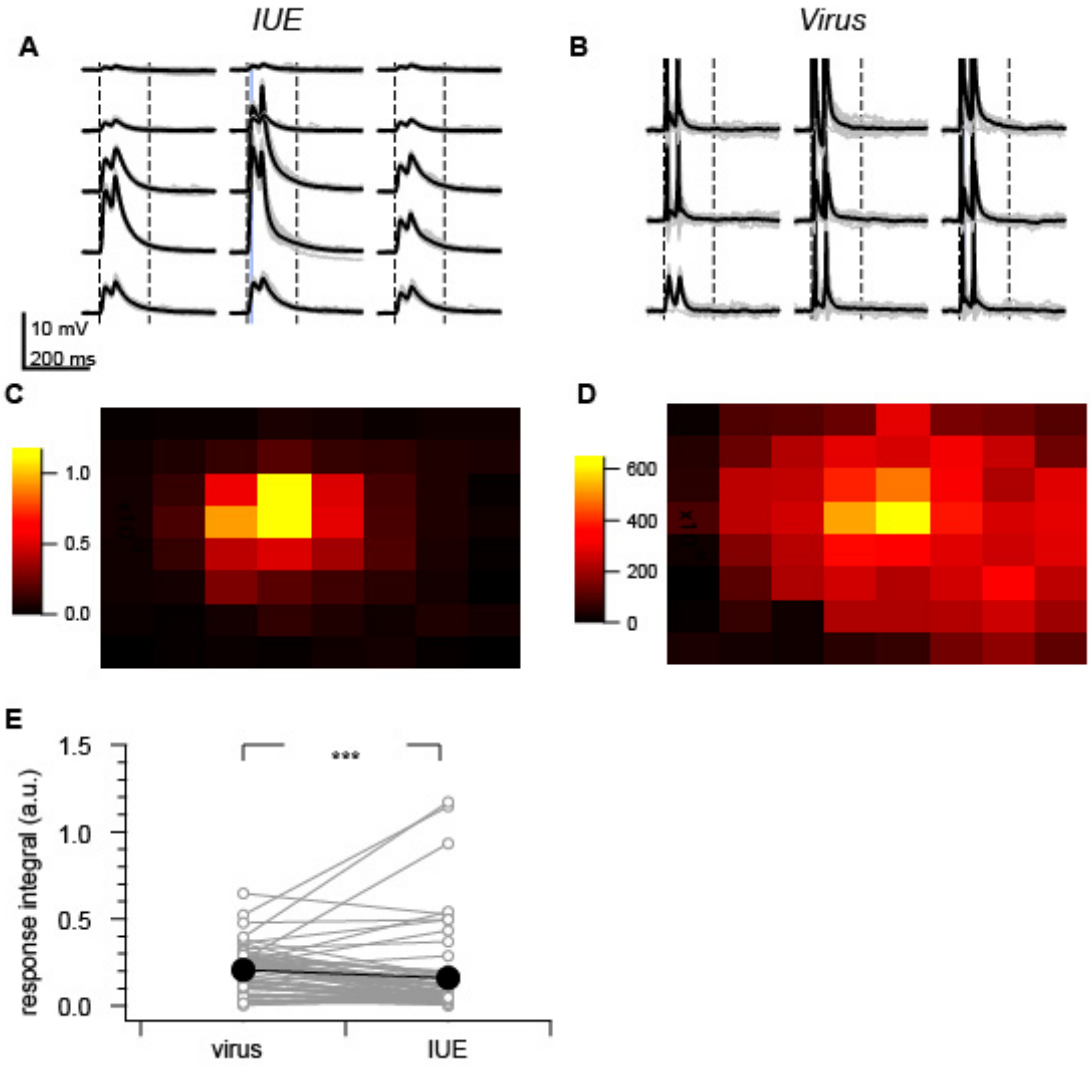

Figure 4.4 Comparison of in-utero electroporation (IUE) and virus injection for CRACM

(A) Evoked responses recorded in M1 after optogenetic laser stimulation of PCs in a ChR2-expressing slice after IUE. The three central columns of an 8-by-8 grid are shown for clarity. The evoked responses come from the postsynaptic cell which was recorded in whole-cell current clamp during presynaptic stimulation.

(B) Evoked responses recorded in M1 after optogenetic laser stimulation of PCs in a ChR2-expressing slice after viral injection. The three central columns of an 8-by-8

grid are shown for clarity. The evoked responses come from the postsynaptic cell which was recorded in whole-cell current clamp during presynaptic stimulation.

(C) 8-by-8 grid matrix of the integral of responses recorded in the postsynaptic cell after presynaptic stimulation of ChR2-expressing PCs in a grid like fashion across the slice. This grid was generated by measuring the integral inside dashed lines in (A). 20 responses were averaged to create each grid piece.

(D) 8-by-8 grid matrix of the integral of responses recorded in the postsynaptic cell after presynaptic stimulation of ChR2-expressing PCs in a grid like fashion across the slice. This grid was generated by measuring the integral inside dashed lines in (B). 20 responses were averaged to create each grid piece.

(E) Comparison of area under the curve (integral) of 64 responses recorded in IUE slices compared to virus injected slices. Cells recorded from virus-injected slices had higher average integral signals than IUE transfected slices (Wilcoxon signed rank test, virus = $2.06 \times 10^{-4} \pm 1.62 \times 10^{-5}$, IUE = $1.60 \times 10^{-4} \pm 3.07 \times 10^{-5}$, n =64 responses, $p < 0.001$)

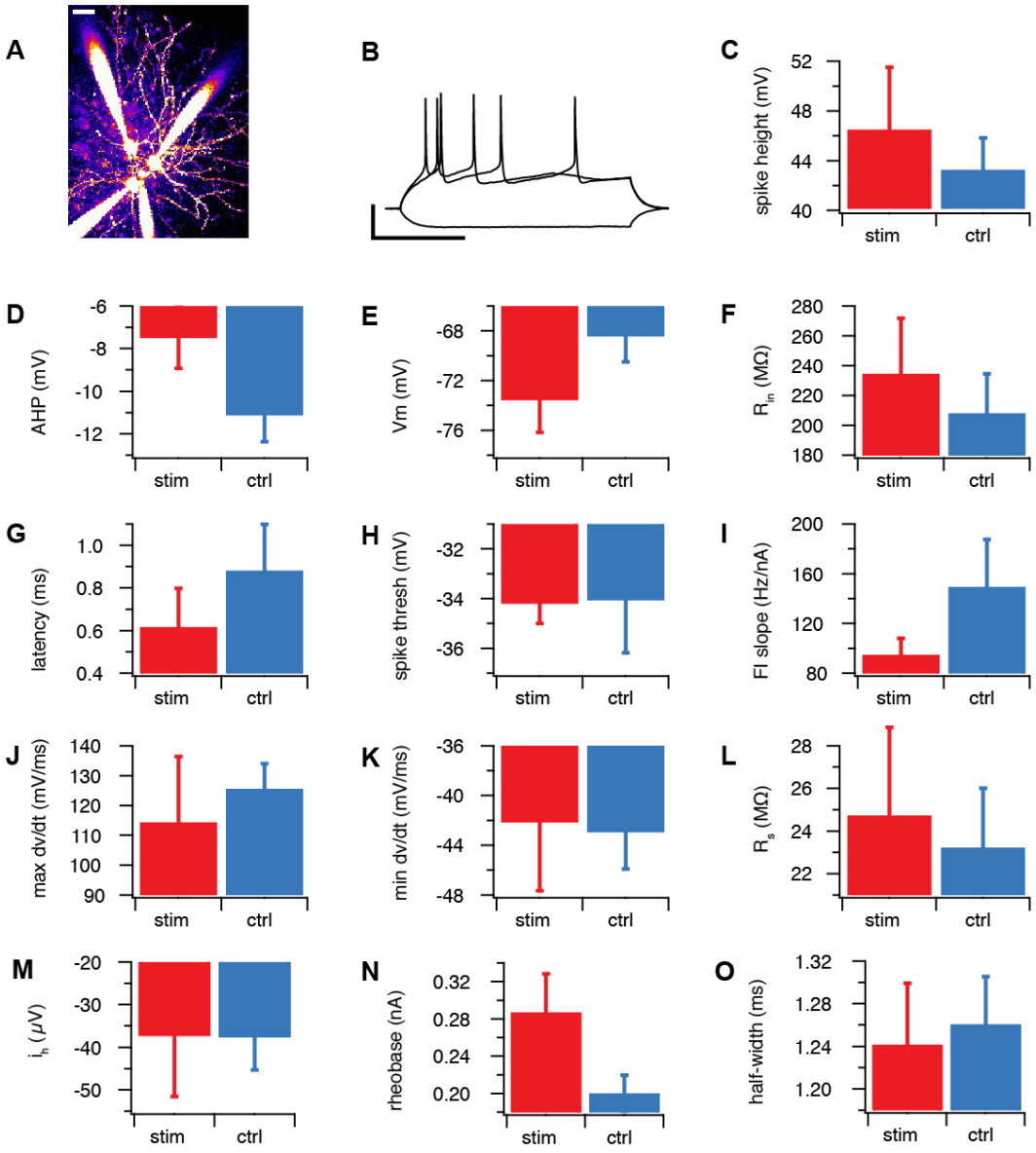

Figure 4.5 Intrinsic properties were indistinguishable in optokindled and control animals

(A) Sample flattened 2PLSM stack of Alexa-594- filled M1 L2/3 PCs. Scale bar: 20 μm.

(B) Three sample voltage traces recorded in an M1 L2/3 PC in response to a series of current pulses (rheobase sweep in black). The hyperpolarizing current was -100 pA, followed by a total of 14 depolarizing pulses starting at 100 pA, spaced by 20 pA up to 200 pA, and by

50 pA subsequently. From such sweeps, the intrinsic cellular properties were automatically extracted, as previously described(Buchanan et al., 2012). Scale bar: 200 ms, 25 mV.

(C) Properties such as spike height, width, threshold (measured at inflexion point), and after-hyperpolarization (AHP, measured 30 ms after the inflexion point(Bean, 2007)) were automatically extracted (Buchanan et al., 2012) from the first action potential at rheobase (see panel B). Scale bar: 20 ms, 20 mV.

(D) AHPs in PCs recorded in acute slices from kindled ("stim ChR2", n = 8 cells, n = 3 animals) and control animals ("no stim ChR2", compare **Figure 2.2A**, n = 17 cells, n = 3 animals) were indistinguishable (p = 0.067). No differences were found for any of the other intrinsic properties either: **(E)** resting membrane potential (V_{rest}, p = 0.133), **(F)** input resistance (R_{in}, p = 0.566), **(G)** latency to spike at rheobase (p = 0.359), **(H)** spike threshold (p = 0.947), **(I)** firing rate/current slope (p = 0.191), **(J)** maximum voltage time derivative (dv/dt, p = 0.637), **(K)** minimum voltage time derivative (p = 0.899), **(L)** spike height (p = 0.571), **(M)** hyperpolarization-activated current (I_h, measured as the sag at steady state due to hyperpolarizing step, p = 0.982), **(N)** rheobase current (p = 0.063), or **(O)** spike half-width (p = 0.793). Finally, series resistance (not shown, not compensated, measured from the fast component of a double-exponential fit to a hyperpolarizing pulse) was also indistinguishable (stim: ChR2: 25 MΩ ± 3 MΩ vs. no stim ChR2: 23 MΩ ± 2 MΩ, p = 0.647). Student's *t* test was used throughout except panel N, where Wilcoxon's rank test was applied since current injections were distributed at discrete intervals.

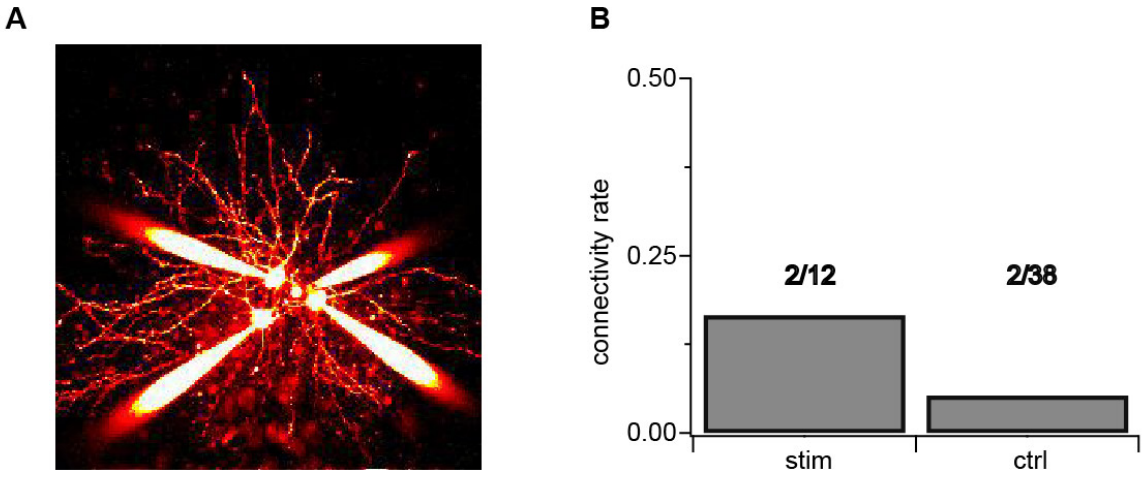

Figure 4.6 Connectivity rates in stimulated and control slices.

(A) 2PLSM flattened stack depicting paired whole-cell recording from PCs in L2/3 filled with Alexa-594 for visualization. Connectivity is tested for pairs of at least two cells recorded simultaneously.

(B) No difference in connectivity rates between stimulated and control slices was found. (Fisher's exact test, p = 0.24, n = 2/12 connections stimulated, n = 2/38 connections control)

5 General Discussion

5.1 Summary of the findings

The main findings can be summarized as follows:

1. A novel optogenetic kindling model of epilepsy was established using repeated activation of PCs through ChR2 activation in awake behaving animals (Cela et al., 2019). Seizures emerged gradually and increased in number over time. In agreement with classical kindling, seizure threshold decreased over sessions as seizure duration increased (Racine, 1972a). Seizure occurrence could not be explained by gross brain damage resulting from the experimental method as neuronal cell counts and astroglial activation wasn't different in control animals compared to stimulated.
2. In a two-hit model, we combined rimonabant injections with our neocortical optokindling protocol and found this accelerated seizure development with no change in seizure properties such as duration and latency.
3. Finally, we established the groundwork for and preformed preliminary experiments outlining possible optogenetic circuit mapping methods to probe circuit alterations following seizures.

5.2 A novel optokindling model of epilepsy

The development of seizures has been studied through acquired and genetic animal models of epilepsy. Acquired models, whereby seizures are induced by chemical proconvulsants or repeated electrical activity, have endured for decades giving rise to a plethora of insights about ictogenesis (Löscher, 2002). In particular, kindling, as an electrical induction model, has been extensively employed in the literature since its initial discovery (Goddard, 1967).

However, the relatively unchanged acquired induction models also suffer from common setbacks. Two examples of setbacks are the lack of cellular specificity in targeting the model and additional damage that may accompany the model itself through the experimental protocol. During classical kindling, electrical stimulation through a bipolar electrode elicits a response in several different neuronal populations in proximity to the electrode (Racine and Zaide, 1978). This prevents a dissection of the causal mechanisms of seizures due to mixing multiple cell bodies and may explain some of the variability in the model.

Recently novel techniques like optogenetics have made it possible to control neuronal firing with millisecond precision whilst identifying cells through genetic tags. Researchers are in the early stages of using these techniques and have been able to halt seizures using inhibitory opsins or induce seizures using excitatory opsins (Khoshkhoo et al., 2017; Osawa et al., 2013; Paz et al., 2013; Wykes et al., 2012b). However, these studies have been in the context of an underlying genetic factor or seizures were elicited in a single session precluding a temporal examination of seizure emergence.

Here we were able to take advantage of optogenetics and *in-vivo* recordings in awake behaving animals to establish an optogenetic variant of the classical kindling paradigm

(Cela et al., 2019). We find that repeated activation of a small subset of neurons in M1 every 48hrs is sufficient to gradually give rise to seizures. Additionally, these optogenetic kindling-induced seizures share properties with classical kindling findings such as gradual lowered threshold and increased seizure duration over sessions (Goddard et al., 1969). Also, we were able to show that these seizures can arise without the presence of glial activation or gross neuronal damage. Finally, we showed that 50Hz activation and ChR2 expression are both necessary for seizure emergence. Taken together, our findings suggest that seizures can arise from repeated stimulation of a small subset of PCs and highlight our optogenetic kindling approach as a novel substitute to the classical model. Future studies in other cell populations extending our results may be helpful to produce meaningful outcomes that may be applied in a clinically beneficial manner.

5.3 CB1R blockade accelerates optokindled seizures

The path to seizure emergence and pathological activity is not a one-way street. There are different ways in which the brain's normal mechanisms of maintaining an excitatory-inhibitory balance can be overcome (Avanzini et al., 2014). Indeed, it is widely understood that a second insult added to an underlying factor such as traumatic brain injury can accelerate seizure development (Pitkänen et al., 2009a).

One of the critical factors that determines potential for seizure development is the state of the existing plasticity in the brain before a second factor is added. It is well known for example that multiple brain disorders such as TSC1 mutations which change brain plasticity also have seizures as co-morbidities (Uhlmann et al., 2002). In this respect, it is vital that mechanisms which have the potential to increase the hyperexcitability of the brain are well

understood so the underlying mechanisms of seizure propensity are targeted for therapeutic intervention (Brodie and Dichter, 1996).

The cannabinoid family of receptors, especially CB1R has been shown to be tightly linked to plasticity with agonism of this receptor promoting LTD in normal brain plasticity where it may work with other receptors (Sjöström et al., 2003; Soltesz et al., 2015). In contrast, in the pathologic epileptic brain, CB1R blockade or antagonism leads to a lowering of the threshold to seizures and promotion of hyperexcitability (Marsicano et al., 2003; Vinogradova et al., 2011).

Considering the role of CB1R in the healthy and diseased brain, we sought to understand what would happen if CB1R antagonisms could be used as a second-hit to test its effects on the gradual seizure development induced by our optokindling protocol (Cela et al., 2019).

We injected animals with the CB1R blocker rimonabant 30 minutes before performing optogenetic kindling and carried out the rest of the stimulation unchanged to our optogenetic kindling model. We found that CB1R blockade significantly accelerates optogenetically-kindled seizures with seizures emerging from the first session of stimulation compared to over a dozen sessions required to elicit seizures in our optogenetic model.

We confirmed the role of the CB1R blockade in our kindling model and show the potential of this pathway to be used as a second-hit to add to existing animal models of seizures. Our optokindling model allows for dissection of how nearby neurons that were unstimulated directly or other neurons such as INs can be affected during the second hit. For example, it is known that cholecystokinin INs express CB1Rs at high levels (>85%) and these are likely to be directly affected by CB1R blockade (Katona et al., 1999). Another potential line of investigation which we did not explore is the contribution of astrocytes to promoting

hyperexcitability upon rimonabant injection as they have known to possess CB1Rs and interact closely with neurons (Navarrete and Araque, 2008).

5.4 Using cutting-edge methods for analysing circuit perturbations following seizures

Epileptogenesis is a process of vital importance to understanding the consequences and mechanisms of focal epilepsy. Vast improvements in animal models of epilepsy over the last decades have allowed for accumulating insights about the disease, but the lack of cellular targeting using acquired seizure models has resulted in difficulty tying experimental results to specific cell populations. The lack of control of defined cell populations has precluded insights about the contributions of distinct cell populations to seizures and consequently, local circuit rearrangements. Although the animal models themselves can generate a state of SE, the transition from a healthy to a pathological brain has not been fully studied.

In the last decade, rapid advances in optogenetics have allowed for millisecond activation and deactivation of neuronal activity coupled to targeting of genetically-defined cell populations (Paz et al., 2013). These advances along with those in laser technology and genetically-encoded calcium indicators have recently allowed for exploration of the missing link between seizure outcomes and their respective neuronal underpinnings (Khoshkhoo et al., 2017). On the readout side, techniques such as CRACM and multiple whole-cell paired recordings have allowed for mapping of connectivity differences in acute slices to examine local-circuit plasticity (Petreanu et al., 2007a; Zhang et al., 2009).

We combined optogenetics and CRACM to carry out proof of principle experiments in control and epileptic tissue following optogenetic kindling (Cela et al., 2019). First, using paired recordings in control and epileptic acute slices of L5 cells in M1 we found no changes

in several measures of intrinsic excitability of PCs between control and kindled slices. While previous experiments have been unable to target the cells receiving direct stimulation, intrinsic excitability following seizures has been previously reported to be unchanged in several cases (Avoli and Olivier, 1989; Prince and Wong, 1981). Thus, while we were able to record from cells that were directly stimulated by light, our findings agree with those of previous studies.

We also used CRACM in ChR2-expressing slices to build connectivity maps of the local circuit. We relied on ChR2 expression solely in PCs predominantly in layers 2/3 and 5. Others have used CRACM as a subcellular mapping tool in neocortex or, more recently, glutamate uncaging in seizure-prone animals (Brill et al., 2016; Petreanu et al., 2007a). We put forth that CRACM applied to seizure studies allows for fast rates of circuit mapping and has the advantage of genetically targeting cells. Our experiments serve as a foundation for potential future studies where circuit dynamics can be rapidly examined following seizures in different cell populations simultaneously. For example, the role of INs and PCs can be examined simultaneously by expressing ChR2 using two different promoters. Furthermore, since our optokindling model allows the gradual development of generalized seizures over time, a “snapshot” of circuit plasticity can be taken throughout epileptogenesis.

5.5 Concluding remarks

The field of epilepsy has been rapidly expanding in recent years by take advantage of modern techniques to study seizure development in animal models. The exact mechanisms underpinning seizure development are still not fully clear and this is due to the complexity of multiple types of epilepsy, the failure of some models to fully capture human symptoms and the lack of cell-targeted tractable models. During my PhD I have focused on ameliorating the

latter weakness of animal models and hope that the insights provided within can further enrich our understanding of the processes of pathologic brain activity and provide inspiration for future studies extending and developing these insights.

6 APPENDIX

6.1 445-nm laser power characterization

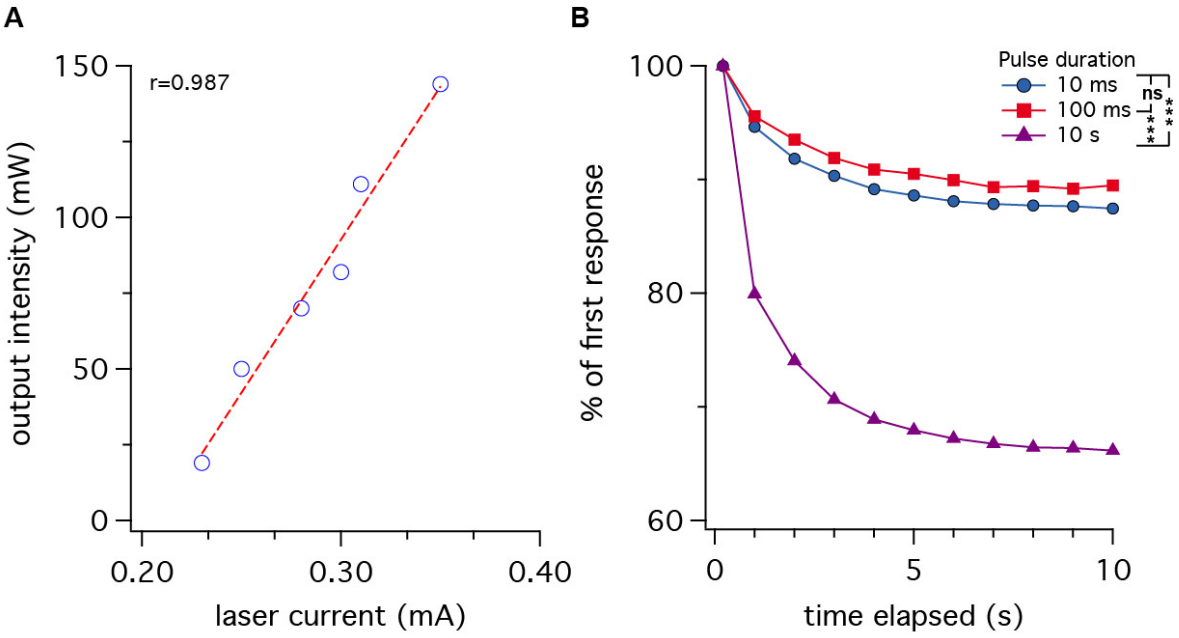

Figure 6.1 Characterization of 445-nm laser used for optogenetic stimulation.

(A) Laser current was linearly correlated with output intensity (Least squares regression, r = 0.987). All stimulations were performed at max current amplitude to ensure suprathreshold stimulation intensity required for ChR2 activation (> 1mW/mm^2).

(B) Laser power was measured over 10 seconds using 50 Hz stimulation with variable pulse duration (10 ms, 100 ms, or 10 seconds). Power intensity decreases exponentially but remains above 90% of initial power (for 10 and 100 ms pulse widths) within 3 seconds and plateaus thereafter. Power was significantly different

between the three pulse widths over 10 seconds (One-way ANOVA, 10ms vs 100 ms: $p = 0.99$, 10 or 100 ms vs 10 seconds: $p < 0.001$).

6.2 *In-vivo* optogenetic stimulation and EEG recording setup

I assembled the following set-up used for the central experiments of my PhD for *in-vivo* optogenetic stimulation and EEG recordings. The platform was put together from scratch using off-the-shelf components available widely. Further explanation of how simultaneous acquisition and light stimulation was achieved, including parts used, can be found in the Methods section of **Chapter 2** (Section 2.3.2). Briefly, two 445 nm lasers are air-coupled to fibreoptic adapters that connect to fibreoptic cables and subsequently the mouse's head during experiments. These lasers and fibreoptic cables are used for bihemispheric optogenetic light stimulation. The animals are allowed to move freely around the cylindrical recording cage where EEG signals are collected by the extracellular amplifier whilst being digitized by NIDAQ boards (#6229, Austin, TX, USA). The simultaneous EEG acquisition and light stimulation is controlled by the computer running Igor Pro v.6.34 software (Wavemetrics Inc., Lake Oswego, OR, USA).

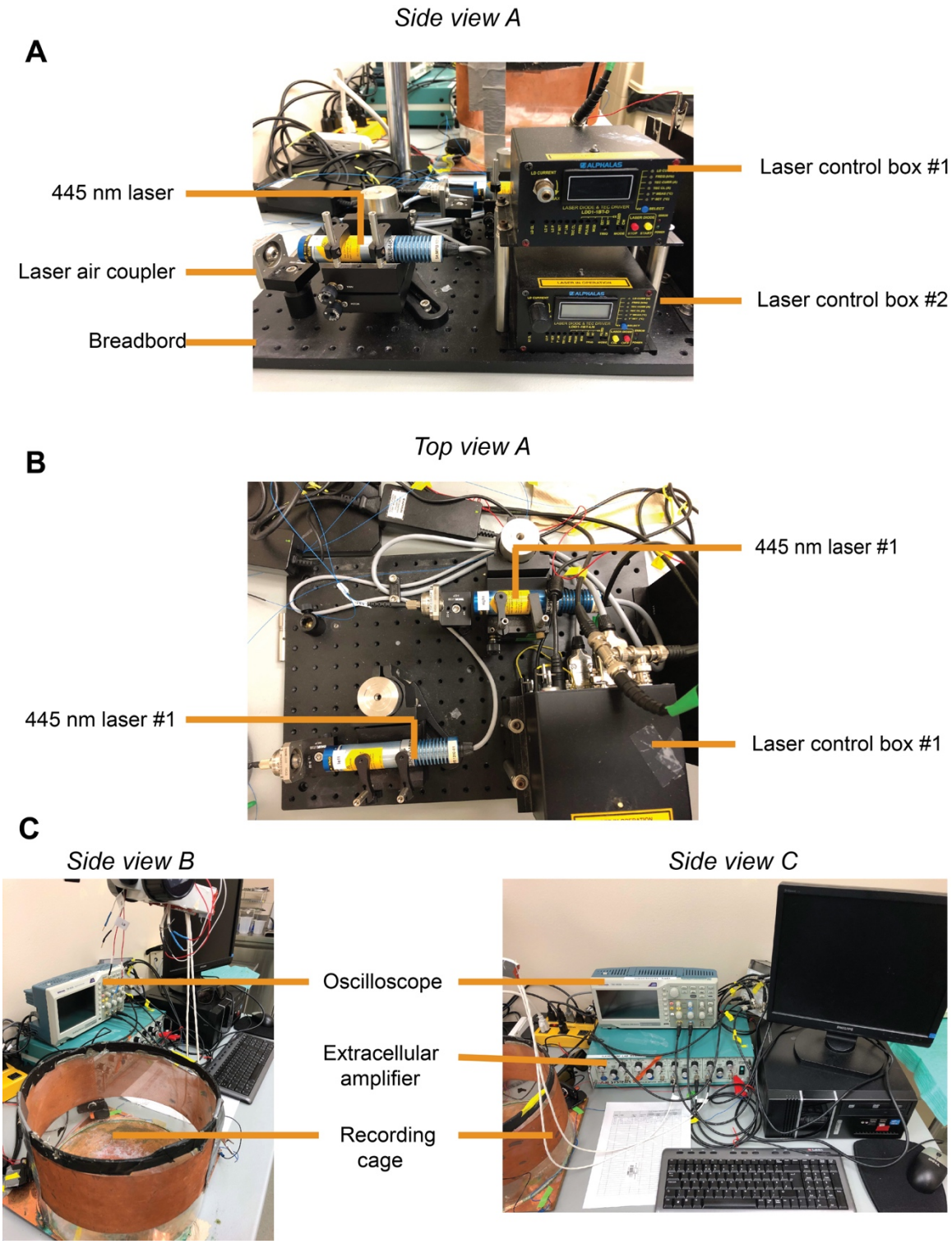

Figure 6.2 *In-vivo* optokindling platform for simultaneous ChR2 excitation and EEG recording

(A) Side view A showing both laser control boxes with one 445-nm laser visible mounted to a breadboard. The laser air coupler collects the laser beam into an FC-PC fiber optic cable using a large NA lens.

(B) Top view A showing both 445-nm lasers mounted on the breadboard.

(C) Side view B shows the Faraday cage where EEG recordings are performed as well as the extracellular amplifier used during recordings. Side view C shows the oscilloscope used to display EEG signals during acquisition as they are digitized by the data acquisition board and stored on the computer.

6.3 Dual acute slice recording and optogenetics setup for *in-vitro* electrophysiology

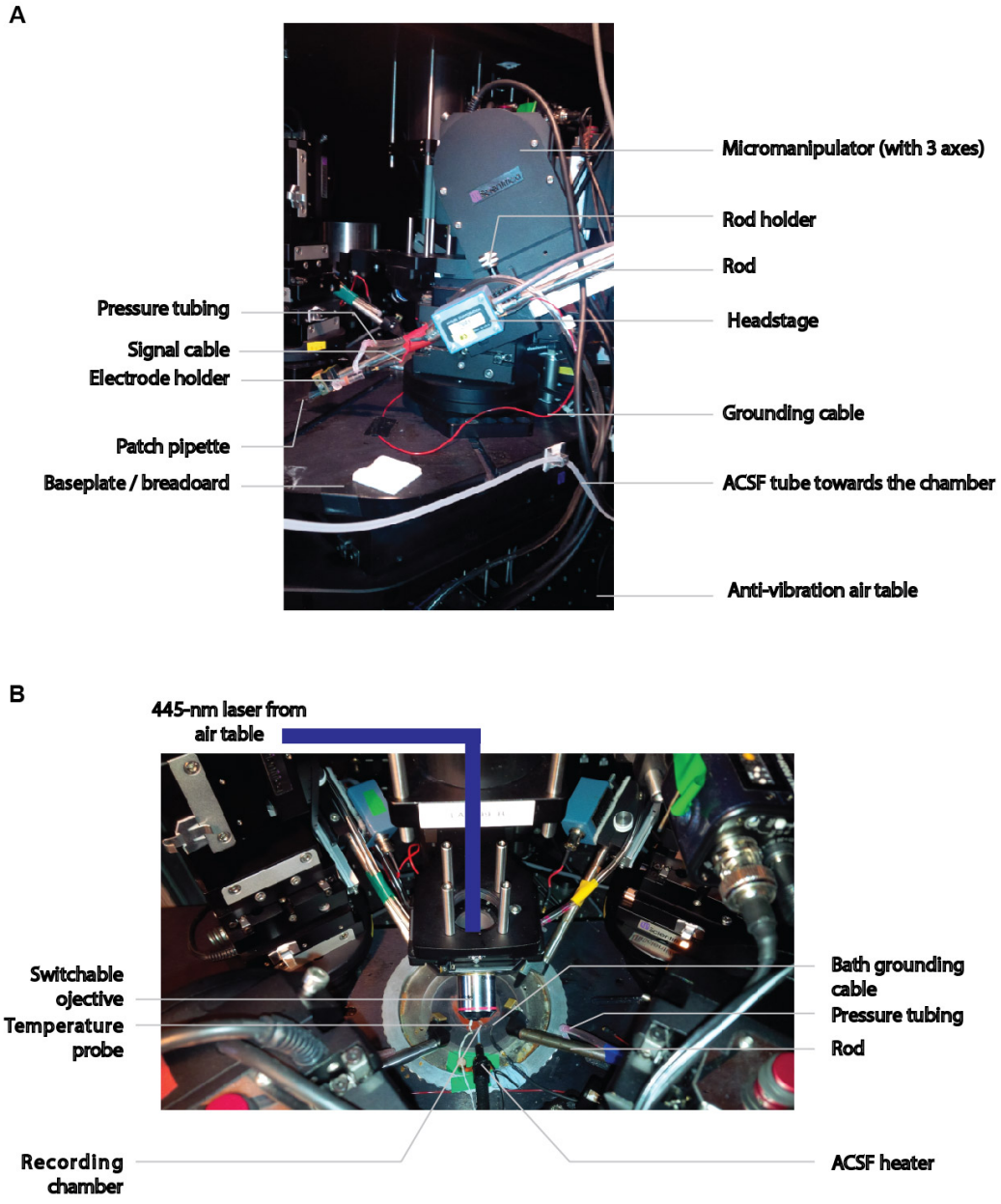

Figure 6.3 *In-vitro* setup for electrophysiological acute slice recording and optogenetics stimulation

Adapted from Lalanne et al. (2016).

(A) Motorized micromanipulator with attached pipette for whole-cell patch clamp recording experiments. The entire setup is placed on an anti-vibration table to minimize drift during recording experiments.

(B) Top-down view of recording setup showing the 445-nm laser guided into the objective for optogenetic stimulation experiments. The 445-nm laser is co-aligned with a two-photon beam (not shown) which allows near-simultaneous imaging and stimulation of ChR2-expressing cells.

6.4 Code

During my PhD I wrote code for several steps of seizure analysis such as peak-finding, array manipulation as well as various automated calculations of central tendencies (mean, standard deviation etc.) A selection of code I wrote is preserved on Github and available for public use. All code is written in Igor Pro version 6.4 and older (Wavemetrics Inc., Lake Oswego, OR, USA).

6.4.1 Assorted array manipulation functions

The code for the various functions is stored on Github at: https://github.com/ec10K/Seizure-Analysis/blob/master/Array_manipulation.ipf

6.4.2 Seizure analysis code

The code for seizure analysis is stored on Github at: https://github.com/ec10K/Seizure-Analysis/blob/master/Seizure%20functions.ipf

7 References

Abrahamsson, T., Lalanne, T., Watt, A.J., and Sjöström, P.J. (2016). Long-Term Potentiation by Theta-Burst Stimulation Using Extracellular Field Potential Recordings in Acute Hippocampal Slices. Cold Spring Harb Protoc *2016*, pdb prot091298.

Airan, R.D., Thompson, K.R., Fenno, L.E., Bernstein, H., and Deisseroth, K. (2009). Temporally precise in vivo control of intracellular signalling. Nature *458*, 1025-1029.

Amzica, F., and Neckelmann, D. (1999). Membrane capacitance of cortical neurons and glia during sleep oscillations and spike-wave seizures. J Neurophysiol *82*, 2731-2746.

Annegers, J.F., Hauser, W.A., Coan, S.P., and Rocca, W.A. (1998). A population-based study of seizures after traumatic brain injuries. N Engl J Med *338*, 20-24.

Annegers, J.F., Rocca, W.A., and Hauser, W.A. (1996). Causes of Epilepsy: Contributions of the Rochester Epidemiology Project. Mayo Clinic Proceedings *71*, 570-575.

Anwyl, R. (2009). Metabotropic glutamate receptor-dependent long-term potentiation. Neuropharmacology *56*, 735-740.

Applegate, C.D., and Burchfiel, J.L. (1990). Evidence for a norepinephrine-dependent brain-stem substrate in the development of kindling antagonism. Epilepsy Res *6*, 23-32.

Aravanis, A.M., Wang, L.P., Zhang, F., Meltzer, L.A., Mogri, M.Z., Schneider, M.B., and Deisseroth, K. (2007). An optical neural interface: in vivo control of rodent motor cortex with integrated fiberoptic and optogenetic technology. J Neural Eng *4*, S143-156.

Armstrong, C., Morgan, R.J., and Soltesz, I. (2009). Pursuing paradoxical proconvulsant prophylaxis for epileptogenesis. Epilepsia *50*, 1657-1669.

Assaf, F., and Schiller, Y. (2016). The antiepileptic and ictogenic effects of optogenetic neurostimulation of PV-expressing interneurons. J Neurophysiol *116*, 1694-1704.

Avaliani, N., Andersson, M., Runegaard, A.H., Woldbye, D., and Kokaia, M. (2016). DREADDs suppress seizure-like activity in a mouse model of pharmacoresistant epileptic brain tissue. Gene Ther *23*, 760-766.

Avanzini, G., Forcelli, P.A., and Gale, K. (2014). Are there really "epileptogenic" mechanisms or only corruptions of "normal" plasticity? Adv Exp Med Biol *813*, 95-107.

Avoli, M. (1996). GABA-mediated synchronous potentials and seizure generation. Epilepsia *37*, 1035-1042.

Avoli, M., and Olivier, A. (1989). Electrophysiological properties and synaptic responses in the deep layers of the human epileptogenic neocortex in vitro. J Neurophysiol *61*, 589-606.

Avramescu, S., Nita, D.A., and Timofeev, I. (2009). Neocortical post-traumatic epileptogenesis is associated with loss of GABAergic neurons. J Neurotrauma *26*, 799-812.

Bains, J.S., Longacher, J.M., and Staley, K.J. (1999). Reciprocal interactions between CA3 network activity and strength of recurrent collateral synapses. Nat Neurosci *2*, 720-726.

Bean, B.P. (2007). The action potential in mammalian central neurons. Nat Rev Neurosci *8*, 451-465.

Beck, H., and Yaari, Y. (2008). Plasticity of intrinsic neuronal properties in CNS disorders. Nat Rev Neurosci *9*, 357-369.

Behr, J., Heinemann, U., and Mody, I. (2001). Kindling induces transient NMDA receptor-mediated facilitation of high-frequency input in the rat dentate gyrus. J Neurophysiol *85*, 2195-2202.

Ben-Ari, Y., Crepel, V., and Represa, A. (2008). Seizures Beget Seizures in Temporal Lobe Epilepsies: The Boomerang Effects of Newly Formed Aberrant Kainatergic Synapses. Epilepsy Currents *8*, 68-72.

Berglind, F., Andersson, M., and Kokaia, M. (2018). Dynamic interaction of local and transhemispheric networks is necessary for progressive intensification of hippocampal seizures. Sci Rep *8*, 5669.

Berglind, F., Ledri, M., Sorensen, A.T., Nikitidou, L., Melis, M., Bielefeld, P., Kirik, D., Deisseroth, K., Andersson, M., and Kokaia, M. (2014). Optogenetic inhibition of chemically induced hypersynchronized bursting in mice. Neurobiol Dis *65*, 133-141.

Berkovic, S.F., Mulley, J.C., Scheffer, I.E., and Petrou, S. (2006). Human epilepsies: interaction of genetic and acquired factors. Trends Neurosci *29*, 391-397.

Berndt, A., Lee, S.Y., Ramakrishnan, C., and Deisseroth, K. (2014). Structure-guided transformation of channelrhodopsin into a light-activated chloride channel. Science *344*, 420-424.

Berndt, A., Schoenenberger, P., Mattis, J., Tye, K.M., Deisseroth, K., Hegemann, P., and Oertner, T.G. (2011). High-efficiency channelrhodopsins for fast neuronal stimulation at low light levels. Proc Natl Acad Sci U S A *108*, 7595-7600.

Bertram, E. (2007). The Relevance of Kindling for Human Epilepsy. Epilepsia *48*, 65-74.

Bezzi, P., Gundersen, V., Galbete, J.L., Seifert, G., Steinhauser, C., Pilati, E., and Volterra, A. (2004). Astrocytes contain a vesicular compartment that is competent for regulated exocytosis of glutamate. Nat Neurosci *7*, 613-620.

Binder, D.K., Routbort, M.J., and McNamara, J.O. (1999). Immunohistochemical evidence of seizure-induced activation of trk receptors in the mossy fiber pathway of adult rat hippocampus. Journal of Neuroscience *19*, 4616-4626.

Boison, D. (2008). The adenosine kinase hypothesis of epileptogenesis. Progress in Neurobiology *84*, 249-262.

Borges, K., Gearing, M., McDermott, D.L., Smith, A.B., Almonte, A.G., Wainer, B.H., and Dingledine, R. (2003). Neuronal and glial pathological changes during epileptogenesis in the mouse pilocarpine model. Exp Neurol *182*, 21-34.

Bortel, A., Levesque, M., Biagini, G., Gotman, J., and Avoli, M. (2010). Convulsive status epilepticus duration as determinant for epileptogenesis and interictal discharge generation in the rat limbic system. Neurobiol Dis *40*, 478-489.

Boyden, E.S., Zhang, F., Bamberg, E., Nagel, G., and Deisseroth, K. (2005). Millisecond-timescale, genetically targeted optical control of neural activity. Nat Neurosci *8*, 1263-1268.

Braakman, H.M., van Oostenbrugge, R.J., van Kranen-Mastenbroek, V.H., and de Krom, M.C. (2009). Rimonabant induces partial seizures in a patient with a history of generalized epilepsy. Epilepsia *50*, 2171-2172.

Bragin, A., Azizyan, A., Almajano, J., Wilson, C.L., and Engel, J., Jr. (2005). Analysis of chronic seizure onsets after intrahippocampal kainic acid injection in freely moving rats. Epilepsia *46*, 1592-1598.

Bragin, A., Engel, J., Jr., Wilson, C.L., Fried, I., and Mathern, G.W. (1999a). Hippocampal and entorhinal cortex high-frequency oscillations (100--500 Hz) in human epileptic brain and in kainic acid--treated rats with chronic seizures. Epilepsia *40*, 127-137.

Bragin, A., Engel, J., Jr., Wilson, C.L., Vizentin, E., and Mathern, G.W. (1999b). Electrophysiologic analysis of a chronic seizure model after unilateral hippocampal KA injection. Epilepsia *40*, 1210-1221.

Bragin, A., Wilson, C.L., Almajano, J., Mody, I., and Engel, J., Jr. (2004). High-frequency oscillations after status epilepticus: epileptogenesis and seizure genesis. Epilepsia *45*, 1017-1023.

Bragin, A., Wilson, C.L., and Engel, J. (2003). Spatial stability over time of brain areas generating fast ripples in the epileptic rat. Epilepsia *44*, 1233-1237.

Bragin, A., Wilson, C.L., and Engel, J., Jr. (2000). Chronic epileptogenesis requires development of a network of pathologically interconnected neuron clusters: a hypothesis. Epilepsia *41 Suppl 6*, S144-152.

Brill, J., Mattis, J., Deisseroth, K., and Huguenard, J.R. (2016). LSPS/Optogenetics to Improve Synaptic Connectivity Mapping: Unmasking the Role of Basket Cell-Mediated Feedforward Inhibition. eNeuro *3*.

Brodie, M.J., and Dichter, M.A. (1996). Antiepileptic drugs. N Engl J Med *334*, 168-175.

Brodie, M.J., Elder, A.T., and Kwan, P. (2009). Epilepsy in later life. Lancet Neurol *8*, 1019-1030.

Brophy, G.M., Bell, R., Claassen, J., Alldredge, B., Bleck, T.P., Glauser, T., Laroche, S.M., Riviello, J.J., Jr., Shutter, L., Sperling, M.R., *et al*. (2012). Guidelines for the evaluation and management of status epilepticus. Neurocrit Care *17*, 3-23.

Brown, D.A., and Griffith, W.H. (1983). Calcium-activated outward current in voltage-clamped hippocampal neurones of the guinea-pig. J Physiol *337*, 287-301.

Buchanan, K.A., Blackman, A.V., Moreau, A.W., Elgar, D., Costa, R.P., Lalanne, T., Tudor Jones, A.A., Oyrer, J., and Sjostrom, P.J. (2012). Target-specific expression of presynaptic NMDA receptors in neocortical microcircuits. Neuron *75*, 451-466.

Buchholz, F., Angrand, P.O., and Stewart, A.F. (1998). Improved properties of FLP recombinase evolved by cycling mutagenesis. Nat Biotechnol *16*, 657-662.

Bui, A.D., Nguyen, T.M., Limouse, C., Kim, H.K., Szabo, G.G., Felong, S., Maroso, M., and Soltesz, I. (2018). Dentate gyrus mossy cells control spontaneous convulsive seizures and spatial memory. Science *359*, 787-790.

Burger, C., Gorbatyuk, O.S., Velardo, M.J., Peden, C.S., Williams, P., Zolotukhin, S., Reier, P.J., Mandel, R.J., and Muzyczka, N. (2004). Recombinant AAV viral vectors pseudotyped with viral capsids from serotypes 1, 2, and 5 display differential efficiency and cell tropism after delivery to different regions of the central nervous system. Mol Ther *10*, 302-317.

Buzsaki, G. (1996). The hippocampo-neocortical dialogue. Cereb Cortex *6*, 81-92.

Buzsaki, G., Horvath, Z., Urioste, R., Hetke, J., and Wise, K. (1992). High-frequency network oscillation in the hippocampus. Science *256*, 1025-1027.

Cain, D.P. (1981). Transfer of pentylenetetrazol sensitization to amygdaloid kindling. Pharmacol Biochem Behav *15*, 533-536.

Cain, D.P. (1982). Kindling in sensory systems: Neocortex. Experimental Neurology *76*, 276-283.

Cain, D.P. (1983). Bidirectional transfer of electrical and carbachol kindling. Brain Res *260*, 135-138.

Cain, D.P., Corcoran, M.E., and Staines, W.A. (1980). Effects of protein synthesis inhibition on kindling in the mouse. Experimental Neurology *68*, 409-419.

Callaway, E.M., and Katz, L.C. (1993). Photostimulation using caged glutamate reveals functional circuitry in living brain slices. Proc Natl Acad Sci U S A *90*, 7661-7665.

Campanac, E., Gasselin, C., Baude, A., Rama, S., Ankri, N., and Debanne, D. (2013). Enhanced intrinsic excitability in basket cells maintains excitatory-inhibitory balance in hippocampal circuits. Neuron *77*, 712-722.

Campbell, S.L., and Hablitz, J.J. (2008). Decreased glutamate transport enhances excitability in a rat model of cortical dysplasia. Neurobiol Dis *32*, 254-261.

Cardin, J.A., Carlén, M., Meletis, K., Knoblich, U., Zhang, F., Deisseroth, K., Tsai, L.-H., and Moore, C.I. (2010). Targeted optogenetic stimulation and recording of neurons in vivo using cell-type-specific expression of Channelrhodopsin-2. Nat Protocols *5*, 247-254.

Cardin, J.A., Carlen, M., Meletis, K., Knoblich, U., Zhang, F., Deisseroth, K., Tsai, L.H., and Moore, C.I. (2009). Driving fast-spiking cells induces gamma rhythm and controls sensory responses. Nature *459*, 663-667.

Cavalheiro, E.A., Leite, J.P., Bortolotto, Z.A., Turski, W.A., Ikonomidou, C., and Turski, L. (1991). Long-term effects of pilocarpine in rats: structural damage of the brain triggers kindling and spontaneous recurrent seizures. Epilepsia *32*, 778-782.

Cavazos, J.E., Das, I., and Sutula, T.P. (1994). Neuronal loss induced in limbic pathways by kindling: evidence for induction of hippocampal sclerosis by repeated brief seizures. The Journal of Neuroscience *14*, 3106-3121.

Cavazos, J.E., Golarai, G., and Sutula, T.P. (1991). Mossy fiber synaptic reorganization induced by kindling: time course of development, progression, and permanence. J Neurosci *11*, 2795-2803.

Cavazos, J.E., and Sutula, T.P. (1990). Progressive neuronal loss induced by kindling: a possible mechanism for mossy fiber synaptic reorganization and hippocampal sclerosis. Brain Res *527*, 1-6.

Cela, E., McFarlan, A.R., Chung, A.J., Wang, T., Chierzi, S., Murai, K.K., and Sjöström, P.J. (2019). An Optogenetic Kindling Model of Neocortical Epilepsy. Scientific Reports *9*, 5236.

Chagnac-Amitai, Y., and Connors, B.W. (1989). Horizontal spread of synchronized activity in neocortex and its control by GABA-mediated inhibition. J Neurophysiol *61*, 747-758.

Chamberlin, N.L., Traub, R.D., and Dingledine, R. (1990). Role of EPSPs in initiation of spontaneous synchronized burst firing in rat hippocampal neurons bathed in high potassium. J Neurophysiol *64*, 1000-1008.

Chang, B.S., and Lowenstein, D.H. (2003). Epilepsy. N Engl J Med *349*, 1257-1266.

Chang, M., Dian, J.A., Dufour, S., Wang, L., Moradi Chameh, H., Ramani, M., Zhang, L., Carlen, P.L., Womelsdorf, T., and Valiante, T.A. (2018). Brief activation of GABAergic interneurons initiates the transition to ictal events through post-inhibitory rebound excitation. Neurobiol Dis *109*, 102-116.

Chatterjee, S., Sullivan, H.A., MacLennan, B.J., Xu, R., Hou, Y., Lavin, T.K., Lea, N.E., Michalski, J.E., Babcock, K.R., Dietrich, S.*, et al*. (2018). Nontoxic, double-deletion-mutant rabies viral vectors for retrograde targeting of projection neurons. Nat Neurosci *21*, 638-646.

Chauvette, S., Soltani, S., Seigneur, J., and Timofeev, I. (2015). In vivo models of cortical acquired epilepsy. Journal of Neuroscience Methods.

Chauvette, S., Soltani, S., Seigneur, J., and Timofeev, I. (2016). In vivo models of cortical acquired epilepsy. J Neurosci Methods *260*, 185-201.

Chen, S., Weitemier, A.Z., Zeng, X., He, L., Wang, X., Tao, Y., Huang, A.J.Y., Hashimotodani, Y., Kano, M., Iwasaki, H.*, et al*. (2018a). Near-infrared deep brain stimulation via upconversion nanoparticle-mediated optogenetics. Science *359*, 679-684.

Chen, Z., Brodie, M.J., Liew, D., and Kwan, P. (2018b). Treatment Outcomes in Patients With Newly Diagnosed Epilepsy Treated With Established and New Antiepileptic Drugs: A 30-Year Longitudinal Cohort Study. JAMA Neurol *75*, 279-286.

Chiang, C.C., Ladas, T.P., Gonzalez-Reyes, L.E., and Durand, D.M. (2014). Seizure Suppression by High Frequency Optogenetic Stimulation Using In Vitro and In Vivo Animal Models of Epilepsy. Brain Stimul *7*, 890-899.

Chow, B.Y., Han, X., Dobry, A.S., Qian, X., Chuong, A.S., Li, M., Henninger, M.A., Belfort, G.M., Lin, Y., Monahan, P.E.*, et al*. (2010). High-performance genetically targetable optical neural silencing by light-driven proton pumps. Nature *463*, 98-102.

Christian, E.P., and Dudek, F.E. (1988). Characteristics of local excitatory circuits studied with glutamate microapplication in the CA3 area of rat hippocampal slices. J Neurophysiol *59*, 90-109.

Christie, I.N., Wells, J.A., Southern, P., Marina, N., Kasparov, S., Gourine, A.V., and Lythgoe, M.F. (2013). fMRI response to blue light delivery in the naive brain: implications for combined optogenetic fMRI studies. Neuroimage *66*, 634-641.

Chu, Y., Jin, X., Parada, I., Pesic, A., Stevens, B., Barres, B., and Prince, D.A. (2010). Enhanced synaptic connectivity and epilepsy in C1q knockout mice. Proc Natl Acad Sci USA *107*, 7975-7980.

Chuong, A.S., Miri, M.L., Busskamp, V., Matthews, G.A., Acker, L.C., Sorensen, A.T., Young, A., Klapoetke, N.C., Henninger, M.A., Kodandaramaiah, S.B., *et al*. (2014). Noninvasive optical inhibition with a red-shifted microbial rhodopsin. Nat Neurosci *17*, 1123-1129.

Clark, M., Post, R.M., Weiss, S.R., Cain, C.J., and Nakajima, T. (1991). Regional expression of c-fos mRNA in rat brain during the evolution of amygdala kindled seizures. Brain Res Mol Brain Res *11*, 55-64.

Clark, M., Post, R.M., Weiss, S.R., and Nakajima, T. (1992). Expression of c-fos mRNA in acute and kindled cocaine seizures in rats. Brain Res *582*, 101-106.

Cobb, S.R., Buhl, E.H., Halasy, K., Paulsen, O., and Somogyi, P. (1995). Synchronization of neuronal activity in hippocampus by individual GABAergic interneurons. Nature *378*, 75-78.

Coenen, A.M. (1975). Frequency analysis of rat hippocampal electrical activity. Physiol Behav *14*, 391-394.

Cohen-Gadol, A.A., Pan, J.W., Kim, J.H., Spencer, D.D., and Hetherington, H.H. (2004). Mesial temporal lobe epilepsy: a proton magnetic resonance spectroscopy study and a histopathological analysis. J Neurosurg *101*, 613-620.

Corcoran, M.E., and Moshé, S.L. (2005). Kindling 6 (New York: Springer).

Couzin, J., and Kaiser, J. (2005). Gene therapy. As Gelsinger case ends, gene therapy suffers another blow. Science *307*, 1028.

Cudmore, R.H., and Turrigiano, G.G. (2004). Long-term potentiation of intrinsic excitability in LV visual cortical neurons. J Neurophysiol *92*, 341-348.

Curry, J.J. (1974). Prepyriform seizure thresholds during the estrous cycle in female rats. Exp Neurol *42*, 300-306.

D'Antuono, M., de Guzman, P., Kano, T., and Avoli, M. (2005). Ripple activity in the dentate gyrus of dishinibited hippocampus-entorhinal cortex slices. J Neurosci Res *80*, 92-103.

dal Maschio, M., Ghezzi, D., Bony, G., Alabastri, A., Deidda, G., Brondi, M., Sato, S.S., Zaccaria, R.P., Di Fabrizio, E., Ratto, G.M., *et al*. (2012). High-performance and site-directed in utero electroporation by a triple-electrode probe. Nat Commun *3*, 960.

de Curtis, M., and Avanzini, G. (2001). Interictal spikes in focal epileptogenesis. Prog Neurobiol *63*, 541-567.

de Curtis, M., Radici, C., and Forti, M. (1999). Cellular mechanisms underlying spontaneous interictal spikes in an acute model of focal cortical epileptogenesis. Neuroscience *88*, 107-117.

De Simoni, M.G., Perego, C., Ravizza, T., Moneta, D., Conti, M., Marchesi, F., De Luigi, A., Garattini, S., and Vezzani, A. (2000). Inflammatory cytokines and related genes are induced in the rat hippocampus by limbic status epilepticus. Eur J Neurosci *12*, 2623-2633.

Deisz, R.A. (2009). PYRAMIDAL CELLS | Intrinsic Mechanisms Contributing to Hyperexcitability of Human Epileptogenic Cortex. In Encyclopedia of Basic Epilepsy Research, P.A. Schwartzkroin, ed. (Oxford: Academic Press), pp. 1266-1272.

Delbeke, J., Hoffman, L., Mols, K., Braeken, D., and Prodanov, D. (2017). And Then There Was Light: Perspectives of Optogenetics for Deep Brain Stimulation and Neuromodulation. Front Neurosci *11*, 663.

Dennison, Z., Teskey, G.C., and Cain, D.P. (1995). Persistence of kindling: effect of partial kindling, retention interval, kindling site, and stimulation parameters. Epilepsy Res *21*, 171-182.

Dheer, P., Chaitanya, G., Pizarro, D., Esteller, R., Majumdar, K., and Pati, S. (2017). Seizure Detection and Network Dynamics of Generalized Convulsive Seizures: Towards Rational Designing of Closed-Loop Neuromodulation. Neurosci J *2017*, 9606213.

Dittgen, T., Nimmerjahn, A., Komai, S., Licznerski, P., Waters, J., Margrie, T.W., Helmchen, F., Denk, W., Brecht, M., and Osten, P. (2004). Lentivirus-based genetic manipulations of cortical neurons and their optical and electrophysiological monitoring in vivo. Proc Natl Acad Sci U S A *101*, 18206-18211.

Dong, Y., and Benveniste, E.N. (2001). Immune function of astrocytes. Glia *36*, 180-190.

Dragunow, M. (1988). Purinergic mechanisms in epilepsy. Prog Neurobiol *31*, 85-108.

Duchowny, M.S., and Burchfiel, J.L. (1981). Facilitation and antagonism of kindled seizure development in the limbic system of the rat. Electroencephalogr Clin Neurophysiol *51*, 403-416.

Dudek, F.E., Pouliot, W.A., Rossi, C.A., and Staley, K.J. (2010). The effect of the cannabinoid-receptor antagonist, SR141716, on the early stage of kainate-induced epileptogenesis in the adult rat. Epilepsia *51 Suppl 3*, 126-130.

During, M.J., Ryder, K.M., and Spencer, D.D. (1995). Hippocampal GABA transporter function in temporal-lobe epilepsy. Nature *376*, 174-177.

Dymecki, S.M., and Kim, J.C. (2007). Molecular neuroanatomy's "Three Gs": a primer. Neuron *54*, 17-34.

Ellender, T.J., Raimondo, J.V., Irkle, A., Lamsa, K.P., and Akerman, C.J. (2014). Excitatory effects of parvalbumin-expressing interneurons maintain hippocampal epileptiform activity via synchronous afterdischarges. J Neurosci *34*, 15208-15222.

Elmer, E., Kokaia, M., Kokaia, Z., Ferencz, I., and Lindvall, O. (1996). Delayed kindling development after rapidly recurring seizures: Relation to mossy fiber sprouting and neurotrophin, GAP-43 and dynorphin gene expression. Brain Research *712*, 19-34.

Emiliani, V., Cohen, A.E., Deisseroth, K., and Häusser, M. (2015). All-Optical Interrogation of Neural Circuits. J Neurosci *35*, 13917-13926.

Engel, J. (2005). Epilepsy : global issues for the practicing neurologist (New York, N.Y.: Demos Medical Pub.).

Engel, J., Jr., and da Silva, F.L. (2012). High-frequency oscillations - where we are and where we need to go. Prog Neurobiol *98*, 316-318.

Engel, J., and Pedley, T.A. (2008). Epilepsy : a comprehensive textbook, 2nd edn (Philadelphia: Wolters Kluwer Health/Lippincott Williams & Wilkins).

Esmaeilpour, K., Sheibani, V., Shabani, M., and Mirnajafi-Zadeh, J. (2017). Low frequency electrical stimulation has time dependent improving effect on kindling-induced impairment in long-term potentiation in rats. Brain Research *1668*, 20-27.

Feeney, D.M., Boyeson, M.G., Linn, R.T., Murray, H.M., and Dail, W.G. (1981). Responses to cortical injury: I. Methodology and local effects of contusions in the rat. Brain Res *211*, 67-77.

Feng, H.J., Naritoku, D.K., Randall, M.E., and Faingold, C.L. (2001). Modulation of audiogenically kindled seizures by gamma-aminobutyric acid-related mechanisms in the amygdala. Exp Neurol *172*, 477-481.

Ferguson, P.L., Smith, G.M., Wannamaker, B.B., Thurman, D.J., Pickelsimer, E.E., and Selassie, A.W. (2010). A population-based study of risk of epilepsy after hospitalization for traumatic brain injury. Epilepsia *51*, 891-898.

Fino, E., and Yuste, R. (2011). Dense inhibitory connectivity in neocortex. Neuron *69*, 1188-1203.

Fisher, R.S. (1989). Animal models of the epilepsies. Brain Res Brain Res Rev *14*, 245-278.

Fisher, R.S., Acevedo, C., Arzimanoglou, A., Bogacz, A., Cross, J.H., Elger, C.E., Engel, J., Jr., Forsgren, L., French, J.A., Glynn, M., *et al*. (2014). ILAE official report: a practical clinical definition of epilepsy. Epilepsia *55*, 475-482.

Fitzsimons, H.L., Bland, R.J., and During, M.J. (2002). Promoters and regulatory elements that improve adeno-associated virus transgene expression in the brain. Methods *28*, 227-236.

Franck, J.E., Kunkel, D.D., Baskin, D.G., and Schwartzkroin, P.A. (1988). Inhibition in kainate-lesioned hyperexcitable hippocampi: physiologic, autoradiographic, and immunocytochemical observations. J Neurosci *8*, 1991-2002.

Freund, T.F., and Buzsaki, G. (1996). Interneurons of the hippocampus. Hippocampus *6*, 347-470.

Friedman, L.K., Pellegrini-Giampietro, D.E., Sperber, E.F., Bennett, M.V., Moshe, S.L., and Zukin, R.S. (1994). Kainate-induced status epilepticus alters glutamate and GABAA receptor gene expression in adult rat hippocampus: an in situ hybridization study. J Neurosci *14*, 2697-2707.

Gabbott, P.L., and Somogyi, P. (1986). Quantitative distribution of GABA-immunoreactive neurons in the visual cortex (area 17) of the cat. Exp Brain Res *61*, 323-331.

Galarreta, M., and Hestrin, S. (1998). Frequency-dependent synaptic depression and the balance of excitation and inhibition in the neocortex. Nat Neurosci *1*, 587-594.

Gall, C.M. (1992). Regulation of brain neurotrophin expression by physiological activity. Trends Pharmacol Sci *13*, 401-403.

Geinisman, Y., Morrell, F., and deToledo-Morrell, L. (1988a). Remodeling of synaptic architecture during hippocampal "kindling". Proc Natl Acad Sci U S A *85*, 3260-3264.

Geinisman, Y., Morrell, F., and deToledo-Morrell, L. (1988b). Remodeling of synaptic architecture during hippocampal "kindling". Proceedings of the National Academy of Sciences *85*, 3260-3264.

Geinisman, Y., Morrell, F., and deToledo-Morrell, L. (1992). Increase in the number of axospinous synapses with segmented postsynaptic densities following hippocampal kindling. Brain Res *569*, 341-347.

Gilbert, M.E. (1992). Proconvulsant activity of endosulfan in amygdala kindling. Neurotoxicol Teratol *14*, 143-149.

Gilbert, T.H., Hannesson, D.K., and Corcoran, M.E. (2000). Hippocampal kindled seizures impair spatial cognition in the Morris water maze. Epilepsy Res *38*, 115-125.

Glasscock, E., Qian, J., Yoo, J.W., and Noebels, J.L. (2007). Masking epilepsy by combining two epilepsy genes. Nat Neurosci *10*, 1554-1558.

Goddard, G.V. (1967). Development of Epileptic Seizures through Brain Stimulation at Low Intensity. Nature *214*, 1020-1021.

Goddard, G.V., McIntyre, D.C., and Leech, C.K. (1969). A permanent change in brain function resulting from daily electrical stimulation. Experimental Neurology *25*, 295-330.

Gotman, J. (1980). Quantitative measurements of epileptic spike morphology in the human EEG. Electroencephalogr Clin Neurophysiol *48*, 551-557.

Grabenstatter, H.L., Del Angel, Y.C., Carlsen, J., Wempe, M.F., White, A.M., Cogswell, M., Russek, S.J., and Brooks-Kayal, A.R. (2014). The effect of STAT3 inhibition on status epilepticus and subsequent spontaneous seizures in the pilocarpine model of acquired epilepsy. Neurobiol Dis *62*, 73-85.

Gradinaru, V., Zhang, F., Ramakrishnan, C., Mattis, J., Prakash, R., Diester, I., Goshen, I., Thompson, K.R., and Deisseroth, K. (2010). Molecular and cellular approaches for diversifying and extending optogenetics. Cell *141*, 154-165.

Haas, K.Z., Sperber, E.F., and Moshe, S.L. (1990). Kindling in developing animals: expression of severe seizures and enhanced development of bilateral foci. Brain Res Dev Brain Res *56*, 275-280.

Haltiner, A.M., Temkin, N.R., and Dikmen, S.S. (1997). Risk of seizure recurrence after the first late posttraumatic seizure. Arch Phys Med Rehabil *78*, 835-840.

Hannesson, D.K., Mohapel, P., and Corcoran, M.E. (2001). Dorsal hippocampal kindling selectively impairs spatial learning/short-term memory. Hippocampus *11*, 275-286.

Hansen, A., Jorgensen, O.S., Bolwig, T.G., and Barry, D.I. (1990). Hippocampal kindling alters the concentration of glial fibrillary acidic protein and other marker proteins in rat brain. Brain Res *531*, 307-311.

Harz, H., and Hegemann, P. (1991). Rhodopsin-Regulated Calcium Currents in Chlamydomonas. Nature *351*, 489-491.

Hebb, D.O. (1949). The Organization of Behavior. In (New York: Wiley).

Hebb, D.O. (1950). Organization of Behavior. Journal of Clinical Psychology *6*, 307-307.

Herman, S.T. (2002). Epilepsy after brain insult: targeting epileptogenesis. Neurology *59*, S21-26.

Hoffmann, A.F., Zhao, Q., and Holmes, G.L. (2004). Cognitive impairment following status epilepticus and recurrent seizures during early development: support for the "two-hit hypothesis". Epilepsy Behav *5*, 873-877.

Hopkins, D.A., and Holstege, G. (1978). Amygdaloid projections to the mesencephalon, pons and medulla oblongata in the cat. Exp Brain Res *32*, 529-547.

Hosford, D.A., Crain, B.J., Cao, Z., Bonhaus, D.W., Friedman, A.H., Okazaki, M.M., Nadler, J.V., and McNamara, J.O. (1991). Increased AMPA-sensitive quisqualate receptor binding

and reduced NMDA receptor binding in epileptic human hippocampus. J Neurosci *11*, 428-434.

Hososhima, S., Yuasa, H., Ishizuka, T., Hoque, M.R., Yamashita, T., Yamanaka, A., Sugano, E., Tomita, H., and Yawo, H. (2015). Near-infrared (NIR) up-conversion optogenetics. Sci Rep *5*, 16533.

Houser, C.R. (1999). Neuronal loss and synaptic reorganization in temporal lobe epilepsy. Adv Neurol *79*, 743-761.

Hsu, B.Y., Wehrli, S.L., Yandrasitz, J.R., Fenstermacher, E.A., Palmieri, M.J., Rea, C.T., McNamara, P.D., Bovee, K.C., and Segal, S. (1994). Renal brush border membrane lipid composition in Basenji dogs with spontaneous idiopathic Fanconi syndrome. Metabolism *43*, 1073-1078.

Hsu, D.A., Rayer, K., Jackson, D.C., Stafstrom, C.E., Hsu, M., Ferrazzano, P.A., Dabbs, K., Worrell, G.A., Jones, J.E., and Hermann, B.P. (2016). Correlation of EEG with neuropsychological status in children with epilepsy. Clin Neurophysiol *127*, 1196-1205.

Huang, J., and Manning, B.D. (2008). The TSC1-TSC2 complex: a molecular switchboard controlling cell growth. Biochem J *412*, 179-190.

Huneau, C., Demont-Guignard, S., Benquet, P., Martin, B., and Wendling, F. (2010). Time-domain features of epileptic spikes as potential bio-markers of the epileptogenesis process. Conf Proc IEEE Eng Med Biol Soc *2010*, 6007-6010.

Iadarola, M.J., Shin, C., McNamara, J.O., and Yang, H.Y. (1986). Changes in dynorphin, enkephalin and cholecystokinin content of hippocampus and substantia nigra after amygdala kindling. Brain Res *365*, 185-191.

Inoue, K., Ono, H., Abe-Yoshizumi, R., Yoshizawa, S., Ito, H., Kogure, K., and Kandori, H. (2013). A light-driven sodium ion pump in marine bacteria. Nat Commun *4*, 1678.

Ishiura, H., Doi, K., Mitsui, J., Yoshimura, J., Matsukawa, M.K., Fujiyama, A., Toyoshima, Y., Kakita, A., Takahashi, H., Suzuki, Y., *et al*. (2018). Expansions of intronic TTTCA and TTTTA repeats in benign adult familial myoclonic epilepsy. Nat Genet *50*, 581-590.

Jabbari, B., Russo, M.B., and Russo, M.L. (2000). Electroencephalogram of asymptomatic adult subjects. Clin Neurophysiol *111*, 102-105.

Jacobs, J., LeVan, P., Chander, R., Hall, J., Dubeau, F., and Gotman, J. (2008). Interictal high-frequency oscillations (80-500 Hz) are an indicator of seizure onset areas independent of spikes in the human epileptic brain. Epilepsia *49*, 1893-1907.

Jacobs, J., Levan, P., Chatillon, C.E., Olivier, A., Dubeau, F., and Gotman, J. (2009a). High frequency oscillations in intracranial EEGs mark epileptogenicity rather than lesion type. Brain *132*, 1022-1037.

Jacobs, J., Zelmann, R., Jirsch, J., Chander, R., Dubeau, C.E., and Gotman, J. (2009b). High frequency oscillations (80-500 Hz) in the preictal period in patients with focal seizures. Epilepsia *50*, 1780-1792.

Jacobs, J., Zijlmans, M., Zelmann, R., Chatillon, C.E., Hall, J., Olivier, A., Dubeau, F., and Gotman, J. (2010). High-frequency electroencephalographic oscillations correlate with outcome of epilepsy surgery. Ann Neurol *67*, 209-220.

Jefferys, J.G., Menendez de la Prida, L., Wendling, F., Bragin, A., Avoli, M., Timofeev, I., and Lopes da Silva, F.H. (2012). Mechanisms of physiological and epileptic HFO generation. Prog Neurobiol *98*, 250-264.

Jin, X., Prince, D.A., and Huguenard, J.R. (2006). Enhanced excitatory synaptic connectivity in layer v pyramidal neurons of chronically injured epileptogenic neocortex in rats. J Neurosci *26*, 4891-4900.

Jones, M.S., and Barth, D.S. (1999). Spatiotemporal organization of fast (>200 Hz) electrical oscillations in rat Vibrissa/Barrel cortex. J Neurophysiol *82*, 1599-1609.

Kamphuis, W., De Rijk, T.C., Talamini, L.M., and Lopes da Silva, F.H. (1994). Rat hippocampal kindling induces changes in the glutamate receptor mRNA expression patterns in dentate granule neurons. Eur J Neurosci *6*, 1119-1127.

Kandel, A., and Buzsaki, G. (1997). Cellular-synaptic generation of sleep spindles, spike-and-wave discharges, and evoked thalamocortical responses in the neocortex of the rat. J Neurosci *17*, 6783-6797.

Kaplitt, M.G., Leone, P., Samulski, R.J., Xiao, X., Pfaff, D.W., O'Malley, K.L., and During, M.J. (1994). Long-term gene expression and phenotypic correction using adeno-associated virus vectors in the mammalian brain. Nat Genet *8*, 148-154.

Katona, I., Sperlagh, B., Sik, A., Kafalvi, A., Vizi, E.S., Mackie, K., and Freund, T.F. (1999). Presynaptically located CB1 cannabinoid receptors regulate GABA release from axon terminals of specific hippocampal interneurons. J Neurosci *19*, 4544-4558.

Katzel, D., Nicholson, E., Schorge, S., Walker, M.C., and Kullmann, D.M. (2014). Chemical-genetic attenuation of focal neocortical seizures. Nat Commun *5*, 3847.

Khoshkhoo, S., Vogt, D., and Sohal, V.S. (2017). Dynamic, Cell-Type-Specific Roles for GABAergic Interneurons in a Mouse Model of Optogenetically Inducible Seizures. Neuron *93*, 291-298.

Khurgel, M., and Ivy, G.O. (1996). Astrocytes in kindling: relevance to epileptogenesis. Epilepsy Res *26*, 163-175.

Ko, H., Hofer, S.B., Pichler, B., Buchanan, K.A., Sjostrom, P.J., and Mrsic-Flogel, T.D. (2011). Functional specificity of local synaptic connections in neocortical networks. Nature *473*, 87-91.

Kogure, S., Kitayama, M., and Matsuda, Y. (2000). Simultaneous kindling of the bilateral hippocampi: an advanced model for epilepsy research. Epilepsia *41*, 929-932.

Koh, S., Storey, T.W., Santos, T.C., Mian, A.Y., and Cole, A.J. (2001). Early-life seizures in rats increase susceptibility to seizure-induced brain injury in adulthood. 1999. Neurology *57*, S22-28.

Kohr, G., De Koninck, Y., and Mody, I. (1993). Properties of NMDA receptor channels in neurons acutely isolated from epileptic (kindled) rats. J Neurosci *13*, 3612-3627.

Kohr, G., Lambert, C.E., and Mody, I. (1991). Calbindin-D28K (CaBP) levels and calcium currents in acutely dissociated epileptic neurons. Exp Brain Res *85*, 543-551.

Kollevold, T. (1976). Immediate and early cerebral seizures after head injuries. Part I. J Oslo City Hosp *26*, 99-114.

Kotloski, R., Lynch, M., Lauersdorf, S., and Sutula, T. (2002). Repeated brief seizures induce progressive hippocampal neuron loss and memory deficits. Prog Brain Res *135*, 95-110.

Krook-Magnuson, E., Armstrong, C., Bui, A., Lew, S., Oijala, M., and Soltesz, I. (2015). In vivo evaluation of the dentate gate theory in epilepsy. J Physiol *593*, 2379-2388.

Krook-Magnuson, E., Armstrong, C., Oijala, M., and Soltesz, I. (2013). On-demand optogenetic control of spontaneous seizures in temporal lobe epilepsy. Nat Commun *4*, 1376.

Krook-Magnuson, E., Szabo, G.G., Armstrong, C., Oijala, M., and Soltesz, I. (2014). Cerebellar Directed Optogenetic Intervention Inhibits Spontaneous Hippocampal Seizures in a Mouse Model of Temporal Lobe Epilepsy. eNeuro *1*.

Kros, L., Eelkman Rooda, O.H., Spanke, J.K., Alva, P., van Dongen, M.N., Karapatis, A., Tolner, E.A., Strydis, C., Davey, N., Winkelman, B.H., *et al*. (2015). Cerebellar output controls generalized spike-and-wave discharge occurrence. Ann Neurol *77*, 1027-1049.

Kubelka, P. (1948). New contributions to the optics of intensely light-scattering materials. J Opt Soc Am *38*, 448-457.

Kwan, P., Schachter, S.C., and Brodie, M.J. (2011). Drug-Resistant Epilepsy. New England Journal of Medicine *365*, 919-926.

Ladas, T.P., Chiang, C.C., Gonzalez-Reyes, L.E., Nowak, T., and Durand, D.M. (2015). Seizure reduction through interneuron-mediated entrainment using low frequency optical stimulation. Experimental Neurology *269*, 120-132.

Lalanne, T., Abrahamsson, T., and Sjöström, P.J. (2016). Using Multiple Whole-Cell Recordings to Study Spike-Timing-Dependent Plasticity in Acute Neocortical Slices. Cold Spring Harb Protoc *2016*.

Larsen, R.S., and Sjöström, P.J. (2015). Synapse-type-specific plasticity in local circuits. Curr Opin Neurobiol *35*, 127-135.

Lefort, S., Tomm, C., Floyd Sarria, J.C., and Petersen, C.C. (2009). The excitatory neuronal network of the C2 barrel column in mouse primary somatosensory cortex. Neuron *61*, 301-316.

Li, H., Chen, A., Xing, G., Wei, M.L., and Rogawski, M.A. (2001). Kainate receptor-mediated heterosynaptic facilitation in the amygdala. Nat Neurosci *4*, 612-620.

Li, T.F., Ren, G.Y., Lusardi, T., Wilz, A., Lan, J.Q., Iwasato, T., Itohara, S., Simon, R.P., and Boison, D. (2008). Adenosine kinase is a target for the prediction and prevention of epileptogenesis in mice. Journal of Clinical Investigation *118*, 571-582.

Libbrecht, S., Van den Haute, C., Malinouskaya, L., Gijsbers, R., and Baekelandt, V. (2017). Evaluation of WGA-Cre-dependent topological transgene expression in the rodent brain. Brain Struct Funct *222*, 717-733.

Lillis, K.P., Wang, Z., Mail, M., Zhao, G.Q., Berdichevsky, Y., Bacskai, B., and Staley, K.J. (2015). Evolution of Network Synchronization during Early Epileptogenesis Parallels Synaptic Circuit Alterations. J Neurosci *35*, 9920-9934.

Lima, S.Q., and Miesenböck, G. (2005). Remote control of behavior through genetically targeted photostimulation of neurons. Cell *121*, 141-152.

Lin, J.Y., Knutsen, P.M., Muller, A., Kleinfeld, D., and Tsien, R.Y. (2013). ReaChR: a red-shifted variant of channelrhodopsin enables deep transcranial optogenetic excitation. Nat Neurosci *16*, 1499-1508.

Lo, L., and Anderson, D.J. (2011). A Cre-dependent, anterograde transsynaptic viral tracer for mapping output pathways of genetically marked neurons. Neuron *72*, 938-950.

Löscher, W. (1999). Animal models of epilepsy and epileptic seizures. In Antiepileptic Drugs (Springer), pp. 19-62.

Löscher, W. (2002). Animal models of epilepsy for the development of antiepileptogenic and disease-modifying drugs. A comparison of the pharmacology of kindling and post-status epilepticus models of temporal lobe epilepsy. Epilepsy Research *50*, 105-123.

Löscher, W. (2011a). Critical review of current animal models of seizures and epilepsy used in the discovery and development of new antiepileptic drugs. Seizure *20*, 359-368.

Löscher, W. (2011b). Critical review of current animal models of seizures and epilepsy used in the discovery and development of new antiepileptic drugs. Seizure *20*, 359-368.

Lothman, E.W., and Williamson, J.M. (1994). Closely Spaced Recurrent Hippocampal Seizures Elicit 2 Types of Heightened Epileptogenesis - a Rapidly Developing, Transient Kindling and a Slowly Developing, Enduring Kindling. Brain Research *649*, 71-84.

Lu, Y., Zhong, C., Wang, L.L., Wei, P.F., He, W., Huang, K., Zhang, Y., Zhan, Y., Feng, G.P., and Wang, L.P. (2016). Optogenetic dissection of ictal propagation in the hippocampal-entorhinal cortex structures. Nature Communications *7*.

Ludanyi, A., Eross, L., Czirjak, S., Vajda, J., Halasz, P., Watanabe, M., Palkovits, M., Magloczky, Z., Freund, T.F., and Katona, I. (2008). Downregulation of the CB1 cannabinoid receptor and related molecular elements of the endocannabinoid system in epileptic human hippocampus. J Neurosci *28*, 2976-2990.

Luo, C., Ikegaya, Y., and Koyama, R. (2016). Microglia and neurogenesis in the epileptic dentate gyrus. Neurogenesis (Austin) *3*, e1235525.

Lynch, M., and Sutula, T. (2000). Recurrent excitatory connectivity in the dentate gyrus of kindled and kainic acid-treated rats. J Neurophysiol *83*, 693-704.

Manford, M., Hart, Y.M., Sander, J.W., and Shorvon, S.D. (1992). National General Practice Study of Epilepsy (NGPSE): partial seizure patterns in a general population. Neurology *42*, 1911-1917.

Mangan, P.S., Rempe, D.A., and Lothman, E.W. (1995). Changes in inhibitory neurotransmission in the CA1 region and dentate gyrus in a chronic model of temporal lobe epilepsy. J Neurophysiol *74*, 829-840.

Manvich, D.F., Webster, K.A., Foster, S.L., Farrell, M.S., Ritchie, J.C., Porter, J.H., and Weinshenker, D. (2018). The DREADD agonist clozapine N-oxide (CNO) is reverse-metabolized to clozapine and produces clozapine-like interoceptive stimulus effects in rats and mice. Sci Rep *8*, 3840.

Mardia, K.V., and Jupp, P.E. (2000). Directional statistics (Chichester ; New York: J. Wiley).

Markram, H., Gerstner, W., and Sjöström, P.J. (2011). A history of spike-timing-dependent plasticity. Frontiers in Synaptic Neuroscience *3*, 1-24.

Markram, H., Lubke, J., Frotscher, M., Roth, A., and Sakmann, B. (1997). Physiology and anatomy of synaptic connections between thick tufted pyramidal neurones in the developing rat neocortex. J Physiol *500 (Pt 2)*, 409-440.

Marsicano, G., Goodenough, S., Monory, K., Hermann, H., Eder, M., Cannich, A., Azad, S.C., Cascio, M.G., Gutiérrez, S.O., Stelt, M.v.d., *et al*. (2003). CB1 Cannabinoid Receptors and On-Demand Defense Against Excitotoxicity. Science *302*, 84-88.

Masseck, O.A., Spoida, K., Dalkara, D., Maejima, T., Rubelowski, J.M., Wallhorn, L., Deneris, E.S., and Herlitze, S. (2014). Vertebrate cone opsins enable sustained and highly sensitive rapid control of Gi/o signaling in anxiety circuitry. Neuron *81*, 1263-1273.

Matsuda, T., and Cepko, C.L. (2007). Controlled expression of transgenes introduced by in vivo electroporation. Proc Natl Acad Sci U S A *104*, 1027-1032.

McDonald, J.W., Fix, A.S., Tizzano, J.P., and Schoepp, D.D. (1993). Seizures and brain injury in neonatal rats induced by 1S,3R-ACPD, a metabotropic glutamate receptor agonist. J Neurosci *13*, 4445-4455.

McNamara, J.O. (1994). Cellular and molecular basis of epilepsy. J Neurosci *14*, 3413-3425.

Meldrum, B.S. (1993). Excitotoxicity and selective neuronal loss in epilepsy. Brain Pathol *3*, 405-412.

Meldrum, B.S. (2000). Glutamate as a neurotransmitter in the brain: Review of physiology and pathology. Journal of Nutrition *130*, 1007s-1015s.

Merlin, L.R., and Wong, R.K. (1997). Role of group I metabotropic glutamate receptors in the patterning of epileptiform activities in vitro. J Neurophysiol *78*, 539-544.

Michael, M., Holsinger, D., Ikeda-Douglas, C., Cammisuli, S., Ferbinteanu, J., DeSouza, C., DeSouza, S., Fecteau, J., Racine, R.J., and Milgram, N.W. (1998). Development of spontaneous seizures over extended electrical kindling: I. Electrographic, behavioral, and transfer kindling correlates. Brain Research *793*, 197-211.

Mobley, J., and Vo-Dinh, T. (2003). Optical Properties of Tissue. In Biomedical Photonics Handbook (CRC Press).

Mody, I. (1993). The molecular basis of kindling. Brain Pathol *3*, 395-403.

Mody, I., and Staley, K.J. (1994). Cell properties in the epileptic hippocampus. Hippocampus *4*, 275-280.

Mody, I., Stanton, P.K., and Heinemann, U. (1988). Activation of N-methyl-D-aspartate receptors parallels changes in cellular and synaptic properties of dentate gyrus granule cells after kindling. J Neurophysiol *59*, 1033-1054.

Monroe, R.R. (1982). Limbic ictus and atypical psychoses. J Nerv Ment Dis *170*, 711-716.

Mori, N., and Wada, J.A. (1989). Bidirectional Transhemispheric Interaction between Amygdaloid Kindling Induced by Excitatory Amino-Acids and Electrical-Stimulation. Epilepsia *30*, 271-275.

Morimoto, K., Fahnestock, M., and Racine, R.J. (2004). Kindling and status epilepticus models of epilepsy: rewiring the brain. Prog Neurobiol *73*, 1-60.

Morimoto, K., Sanei, T., and Sato, K. (1993). Comparative study of the anticonvulsant effect of gamma-aminobutyric acid agonists in the feline kindling model of epilepsy. Epilepsia *34*, 1123-1129.

Morimoto, K., Sato, H., Sato, K., Sato, S., and Yamada, N. (1997). BW1003C87, phenytoin and carbamazepine elevate seizure threshold in the rat amygdala-kindling model of epilepsy. Eur J Pharmacol *339*, 11-15.

Morrell, F. (1960). Secondary epileptogenic lesions. Epilepsia *1*, 538-560.

Morrell, F. (1985). Secondary epileptogenesis in man. Arch Neurol *42*, 318-335.

Morrell, F., Tsuru, N., Hoeppner, T.J., Morgan, D., and Harrison, W.H. (1975). Secondary epileptogenesis in frog forebrain: effect of inhibition of protein synthesis. Can J Neurol Sci *2*, 407-416.

Mucha, R.F., and Pinel, P.J. (1977). Postseizure inhibition of kindled seizures. Exp Neurol *54*, 266-282.

Murphy, J.T., Kwan, H.C., Mackay, W.A., and Wong, Y.C. (1980). Physiologic Basis for Focal Motor Seizures and the Jacksonian March Phenomena. Canadian Journal of Neurological Sciences *7*, 79-85.

Nadler, J.V., Perry, B.W., and Cotman, C.W. (1978). Intraventricular kainic acid preferentially destroys hippocampal pyramidal cells. Nature *271*, 676-677.

Nadler, J.V., Thompson, M.A., and McNamara, J.O. (1994). Kindling reduces sensitivity of CA3 hippocampal pyramidal cells to competitive NMDA receptor antagonists. Neuropharmacology *33*, 147-153.

Nagel, G., Ollig, D., Fuhrmann, M., Kateriya, S., Musti, A.M., Bamberg, E., and Hegemann, P. (2002). Channelrhodopsin-1: a light-gated proton channel in green algae. Science *296*, 2395-2398.

Nathanson, M., Krumholz, A., and Biddle, D. (1978). Seizures of axial structures. Presumptive evidence for brain stem origin. Arch Neurol *35*, 448-452.

Navarrete, M., and Araque, A. (2008). Endocannabinoids mediate neuron-astrocyte communication. Neuron *57*, 883-893.

Nelson, S.B., and Turrigiano, G.G. (1998). Synaptic depression: a key player in the cortical balancing act. Nat Neurosci *1*, 539-541.

Nissinen, J., Andrade, P., Natunen, T., Hiltunen, M., Malm, T., Kanninen, K., Soares, J.I., Shatillo, O., Sallinen, J., Ndode-Ekane, X.E., *et al*. (2017). Disease-modifying effect of atipamezole in a model of post-traumatic epilepsy. Epilepsy Res *136*, 18-34.

Niswender, C.M., and Conn, P.J. (2010). Metabotropic Glutamate Receptors: Physiology, Pharmacology, and Disease. Annu Rev Pharmacol *50*, 295-322.

Ogren, J.A., Wilson, C.L., Bragin, A., Lin, J.J., Salamon, N., Dutton, R.A., Luders, E., Fields, T.A., Fried, I., Toga, A.W., *et al*. (2009). Three-dimensional surface maps link local atrophy and fast ripples in human epileptic hippocampus. Ann Neurol *66*, 783-791.

Ohara, S., Ikeda, A., Kunieda, T., Yazawa, S., Taki, J., Nagamine, T., Taki, W., Miyamoto, S., Hashimoto, N., and Shibasaki, H. (2004). Propagation of tonic posturing in supplementary motor area (SMA) seizures. Epilepsy Res *62*, 179-187.

Olney, J.W., Rhee, V., and Ho, O.L. (1974). Kainic acid: a powerful neurotoxic analogue of glutamate. Brain Res *77*, 507-512.

Osawa, S., Iwasaki, M., Hosaka, R., Matsuzaka, Y., Tomita, H., Ishizuka, T., Sugano, E., Okumura, E., Yawo, H., Nakasato, N., *et al*. (2013). Optogenetically induced seizure and the longitudinal hippocampal network dynamics. PLoS One *8*, e60928.

Oyegbile, T.O., Dow, C., Jones, J., Bell, B., Rutecki, P., Sheth, R., Seidenberg, M., and Hermann, B.P. (2004). The nature and course of neuropsychological morbidity in chronic temporal lobe epilepsy. Neurology *62*, 1736-1742.

Ozen, L.J., and Teskey, G.C. (2009). One hertz stimulation to the corpus callosum quenches seizure development and attenuates motor map expansion. Neuroscience *160*, 567-575.

Pascual, O., Casper, K.B., Kubera, C., Zhang, J., Revilla-Sanchez, R., Sul, J.Y., Takano, H., Moss, S.J., McCarthy, K., and Haydon, P.G. (2005). Astrocytic purinergic signaling coordinates synaptic networks. Science *310*, 113-116.

Paz, J.T., Bryant, A.S., Peng, K., Fenno, L., Yizhar, O., Frankel, W.N., Deisseroth, K., and Huguenard, J.R. (2011). A new mode of corticothalamic transmission revealed in the Gria4(-/-) model of absence epilepsy. Nat Neurosci *14*, 1167-1173.

Paz, J.T., Davidson, T.J., Frechette, E.S., Delord, B., Parada, I., Peng, K., Deisseroth, K., and Huguenard, J.R. (2012). Closed-loop optogenetic control of thalamus as a tool for interrupting seizures after cortical injury. Nature Neuroscience *16*, 64-70.

Paz, J.T., Davidson, T.J., Frechette, E.S., Delord, B., Parada, I., Peng, K., Deisseroth, K., and Huguenard, J.R. (2013). Closed-loop optogenetic control of thalamus as a tool for interrupting seizures after cortical injury. Nat Neurosci *16*, 64-70.

Pei, Y., Rogan, S.C., Yan, F., and Roth, B.L. (2008). Engineered GPCRs as tools to modulate signal transduction. Physiology (Bethesda) *23*, 313-321.

Penfield, W., and Rasmussen, T. (1950). The cerebral cortex of man; a clinical study of localization of function (New York,: Macmillan).

Perescis, M.F., de Bruin, N., Heijink, L., Kruse, C., Vinogradova, L., Luttjohann, A., van Luijtelaar, G., and van Rijn, C.M. (2017). Cannabinoid antagonist SLV326 induces convulsive seizures and changes in the interictal EEG in rats. PLoS One *12*, e0165363.

Perreault, P., and Avoli, M. (1992). 4-aminopyridine-induced epileptiform activity and a GABA-mediated long-lasting depolarization in the rat hippocampus. J Neurosci *12*, 104-115.

Perucca, P., and Gilliam, F.G. (2012). Adverse effects of antiepileptic drugs. Lancet Neurol *11*, 792-802.

Petreanu, L., Huber, D., Sobczyk, A., and Svoboda, K. (2007a). Channelrhodopsin-2-assisted circuit mapping of long-range callosal projections. Nat Neurosci *10*, 663-668.

Petreanu, L., Huber, D., Sobczyk, A., and Svoboda, K. (2007b). Channelrhodopsin-2–assisted circuit mapping of long-range callosal projections. Nature Neuroscience *10*, 663-668.

Petreanu, L., Mao, T., Sternson, S.M., and Svoboda, K. (2009). The subcellular organization of neocortical excitatory connections. Nature *457*, 1142-1145.

Petroff, O.A., Errante, L.D., Rothman, D.L., Kim, J.H., and Spencer, D.D. (2002). Glutamate-glutamine cycling in the epileptic human hippocampus. Epilepsia *43*, 703-710.

Pinel, J.P.J., and Rovner, L.I. (1978). Experimental epileptogenesis: Kindling-induced epilepsy in rats. Experimental Neurology *58*, 190-202.

Pitkänen, A., Immonen, R.J., Grohn, O.H., and Kharatishvili, I. (2009a). From traumatic brain injury to posttraumatic epilepsy: what animal models tell us about the process and treatment options. Epilepsia *50 Suppl 2*, 21-29.

Pitkänen, A., Immonen, R.J., Gröhn, O.H.J., and Kharatishvili, I. (2009b). From traumatic brain injury to posttraumatic epilepsy: What animal models tell us about the process and treatment options. Epilepsia *50*, 21-29.

Pitkanen, A., and McIntosh, T.K. (2006). Animal models of post-traumatic epilepsy. J Neurotrauma *23*, 241-261.

Ponnazhagan, S., Mukherjee, P., Yoder, M.C., Wang, X.S., Zhou, S.Z., Kaplan, J., Wadsworth, S., and Srivastava, A. (1997). Adeno-associated virus 2-mediated gene transfer in vivo: organ-tropism and expression of transduced sequences in mice. Gene *190*, 203-210.

Prince, D.A., and Tseng, G.F. (1993). Epileptogenesis in chronically injured cortex: in vitro studies. J Neurophysiol *69*, 1276-1291.

Prince, D.A., and Wong, R.K. (1981). Human epileptic neurons studied in vitro. Brain Res *210*, 323-333.

Qian, Z., Gilbert, M.E., Colicos, M.A., Kandel, E.R., and Kuhl, D. (1993). Tissue-plasminogen activator is induced as an immediate-early gene during seizure, kindling and long-term potentiation. Nature *361*, 453-457.

Quigg, M., Clayburn, H., Straume, M., Menaker, M., and Bertram, E.H., 3rd (2000). Effects of circadian regulation and rest-activity state on spontaneous seizures in a rat model of limbic epilepsy. Epilepsia *41*, 502-509.

Racine, R. (1978). Kindling: the first decade. Neurosurgery *3*, 234-252.

Racine, R., and Zaide, J. (1978). A Further Investigation into the Mechanisms Underlying the Kindling Phenomenon. In Limbic Mechanisms, K.E. Livingston, and O. Hornykiewicz, eds. (Springer US), pp. 457-493.

Racine, R.J. (1972a). Modification of seizure activity by electrical stimulation: I. After-discharge threshold. Electroencephalography and Clinical Neurophysiology *32*, 269-279.

Racine, R.J. (1972b). Modification of seizure activity by electrical stimulation: II. Motor seizure. Electroencephalography and Clinical Neurophysiology *32*, 281-294.

Racine, R.J. (1972c). Modification of seizure activity by electrical stimulation. II. Motor seizure. Electroencephalography and clinical neurophysiology *32*, 281-294.

Racine, R.J. (1975). Modification of seizure activity by electrical stimulation: Cortical areas. Electroencephalography and Clinical Neurophysiology *38*, 1-12.

Racine, R.J., Burnham, W.M., Gartner, J.G., and Levitan, D. (1973). Rates of motor seizure development in rats subjected to electrical brain stimulation: strain and inter-stimulation interval effects. Electroencephalogr Clin Neurophysiol *35*, 553-556.

Racine, R.J., Mosher, M., and Kairiss, E.W. (1988). The role of the pyriform cortex in the generation of interictal spikes in the kindled preparation. Brain Res *454*, 251-263.

Rancz, E.A., Franks, K.M., Schwarz, M.K., Pichler, B., Schaefer, A.T., and Margrie, T.W. (2011). Transfection via whole-cell recording in vivo: bridging single-cell physiology, genetics and connectomics. Nat Neurosci *14*, 527-532.

Represa, A., Le Gall La Salle, G., and Ben-Ari, Y. (1989). Hippocampal plasticity in the kindling model of epilepsy in rats. Neurosci Lett *99*, 345-350.

Rosen, J.B., Cain, C.J., Weiss, S.R., and Post, R.M. (1992). Alterations in mRNA of enkephalin, dynorphin and thyrotropin releasing hormone during amygdala kindling: an in situ hybridization study. Brain Res Mol Brain Res *15*, 247-255.

Rossetti, A.O., and Lowenstein, D.H. (2011). Management of refractory status epilepticus in adults: still more questions than answers. Lancet Neurol *10*, 922-930.

Sajatovic, M., and Meltzer, H.Y. (1996). Clozapine-induced myoclonus and generalized seizures. Biol Psychiatry *39*, 367-370.

Salanova, V., Andermann, F., Rasmussen, T., Olivier, A., and Quesney, L. (1996). The running down phenomenon in temporal lobe epilepsy. Brain *119 (Pt 3)*, 989-996.

Sato, M., Racine, R.J., and McIntyre, D.C. (1990). Kindling: basic mechanisms and clinical validity. Electroencephalogr Clin Neurophysiol *76*, 459-472.

Sato, T., Yamada, N., Morimoto, K., Uemura, S., and Kuroda, S. (1998). A behavioral and immunohistochemical study on the development of perirhinal cortical kindling: a comparison with other types of limbic kindling. Brain Res *811*, 122-132.

Sauer, B. (1987). Functional expression of the cre-lox site-specific recombination system in the yeast Saccharomyces cerevisiae. Mol Cell Biol *7*, 2087-2096.

Sayin, U., Osting, S., Hagen, J., Rutecki, P., and Sutula, T. (2003). Spontaneous seizures and loss of axo-axonic and axo-somatic inhibition induced by repeated brief seizures in kindled rats. J Neurosci *23*, 2759-2768.

Schevon, C.A., Trevelyan, A.J., Schroeder, C.E., Goodman, R.R., McKhann, G., Jr., and Emerson, R.G. (2009). Spatial characterization of interictal high frequency oscillations in epileptic neocortex. Brain *132*, 3047-3059.

Schidlitzki, A., Twele, F., Klee, R., Waltl, I., Romermann, K., Broer, S., Meller, S., Gerhauser, I., Rankovic, V., Li, D., *et al*. (2017). A combination of NMDA and AMPA receptor antagonists retards granule cell dispersion and epileptogenesis in a model of acquired epilepsy. Sci Rep *7*, 12191.

Schneider, C.A., Rasband, W.S., and Eliceiri, K.W. (2012). NIH Image to ImageJ: 25 years of image analysis. Nat Methods *9*, 671-675.

Schwartzkroin, P.A., and Prince, D.A. (1980). Changes in excitatory and inhibitory synaptic potentials leading to epileptogenic activity. Brain Res *183*, 61-76.

Schwarzer, C., and Sperk, G. (1995). Hippocampal granule cells express glutamic acid decarboxylase-67 after limbic seizures in the rat. Neuroscience *69*, 705-709.

Seifert, G., Schilling, K., and Steinhauser, C. (2006). Astrocyte dysfunction in neurological disorders: a molecular perspective. Nat Rev Neurosci *7*, 194-206.

Semyanov, A., Morenkov, E., Savin, A., and Godukhin, O. (2000). In vivo hippocampal kindling occludes the development of in vitro kindling-like state in CA1 area of rat hippocampal slices. Epilepsy Research *38*, 75-85.

Serbanescu, I., Cortez, M.A., McKerlie, C., and Snead, O.C., 3rd (2004). Refractory atypical absence seizures in rat: a two hit model. Epilepsy Res *62*, 53-63.

Sessolo, M., Marcon, I., Bovetti, S., Losi, G., Cammarota, M., Ratto, G.M., Fellin, T., and Carmignoto, G. (2015). Parvalbumin-Positive Inhibitory Interneurons Oppose Propagation But Favor Generation of Focal Epileptiform Activity. J Neurosci *35*, 9544-9557.

Shah, M.M., Anderson, A.E., Leung, V., Lin, X., and Johnston, D. (2004). Seizure-induced plasticity of h channels in entorhinal cortical layer III pyramidal neurons. Neuron *44*, 495-508.

Shiri, Z., Manseau, F., Lévesque, M., Williams, S., and Avoli, M. (2015). Interneuron activity leads to initiation of low-voltage fast-onset seizures. Annals of Neurology *77*, 541-546.

Shorvon, S.D., and Goodridge, D.M. (2013). Longitudinal cohort studies of the prognosis of epilepsy: contribution of the National General Practice Study of Epilepsy and other studies. Brain *136*, 3497-3510.

Shu, X., Lev-Ram, V., Deerinck, T.J., Qi, Y., Ramko, E.B., Davidson, M.W., Jin, Y., Ellisman, M.H., and Tsien, R.Y. (2011). A genetically encoded tag for correlated light and electron microscopy of intact cells, tissues, and organisms. PLoS Biol *9*, e1001041.

Sjostrom, P.J., Turrigiano, G.G., and Nelson, S.B. (2001). Rate, timing, and cooperativity jointly determine cortical synaptic plasticity. Neuron *32*, 1149-1164.

Sjöström, P.J., Turrigiano, G.G., and Nelson, S.B. (2003). Neocortical LTD via Coincident Activation of Presynaptic NMDA and Cannabinoid Receptors. Neuron *39*, 641-654.

Sjulson, L., Cassataro, D., DasGupta, S., and Miesenböck, G. (2016). Cell-Specific Targeting of Genetically Encoded Tools for Neuroscience. Annu Rev Genet *50*, 571-594.

Sloviter, R.S., Dean, E., Sollas, A.L., and Goodman, J.H. (1996). Apoptosis and necrosis induced in different hippocampal neuron populations by repetitive perforant path stimulation in the rat. J Comp Neurol *366*, 516-533.

Sohal, V.S., Zhang, F., Yizhar, O., and Deisseroth, K. (2009). Parvalbumin neurons and gamma rhythms enhance cortical circuit performance. Nature *459*, 698-702.

Soltesz, I., Alger, B.E., Kano, M., Lee, S.-H., Lovinger, D.M., Ohno-Shosaku, T., and Watanabe, M. (2015). Weeding out bad waves: towards selective cannabinoid circuit control in epilepsy. Nature Reviews Neuroscience *16*, 264-277.

Somjen, G.G. (2009). Non-Synaptic Mechanisms in Seizures: The Role of Ion Fluxes and Intrinsic Membrane Properties. Encyclopedia of Basic Epilepsy Research, Vols 1-3, 964-973.

Sonnenberg, J.L., Frantz, G.D., Lee, S., Heick, A., Chu, C., Tobin, A.J., and Christakos, S. (1991). Calcium binding protein (calbindin-D28k) and glutamate decarboxylase gene expression after kindling induced seizures. Brain Res Mol Brain Res *9*, 179-190.

Soper, C., Wicker, E., Kulick, C.V., N'Gouemo, P., and Forcelli, P.A. (2016). Optogenetic activation of superior colliculus neurons suppresses seizures originating in diverse brain networks. Neurobiol Dis *87*, 102-115.

Sorokin, J.M., Davidson, T.J., Frechette, E., Abramian, A.M., Deisseroth, K., Huguenard, J.R., and Paz, J.T. (2017). Bidirectional Control of Generalized Epilepsy Networks via Rapid Real-Time Switching of Firing Mode. Neuron *93*, 194-210.

Sramka, M., Fritz, G., Galanda, M., and Nadvornik, P. (1976). Some observations in treatment stimulation of epilepsy. Acta Neurochir (Wien), 257-262.

Staba, R.J., Frighetto, L., Behnke, E.J., Mathern, G.W., Fields, T., Bragin, A., Ogren, J., Fried, I., Wilson, C.L., and Engel, J., Jr. (2007). Increased fast ripple to ripple ratios correlate with reduced hippocampal volumes and neuron loss in temporal lobe epilepsy patients. Epilepsia *48*, 2130-2138.

Staba, R.J., Wilson, C.L., Bragin, A., Fried, I., and Engel, J., Jr. (2002). Quantitative analysis of high-frequency oscillations (80-500 Hz) recorded in human epileptic hippocampus and entorhinal cortex. J Neurophysiol *88*, 1743-1752.

Staley, K.J., Soldo, B.L., and Proctor, W.R. (1995). Ionic mechanisms of neuronal excitation by inhibitory GABAA receptors. Science *269*, 977-981.

Staley, K.J., White, A., and Dudek, F.E. (2011). Interictal spikes: harbingers or causes of epilepsy? Neurosci Lett *497*, 247-250.

Stanton, P.K., Jones, R.S., Mody, I., and Heinemann, U. (1987). Epileptiform activity induced by lowering extracellular [Mg2+] in combined hippocampal-entorhinal cortex slices:

modulation by receptors for norepinephrine and N-methyl-D-aspartate. Epilepsy Res *1*, 53-62.

Storm, J.F. (1988). Temporal integration by a slowly inactivating K+ current in hippocampal neurons. Nature *336*, 379-381.

Stripling, J.S., and Ellinwood, E.H., Jr. (1977). Augmentation of the behavioral and electrophysiologic response to cocaine by chronic administration in the rat. Exp Neurol *54*, 546-564.

Sukhotinsky, I., Chan, A.M., Ahmed, O.J., Rao, V.R., Gradinaru, V., Ramakrishnan, C., Deisseroth, K., Majewska, A.K., and Cash, S.S. (2013). Optogenetic delay of status epilepticus onset in an in vivo rodent epilepsy model. PLoS One *8*, e62013.

Sutula, T., Xiao-Xian, H., Cavazos, J., and Scott, G. (1988). Synaptic Reorganization in the Hippocampus Induced by Abnormal Functional Activity. Science *239*, 1147-1150.

Sutula, T.P. (2004). Mechanisms of epilepsy progression: current theories and perspectives from neuroplasticity in adulthood and development. Epilepsy Res *60*, 161-171.

Sutula, T.P., Golarai, G., and Cavazos, J. (1992). Assessing the functional significance of mossy fiber sprouting. Epilepsy Res Suppl *7*, 251-259.

Taniguchi, Y., Young-Pearse, T., Sawa, A., and Kamiya, A. (2012). In utero electroporation as a tool for genetic manipulation in vivo to study psychiatric disorders: from genes to circuits and behaviors. Neuroscientist *18*, 169-179.

Taylor, G.W., Merlin, L.R., and Wong, R.K. (1995). Synchronized oscillations in hippocampal CA3 neurons induced by metabotropic glutamate receptor activation. J Neurosci *15*, 8039-8052.

Temkin, N.R. (2003). Risk factors for posttraumatic seizures in adults. Epilepsia *44 Suppl 10*, 18-20.

Teskey, G.C. (2001a). In Toward a theory of neuroplasticity C.A. Shaw, and McEachern, J.C., ed. (Psychology Press), pp. 347-358.

Teskey, G.C. (2001b). Using kindling to model the neuroplastic changes associated with learning and memory, neuropsychiatric disorders, and epilepsy. In Toward a theory of neuroplasticity, C.A. Shaw, and J.C. McEachern, eds. (New York, NY: Psychology Press), pp. 347-358.

Teskey, G.C., Monfils, M.H., Silasi, G., and Kolb, B. (2006). Neocortical kindling is associated with opposing alterations in dendritic morphology in neocortical layer V and striatum from neocortical layer III. Synapse *59*, 1-9.

Teskey, G.C., Monfils, M.H., VandenBerg, P.M., and Kleim, J.A. (2002). Motor map expansion following repeated cortical and limbic seizures is related to synaptic potentiation. Cereb Cortex *12*, 98-105.

Teskey, G.C., Thiessen, E.J., and Gilbert, T.H. (1999). Alternate-site kindling in the guinea-pig results in accelerated seizure progression and generalization. Epilepsy Res *34*, 151-159.

Teyler, T.J., and DiScenna, P. (1987). Long-term potentiation. Annu Rev Neurosci *10*, 131-161.

Timofeev, I., Bazhenov, M., Sejnowski, T., and Steriade, M. (2002). Cortical hyperpolarization-activated depolarizing current takes part in the generation of focal paroxysmal activities. Proc Natl Acad Sci U S A *99*, 9533-9537.

Timofeev, I., Chauvette, S., and Soltani, S. (2014). Neocortical focus: experimental view. Int Rev Neurobiol *114*, 9-33.

Ting, J.T., Daigle, T.L., Chen, Q., and Feng, G. (2014). Acute brain slice methods for adult and aging animals: application of targeted patch clamp analysis and optogenetics. Methods Mol Biol *1183*, 221-242.

Tonnesen, J., Sorensen, A.T., Deisseroth, K., Lundberg, C., and Kokaia, M. (2009). Optogenetic control of epileptiform activity. Proc Natl Acad Sci U S A *106*, 12162-12167.

Traub, R.D. (1982). Simulation of Intrinsic Bursting in Ca3 Hippocampal-Neurons. Neuroscience *7*, 1233-1242.

Tsaur, M.L., Sheng, M., Lowenstein, D.H., Jan, Y.N., and Jan, L.Y. (1992). Differential expression of K+ channel mRNAs in the rat brain and down-regulation in the hippocampus following seizures. Neuron *8*, 1055-1067.

Tsuchiya, K., and Kogure, S. (2012). Spectral analysis of bilateral or alternate-site kindling-induced afterdischarges in the rabbit hippocampi. Epilepsy Research *101*, 228-236.

Turrigiano, G.G. (2017). The dialectic of Hebb and homeostasis. Philos Trans R Soc Lond B Biol Sci *372*.

Uematsu, S., Lesser, R., Fisher, R.S., Gordon, B., Hara, K., Krauss, G.L., Vining, E.P., and Webber, R.W. (1992). Motor and sensory cortex in humans: topography studied with chronic subdural stimulation. Neurosurgery *31*, 59-71; discussion 71-52.

Uhlmann, E.J., Wong, M., Baldwin, R.L., Bajenaru, M.L., Onda, H., Kwiatkowski, D.J., Yamada, K., and Gutmann, D.H. (2002). Astrocyte-specific TSC1 conditional knockout mice exhibit abnormal neuronal organization and seizures. Ann Neurol *52*, 285-296.

Urrestarazu, E., Chander, R., Dubeau, F., and Gotman, J. (2007). Interictal high-frequency oscillations (100-500 Hz) in the intracerebral EEG of epileptic patients. Brain *130*, 2354-2366.

Valentine, P.A., Teskey, G.C., and Eggermont, J.J. (2004). Kindling changes burst firing, neural synchrony and tonotopic organization of cat primary auditory cortex. Cereb Cortex *14*, 827-839.

van Lier, H., Coenen, A.M., and Drinkenburg, W.H. (2003). Behavioral transitions modulate hippocampal electroencephalogram correlates of open field behavior in the rat: support for a sensorimotor function of hippocampal rhythmical synchronous activity. J Neurosci *23*, 2459-2465.

van Rijn, C.M., Gaetani, S., Santolini, I., Badura, A., Gabova, A., Fu, J., Watanabe, M., Cuomo, V., van Luijtelaar, G., Nicoletti, F.*, et al.* (2010). WAG/Rij rats show a reduced expression of CB(1) receptors in thalamic nuclei and respond to the CB(1) receptor agonist, R(+)WIN55,212-2, with a reduced incidence of spike-wave discharges. Epilepsia *51*, 1511-1521.

Vezzani, A., Speciale, C., DellaVedova, F., Tamburin, M., and Benatti, L. (1995). Alternative splicing at the C-terminal but not at the N-terminal domain of the NMDA receptor NR1 is altered in the kindled hippocampus. European Journal of Neuroscience *7*, 2513-2517.

Vinogradova, L.V., Shatskova, A.B., and van Rijn, C.M. (2011). Pro-epileptic effects of the cannabinoid receptor antagonist SR141716 in a model of audiogenic epilepsy. Epilepsy Research *96*, 250-256.

Volgraf, M., Gorostiza, P., Numano, R., Kramer, R.H., Isacoff, E.Y., and Trauner, D. (2006). Allosteric control of an ionotropic glutamate receptor with an optical switch. Nat Chem Biol *2*, 47-52.

Vreugdenhil, M., and Wadman, W.J. (1992). Enhancement of calcium currents in rat hippocampal CA1 neurons induced by kindling epileptogenesis. Neuroscience *49*, 373-381.

Wada, J.A., Osawa, T., and Mizoguchi, T. (1975). Recurrent spontaneous seizure state induced by prefrontal kindling in senegalese baboons, Papio papio. Can J Neurol Sci *2*, 477-492.

Wada, J.A., Sato, M., and Corcoran, M.E. (1974). Persistent seizure susceptibility and recurrent spontaneous seizures in kindled cats. Epilepsia *15*, 465-478.

Wada, Y., Hasegawa, H., Okuda, H., Yoshida, K., and Yamaguchi, N. (1989). Kindling of the Visual-Cortex in Cats - Comparison with Amygdaloid Kindling. Jpn J Psychiat Neur *43*, 245-253.

Waddington, S.N., Kramer, M.G., Hernandez-Alcoceba, R., Buckley, S.M., Themis, M., Coutelle, C., and Prieto, J. (2005). In utero gene therapy: current challenges and perspectives. Mol Ther *11*, 661-676.

Wagner, F.B., Truccolo, W., Wang, J., and Nurmikko, A.V. (2015). Spatiotemporal dynamics of optogenetically induced and spontaneous seizure transitions in primary generalized epilepsy. Journal of Neurophysiology *113*, 2321-2341.

Wang, Y., Xu, C., Xu, Z., Ji, C., Liang, J., Wang, Y., Chen, B., Wu, X., Gao, F., Wang, S.*, et al*. (2017). Depolarized GABAergic Signaling in Subicular Microcircuits Mediates Generalized Seizure in Temporal Lobe Epilepsy. Neuron *95*, 1221.

Way, S.W., Rozas, N.S., Wu, H.C., McKenna, J., 3rd, Reith, R.M., Hashmi, S.S., Dash, P.K., and Gambello, M.J. (2012). The differential effects of prenatal and/or postnatal rapamycin on neurodevelopmental defects and cognition in a neuroglial mouse model of tuberous sclerosis complex. Hum Mol Genet *21*, 3226-3236.

Weitz, A.J., Fang, Z., Lee, H.J., Fisher, R.S., Smith, W.C., Choy, M., Liu, J., Lin, P., Rosenberg, M., and Lee, J.H. (2015). Optogenetic fMRI reveals distinct, frequency-dependent networks recruited by dorsal and intermediate hippocampus stimulations. Neuroimage *107*, 229-241.

Wicker, E., and Forcelli, P.A. (2016). Chemogenetic silencing of the midline and intralaminar thalamus blocks amygdala-kindled seizures. Exp Neurol *283*, 404-412.

Wierenga, C.J., and Wadman, W.J. (1999). Miniature inhibitory postsynaptic currents in CA1 pyramidal neurons after kindling epileptogenesis. J Neurophysiol *82*, 1352-1362.

Wilder, B.J., King, R.L., and Schmidt, R.P. (1968). Comparative study of secondary epileptogenesis. Epilepsia *9*, 275-289.

Wong, M. (2008). Mechanisms of epileptogenesis in tuberous sclerosis complex and related malformations of cortical development with abnormal glioneuronal proliferation. Epilepsia *49*, 8-21.

Wong, R.K., and Prince, D.A. (1978). Participation of calcium spikes during intrinsic burst firing in hippocampal neurons. Brain Res *159*, 385-390.

Worrell, G.A., Parish, L., Cranstoun, S.D., Jonas, R., Baltuch, G., and Litt, B. (2004). High-frequency oscillations and seizure generation in neocortical epilepsy. Brain *127*, 1496-1506.

Wuarin, J.P., and Dudek, F.E. (1996). Electrographic seizures and new recurrent excitatory circuits in the dentate gyrus of hippocampal slices from kainate-treated epileptic rats. J Neurosci *16*, 4438-4448.

Wykes, R.C., Heeroma, J.H., Mantoan, L., Zheng, K., MacDonald, D.C., Deisseroth, K., Hashemi, K.S., Walker, M.C., Schorge, S., and Kullmann, D.M. (2012a). Optogenetic and potassium channel gene therapy in a rodent model of focal neocortical epilepsy. Sci Transl Med *4*, 161ra152.

Wykes, R.C., Heeroma, J.H., Mantoan, L., Zheng, K., MacDonald, D.C., Deisseroth, K., Hashemi, K.S., Walker, M.C., Schorge, S., and Kullmann, D.M. (2012b). Optogenetic and Potassium Channel Gene Therapy in a Rodent Model of Focal Neocortical Epilepsy. Science Translational Medicine *4*, 161ra152-161ra152.

Ye, Z.C., and Sontheimer, H. (1996). Cytokine modulation of glial glutamate uptake: a possible involvement of nitric oxide. Neuroreport *7*, 2181-2185.

Yekhlef, L., Breschi, G.L., Lagostena, L., Russo, G., and Taverna, S. (2015). Selective activation of parvalbumin- or somatostatin-expressing interneurons triggers epileptic seizurelike activity in mouse medial entorhinal cortex. J Neurophysiol *113*, 1616-1630.

Yizhar, O., Fenno, Lief E., Davidson, Thomas J., Mogri, M., and Deisseroth, K. (2011). Optogenetics in Neural Systems. Neuron *71*, 9-34.

Zemelman, B.V., Lee, G.A., Ng, M., and Miesenböck, G. (2002). Selective photostimulation of genetically chARGed neurons. Neuron *33*, 15-22.

Zeng, L.H., Xu, L., Gutmann, D.H., and Wong, M. (2008). Rapamycin prevents epilepsy in a mouse model of tuberous sclerosis complex. Ann Neurol *63*, 444-453.

Zhang, F., Wang, L.P., Brauner, M., Liewald, J.F., Kay, K., Watzke, N., Wood, P.G., Bamberg, E., Nagel, G., Gottschalk, A., *et al*. (2007). Multimodal fast optical interrogation of neural circuitry. Nature *446*, 633-639.

Zhang, H.H., Zhao, H.T., Zeng, C., Van Dort, C., Faingold, C.L., Taylor, N.E., Solt, K., and Feng, H.J. (2018a). Optogenetic activation of 5-HT neurons in the dorsal raphe suppresses seizure-induced respiratory arrest and produces anticonvulsant effect in the DBA/1 mouse SUDEP model. Neurobiology of Disease *110*, 47-58.

Zhang, W., Yamawaki, R., Wen, X., Uhl, J., Diaz, J., Prince, D.A., and Buckmaster, P.S. (2009). Surviving hilar somatostatin interneurons enlarge, sprout axons, and form new synapses with granule cells in a mouse model of temporal lobe epilepsy. J Neurosci *29*, 14247-14256.

Zhang, Z., Russell, L.E., Packer, A.M., Gauld, O.M., and Hausser, M. (2018b). Closed-loop all-optical interrogation of neural circuits in vivo. Nat Methods *15*, 1037-1040.

Zhao, W.F., Bianchi, R., Wang, M., and Wong, R.K.S. (2004). Extracellular signal-regulated kinase 1/2 is required for the induction of group I metabotropic glutamate receptor-mediated epileptiform discharges. Journal of Neuroscience *24*, 76-84.

Zhu, Z.Q., Armstrong, D.L., Hamilton, W.J., and Grossman, R.G. (1997). Disproportionate loss of CA4 parvalbumin-immunoreactive interneurons in patients with Ammon's horn sclerosis. J Neuropathol Exp Neurol *56*, 988-998.

Zijlmans, M., Jacobs, J., Zelmann, R., Dubeau, F., and Gotman, J. (2009). High frequency oscillations and seizure frequency in patients with focal epilepsy. Epilepsy Res *85*, 287-292.

Zingg, B., Chou, X.L., Zhang, Z.G., Mesik, L., Liang, F., Tao, H.W., and Zhang, L.I. (2017). AAV-Mediated Anterograde Transsynaptic Tagging: Mapping Corticocollicular Input-Defined Neural Pathways for Defense Behaviors. Neuron *93*, 33-47.